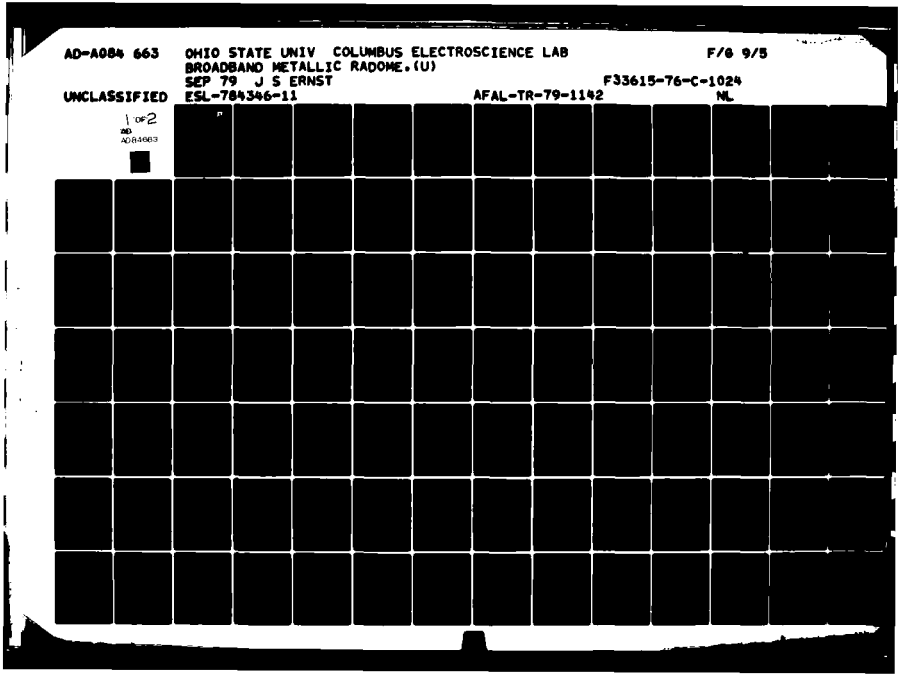
AD-A084 663
OHIO STATE UNIV COLUMBUS ELECTROSCIENCE LAB
F/G 9/5
BROADBAND METALLIC RADOME,(U)
SEP 79 J S ERNST
F33615-76-C-1024
UNCLASSIFIED
ESL-784346-11
AFAL-TR-79-1142
NL
1 OF 2
AD
A084663

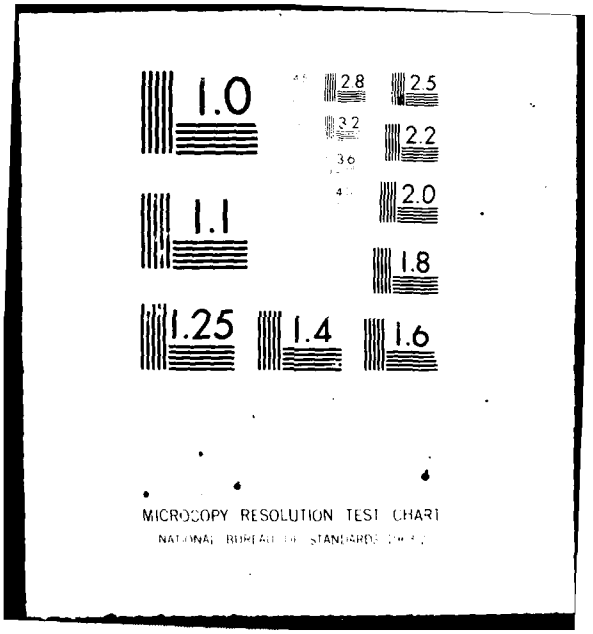
1.0
2.8
2.5
3.2
2.2
3.6
4.0
2.0
1.1
1.8
1.25
1.4
1.6
MICROCOPY RESOLUTION TEST CHART
NATIONAL BUREAU OF STANDARDS 1963-A

AFAL-TR-79-1142




# BROADBAND METALLIC RADOME

*THE OHIO STATE UNIVERSITY*
*ELECTROSCIENCE LABORATORY*
*DEPARTMENT OF ELECTRICAL ENGINEERING*
*COLUMBUS, OHIO 43212*

SEPTEMBER 1979



TECHNICAL REPORT AFAL-TR-79-1142
Interim Report for January 1976 to September 1979

Approved for public release; distribution unlimited.



AIR FORCE AVIONICS LABORATORY
AIR FORCE WRIGHT AERONAUTICAL LABORATORIES
AIR FORCE SYSTEMS COMMAND
WRIGHT-PATTERSON AIR FORCE BASE, OHIO 45433

NOTICE

When Government drawings, specifications, or other data are used for any purpose other than in connection with a definitely related Government procurement operation, the United States government thereby incurs no responsibility nor any obligation whatsoever; and the fact that the government may have formulated, furnished, or in any way supplied the said drawings, specifications, or other data, is not to be regarded by implication or otherwise as in any manner licensing the holder or any other person or corporation, or conveying any rights or permission to manufacture, use, or sell any patented invention that may in any way be related thereto.

This report has been reviewed by the Information Office (OI), and is releasable to the National Technical Information Service (NTIS). At NTIS, it will be available to the general public, including foreign nations.

This technical report has been reviewed and is approved for publication.

Carl A. Mentzer
Project Engineer

William F. Bahret
William F. Bahret, Chief
Passive ECM Br, EW Division
Avionics Laboratory

FOR THE COMMANDER

Joseph H. Jacobs
Joseph H. Jacobs, Colonel, USAF
Chief, Electronic Warfare Division
Avionics Laboratory

*"If your address has changed, if you wish to be removed from our mailing list, or if the addressee is no longer employed by your organization please notify AFWAL/AAWP ,W-PAFB, OH 45433 to help us maintain a current mailing list".*

*Copies of this report should not be returned unless return is required by security considerations, contractual obligations, or notice on a specific document.*

AIR FORCE/56780/1 May 1980 — 80

# DISCLAIMER NOTICE

THIS DOCUMENT IS BEST QUALITY PRACTICABLE. THE COPY FURNISHED TO DTIC CONTAINED A SIGNIFICANT NUMBER OF PAGES WHICH DO NOT REPRODUCE LEGIBLY.

SECURITY CLASSIFICATION OF THIS PAGE (When Data Entered)

## REPORT DOCUMENTATION PAGE

READ INSTRUCTIONS BEFORE COMPLETING FORM

| | |
|---|---|
| 1. REPORT NUMBER: AFAL-TR-79-1142 | 2. GOVT ACCESSION NO.: AD-A084 663 |
| 3. RECIPIENT'S CATALOG NUMBER: | |
| 4. TITLE (and Subtitle): BROADBAND METALLIC RADOME | 5. TYPE OF REPORT & PERIOD COVERED: Interim Report, for January 1976 to September 1979 |
| 6. PERFORMING ORG. REPORT NUMBER: ESL-784346-11 | |
| 7. AUTHOR(s): J.S. Ernst | 8. CONTRACT OR GRANT NUMBER(s): Contract F33615-76-C-1024 |
| 9. PERFORMING ORGANIZATION NAME AND ADDRESS: The Ohio State University ElectroScience Laboratory, Department of Electrical Engineering, Columbus, Ohio 43212 | 10. PROGRAM ELEMENT, PROJECT, TASK AREA & WORK UNIT NUMBERS: 7633-13-28 |
| 11. CONTROLLING OFFICE NAME AND ADDRESS: Air Force Avionics Laboratory (AFAL/WRP) Air Force Wright Aeronautical Laboratories Wright-Patterson Air Force Base, Ohio 45433 | 12. REPORT DATE: September 1979 |
| | 13. NUMBER OF PAGES: 111 |
| 14. MONITORING AGENCY NAME & ADDRESS (if different from Controlling Office) | 15. SECURITY CLASS. (of this report): Unclassified |
| | 15a. DECLASSIFICATION/DOWNGRADING SCHEDULE |

16. DISTRIBUTION STATEMENT (of this Report)

Approved for public release; distribution unlimited.

17. DISTRIBUTION STATEMENT (of the abstract entered in Block 20, if different from Report)

18. SUPPLEMENTARY NOTES

The work contained in this report is also used as a thesis submitted to the Department of Electrical Engineering, The Ohio State University as partial fulfillment for the degree Master of Science.

19. KEY WORDS (Continue on reverse side if necessary and identify by block number)

| | |
|---|---|
| Radomes | Periodic Surfaces |
| Broadband Radomes | Interlace Anomaly |
| Metallic Radomes | Luebbers Anomaly |

20. ABSTRACT (Continue on reverse side if necessary and identify by block number)

This report studies the transmission properties of a metallic radome configuration of two slot arrays consisting of three-legged elements imbedded in three dielectric layers. The purpose is to design a bandpass filter with as large a bandwidth as possible while still maintaining a constant bandwidth for all angles of incidence.

DD FORM 1 JAN 73 1473 EDITION OF 1 NOV 65 IS OBSOLETE

SECURITY CLASSIFICATION OF THIS PAGE (When Data Entered)

20.

The method of design involves an iterative procedure carried out through computer calculations. This procedure produces good results.

The final design makes use of a cosinusoidal voltage distribution along the slot when in the non-transmitting (scattering) mode. This should increase the accuracy between measured and calculated transmission curves at the upper portion of the frequency band. A sinusoidal voltage distribution was previously used.

The final design for the metallic radome results in a 1 dB bandwidth for angles of incidence from $0^{\circ}$ to $60^{\circ}$ of approximately 43 percent. For angles of incidence up to $75^{\circ}$, the bandwidth is somewhat reduced. This is the largest and most constant bandwidth to date.

This work is important to the Air Force in that it will allow metallic radomes with large constant bandwidths to be designed.

## ACKNOWLEDGMENTS

The author wishes to express his gratitude to the individuals at the ElectroScience Laboratory who assisted in work involved in this thesis. A special thanks goes to Dr. Benedikt Munk for his counsel in all phases of the investigation and to Prof. Leon Peters for his review of this thesis.

The work reported in this thesis was supported in part by Contract F33615-76-C-1024 between Air Force Avionics Laboratory, Wright-Patterson Air Force Base, Ohio and The Ohio State University Research Foundation.

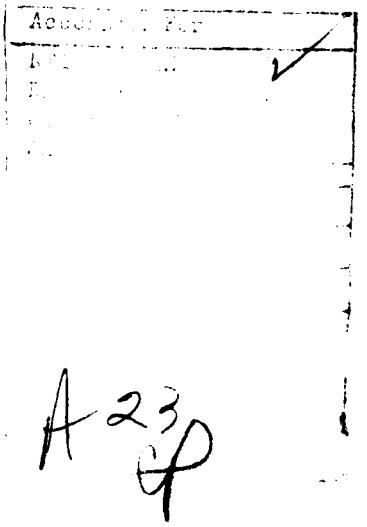

TABLE OF CONTENTS

LIST OF FIGURES

# SECTION I
# INTRODUCTION

In many applications it is necessary to place a protective cover over an antenna. Such a cover is commonly referred to as a radome and the conventional approach has been to use solid or laminated dielectric materials for these covers. Recently, substantial effort has been directed to a study of metallic radomes.

Metallic radomes possess many inherent advantages over conventional dielectric radomes. Some of these are

1) Elimination of the precipitation static (p-static) noise, which may cause certain radars and electronic equipment to malfunction,

2) Inherent lightning protection,

3) Reflection from a thermonuclear flash,

4) Better shielding against low frequency EM-pulses since a metallic radome in general can be regarded as a bandpass filter with high attenuation for low frequencies,

5) Potentially better laser hardening, and

6) Potentially higher mechanical strength.

Periodic surfaces are employed in the design of metallic radomes. Previous designs of periodic surfaces have been used for band rejection of an incident signal by utilizing dipole arrays and they have been used as narrow bandpass filters by utilizing slot arrays. The objective of this study is, through the use of planar periodic slot arrays, to design a passband filter with the largest bandwidth to date. The bandwidth is considered to be that range of frequencies in which the field transmitted through the structure has a loss of less than 1 dB. In some applications a typical constraint is given as 3 dB but this would mean 50% of the energy is lost. This lost energy is not necessarily absorbed but can be reflected in directions different from that on the main beam. This could have the undesirable effect of increasing the side lobe level of the antenna.

The type of metallic radome to achieve the objective is found to be an extension of previous results. From the results in [1], it is determined that the type of element in the planar periodic slot array be a generalized three-legged element. This type of element allows for a closer packing of the elements and also allows the elements to be unloaded. From the results in [2], it is determined that a skewed grid (i.e., interlace design) should improve the bandwidth. From the results in [3], it is determined that two planar periodic slot arrays placed in parallel results in an increase in bandwidth with more control of the shape of the transmission curve. This results in a flat response in the pass-band region and greater attenuation outside the pass-band region.

There must be a dielectric structure to be used to separate and to support the two arrays. From the results in [4] it is determined that dielectric layers are needed. These layers are used to provide a constant bandwidth for the varying angles of incidence. From the results in [5], it is determined that three dielectric layers should be used. The dielectric layers serve the dual function of physical support as well as stabilizing the bandwidth. The outer dielectric layers produce a constant bandwidth and the middle dielectric layer provides the proper coupling between the arrays.

All of this leads to the structure of Figures 1 and 2, that being a biplanar slot array of generalized three-legged elements imbedded in three dielectric slabs. The slabs have relative permittivity, $\varepsilon_{rm}$, and thickness, $d_m$, where m refers to the dielectric media. The theory is described in the next chapter and the actual transmission curves and input variables are determined in Chapter III. The conclusions are presented in Chapter IV.

The approach used in this report is to use the previous solutions as a guide and to apply them with a view toward obtaining as large a bandwidth as possible. Since much of the theory is contained in detail in these prior studies by other authors, it is not repeated here. Only the final equations are presented so that the casual reader can observe what is being achieved. This also allows the achievements to be presented with a minimum of clutter. The serious reader will, of course, refer to these original and rather elaborate reports.

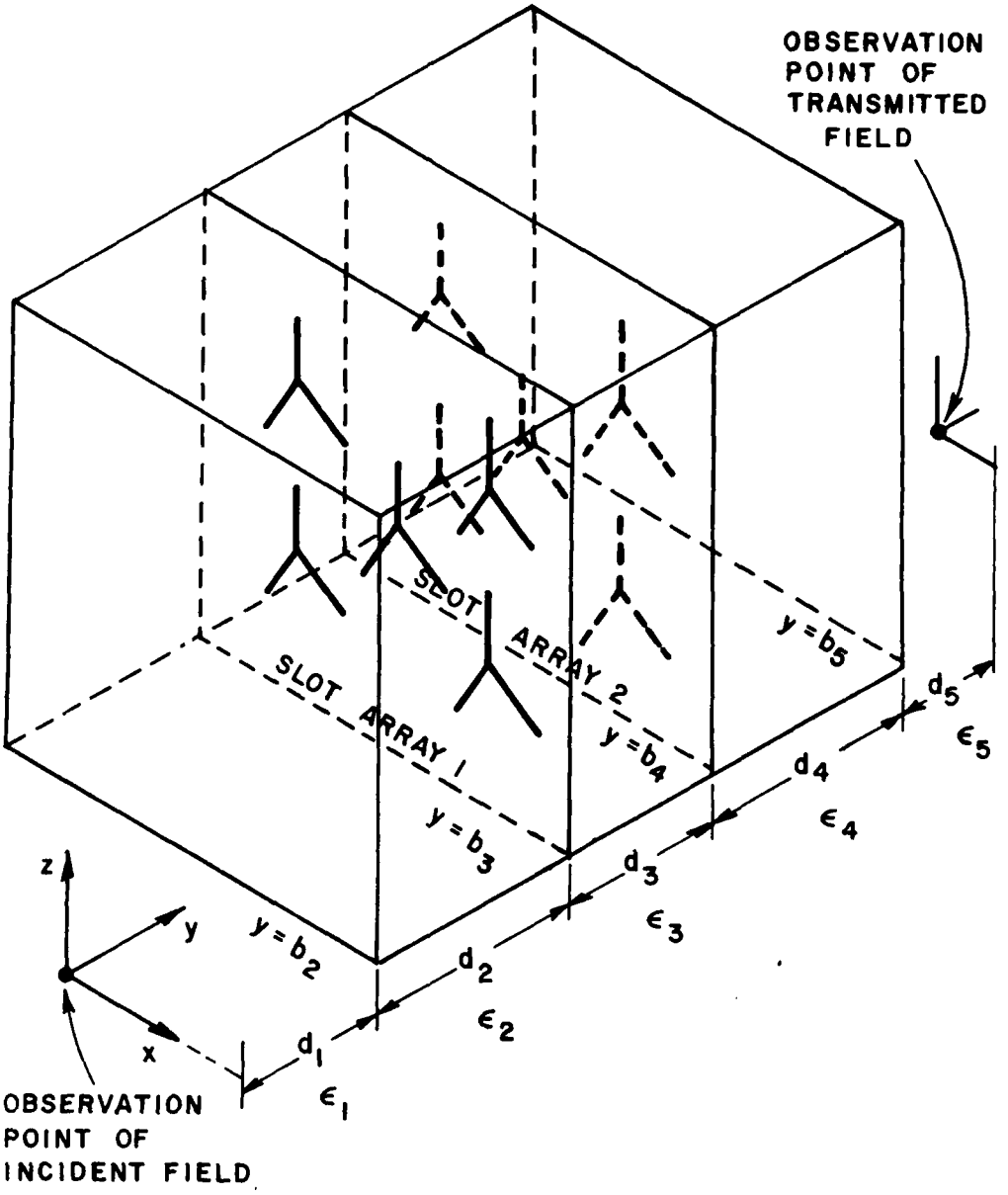


Figure 1. Biplanar slot arrays of three-legged elements imbedded in three dielectric slabs.

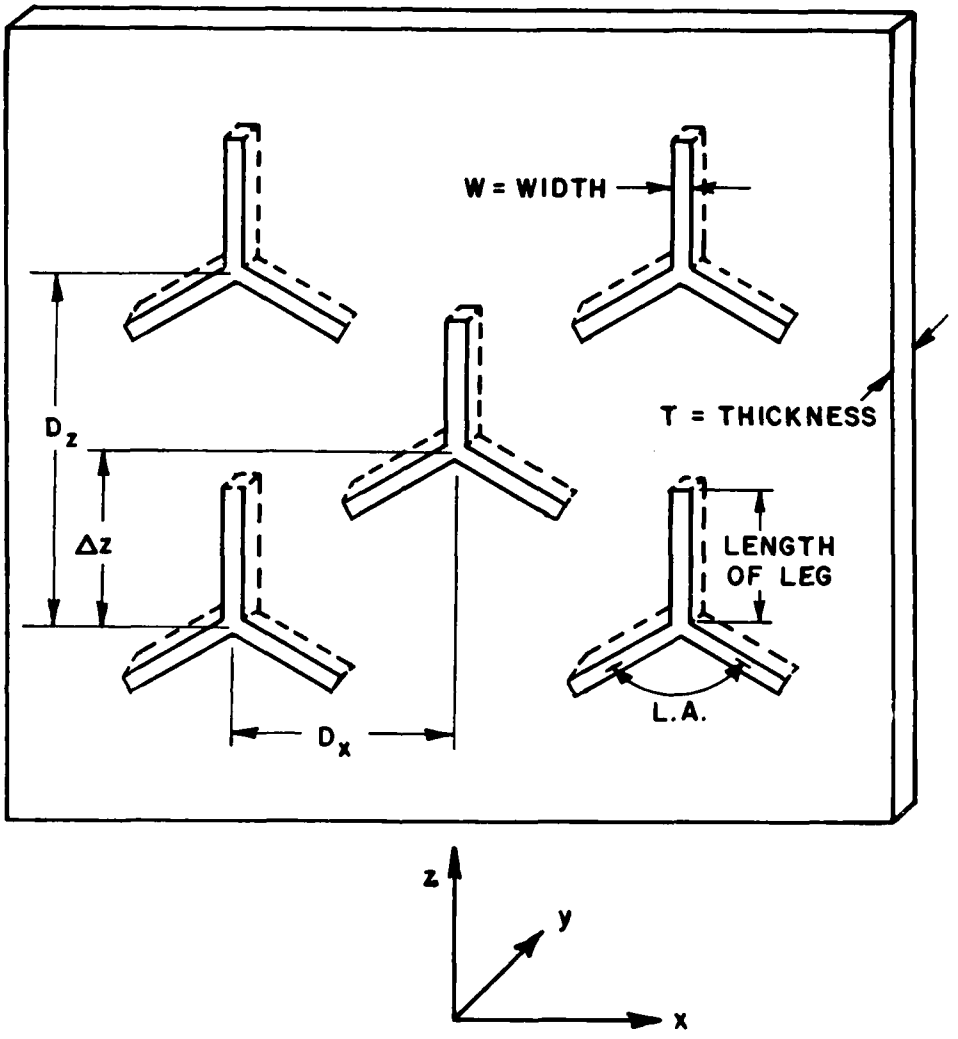


Figure 2. Three-legged slot array geometry.
L. A. denotes Leg Angle.

## SECTION II
## DEVELOPMENT OF THE THEORY

Generalized three legged elements consist of three monopoles connected together at a single point each of arbitrary length and direction. The lengths being $\ell^{1,i}$, $\ell^{2,i}$, $\ell^{3,i}$ and the directions being unit vectors $\hat{p}^{1,i}$, $\hat{p}^{2,i}$, $\hat{p}^{3,i}$ where the superscripts refer to the leg number and array index, respectively* The parameters of the generalized three legged element are illustrated in Figure 3. The lengths and unit vectors will remain fixed in each array but may differ between arrays for the remainder of this report. It has been shown in earlier work[6] that the voltage distribution along the reference slot in array i is the sum of two modes:

1) the symmetric mode, $V^{s,i}(\ell)$ $\quad i = 1,2$

2) the asymmetric mode $V^{a,i}(\ell)$

as shown in Figure 4.

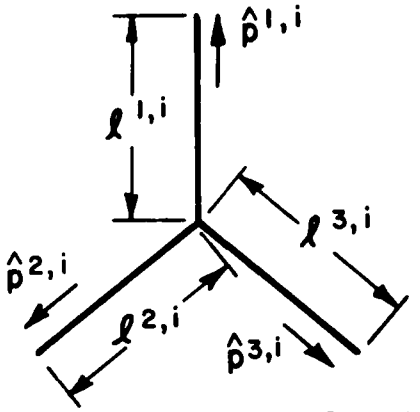


Figure 3. Generalized three legged element showing critical parameters.

* Note: The superscript is sometimes enclosed with a parenthesis so that it is not confused with the power of a variable (i.e., $\hat{p}^{(2)}$ is not $\hat{p}$ squared).

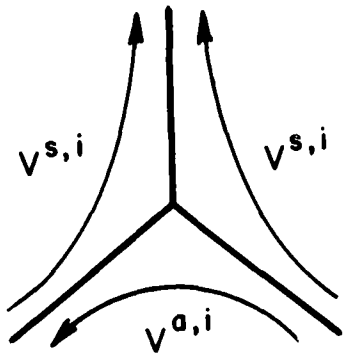


Figure 4. The voltage modes on a generalized three legged element.

To determine the transmission through this structure, the procedure is similar to that of an earlier report[7]. This consists of the following three parts:

A. determination of the symmetric current, $I^{s,in}$, and the asymmetric current, $I^{a,in}$ induced by the incident H-field,

B. determination of the symmetric and asymmetric voltage modes, $V^{s,2}(\ell)$ and $V^{a,2}(\ell)$ respectively, where the superscript 2 refers to the second array,

C. determination of the transmitted H-field reradiated by the two voltage modes above of the second array.

## A. Determination of the induced currents $I^{s,in}$ and $I^{a,in}$

Let the configuration shown in Figure 1 be exposed to the incident plane wave whose magnetic field is given by

$$\overline{H}_1^{inc}(\overline{R}) = \overline{H}_1^{inc}\, e^{-j\beta_1 \overline{R}\cdot\hat{s}_1}$$

where

$\hat{s}_1$ is the direction of the incident plane wave signal in medium 1 (as shown in Figure 5),

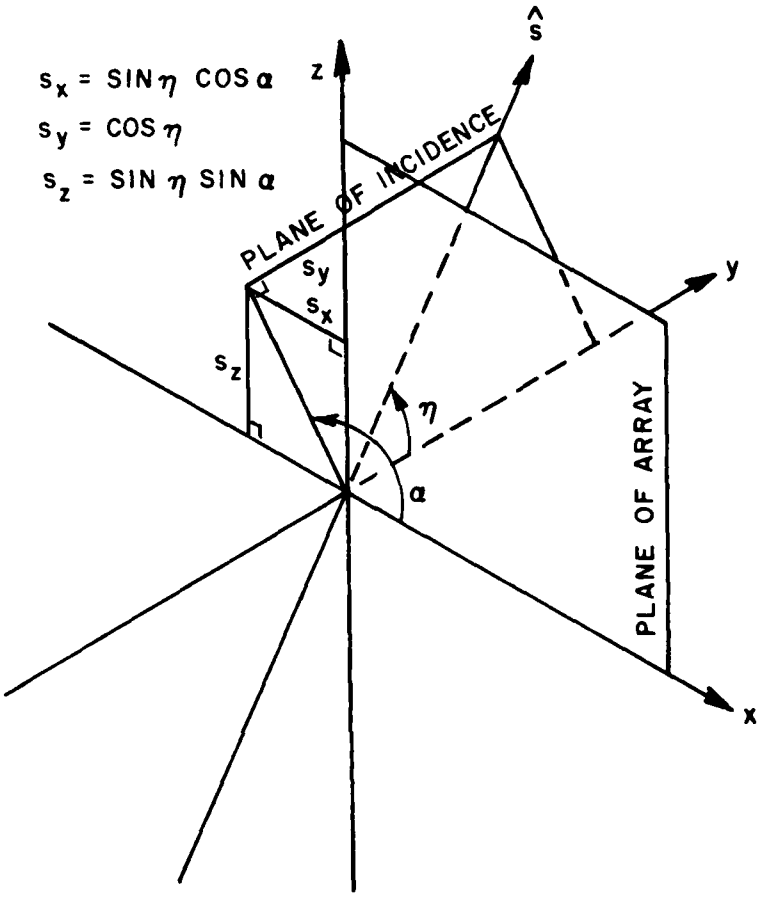


Figure 5. Coordinate system for incident fields.

$\beta_1$ is the propagation constant of medium 1,

$\overline{R}$ is the position vector for the point of observation for the incident field (as shown in Figure 6).

A slot can be considered as a magnetic element mounted directly in front of an electrically perfectly-conducting ground plane[8]. Because of this electric screen effect, the incident plane wave will only induce $I^{s,in}$ and $I^{a,in}$ in array 1. Also the induced currents, $I^{s,in}$ and $I^{a,in}$, are independent of whatever exists behind array 1.* Thus

* The effect of the structure behind array 1 is contained in the mutual coupling terms between the two arrays.

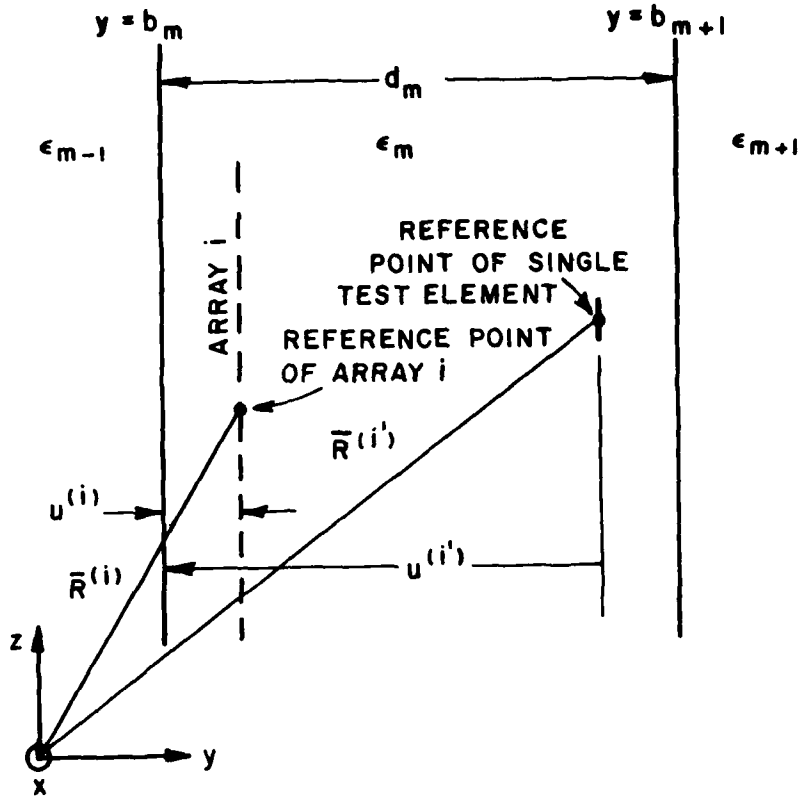


Figure 6. Structure used to define certain variables needed to determine the admittances in slab m bounded by the planes $y=b_m$ and $y=b_{m+1}$.

the induced currents are of the same form as Equations (11) and (12) in [9]. The symmetric and asymmetric current are:

$$I^{s,in} = [\bar{H}_1^{inc}(\bar{R}) \cdot {}_{\perp}\hat{n}_1 \, {}_{\perp}P_1^{slt} \, {}_{\perp}T_{2/1}(0,0) + \bar{H}_1^{inc}(\bar{R}) \cdot {}_{\parallel}\hat{n}_1 \, {}_{\parallel}P^{slt} \, {}_{\parallel}T_{2/1}(0,0)] \, e^{-j\beta_2(\bar{R}^{(1)}-\bar{R})\cdot\hat{s}_2} \quad (1)$$

$$I^{a,in} = [\bar{H}_1^{inc}(\bar{R}) \cdot {}_{\perp}\hat{n}_1 \, {}_{\perp}P^{alt} \, {}_{\perp}T_{2/1}(0,0) + \bar{H}_1^{inc}(\bar{R}) \cdot {}_{\parallel}\hat{n}_1 \, {}_{\parallel}P^{alt} \, {}_{\parallel}T_{2/1}(0,0)] \, e^{-j\beta_2(\bar{R}^{(1)}-\bar{R})\cdot\hat{s}_2} \quad (2)$$

where

$_{\perp}\hat{n}_1$ is a unit vector orthogonal to the plane of incidence in medium 1 (see Appendix C),

$_{\parallel}\hat{n}_1$ is a unit vector parallel to the plane of incidence and orthogonal to the direction of propagation in medium 1 (see Appendix C),

$\overline{R}^{(1)}$ is the position vector for the reference point of the reference element in array 1 (see Figure 6),

$\{^{\perp}_{\parallel}\}P_1^{sit}$ is the composite symmetric transmitting pattern factor for array 1 in medium 1, orthogonal and parallel components,

$\{^{\perp}_{\parallel}\}P_1^{alt}$ is the composite asymmetric transmitting pattern factor for array 1 in medium 1, orthogonal and parallel components,

$\{^{\perp}_{\parallel}\}T_{2/1}(0,0)$ is the transformation function for dielectric media 2 normalized to media 1. (normalized T-factor).

The pattern factors are the far field patterns due to a voltage distribution on an element of the array. They represent the relative magnitude of the plane waves propagating in certain directions. See section B2, The Pattern Factors, for defining equations.

The transformation function represents the transformation of the field as a result of the dielectric interfaces. The plane waves will be partly reflected and partly transmitted at each interface. The transformation function sums up this effect of multiple reflections of the waves and transforms the field from one dielectric media to another. see section B3, The Transformation Functions, for defining equations.

## B. Determination of $V^{s,2}(\ell)$ and $V^{a,2}(\ell)$

Certain quantities needed for the evaluation of $V^{s,2}(\ell)$ and $V^{a,2}(\ell)$ are evaluated in the following sections.

### B1. Determination of Admittances

As developed in [10], the impedances for dipole arrays was defined as

$$Z^{i',i} \equiv - \frac{\text{Voltage induced in the single test element } i'}{\text{Terminal current of the reference element of the array } i^*}$$

*This does not imply that the currents in the remaining slots are zero. In fact they are related to the reference element by Floquet's theorem.

Through use of duality (i.e., the induced voltage becomes the induced current and the terminal current becomes the terminal voltage), the admittance for slot arrays is defined as

$$Y^{i',i} \equiv - \frac{\text{Current induced in the single test element } i'}{\text{Terminal voltage of the reference element of the array } i}$$

Now each voltage mode, $V^{si}(\ell)$ and $V^{ai}(\ell)$ of each array induces a symmetric current in the reference element of each array. Hence there is a total of sixteen admittances.

Using the dual of Equation (44) in [11] with some change of notation and generalizing to the medium m results in

$$Y^{Ai',Bi} = \frac{Y_m}{2D_x D_z} \sum_{k=-\infty}^{\infty} \sum_{n=-\infty}^{\infty} \frac{e^{-j\beta_m(\bar{R}^{(i')}-\bar{R}^{(i)})\cdot\hat{r}_m}}{r_{my}}$$

$$[{}_{\perp}P_m^{Ai't}{}_{\perp}P_m^{Bi}{}_{\perp}T_m(u^{(i)},d_m-u^{(i')}) + {}_{\parallel}P_m^{Ai't}{}_{\parallel}P_m^{Bi}{}_{\parallel}T_m(u^{(i)},d_m-u^{(i')})] \qquad (3)$$

where

A,B are dummy superscripts that refer to the symmetric or asymmetric composite pattern factors,

${}_{\{\perp\atop\parallel\}}P_m^{Ai't}, {}_{\{\perp\atop\parallel\}}P_m^{Bi}$ are defined in the section on Pattern Factors,

$Y_m$ is the characteristic admittance of dielectric media m,

$D_x, D_z$ are the interelement spacings between adjacent slots measured in the $\hat{x}$ and $\hat{z}$ direction respectively,

$\beta_m$ is the propagation constant of media m,

$u^{(i)}, u^{(i')}$ are defined in Figure 6,

$\bar{R}^{(i')}$ is the position vector of the single test element reference point,

$\bar{R}^{(i)}$ is the position vector of the reference point of the reference element of array i,

${}_{\{\perp\atop\parallel\}}T_m(u^{(i)},d_m-u^{(i')})$ is defined in section B3, Transformation Function.

The unit vector, $\hat{r}_m$, indicates the directions in which the bundle of plane, inhomogeneous waves are being scattered by the array. Using Equations (D2) and (D3) in [12] together with results developed in [13], $\hat{r}_m$ for a skewed array is found to be

$$\hat{r}_m = \hat{x}\left(s_{mx} + \frac{k\lambda_m}{D_x} - \frac{n\Delta z\lambda_m}{D_x D_z}\right) + \hat{y} r_{my} + \hat{z}\left(s_{mz} + \frac{n\lambda_m}{D_z}\right) \tag{4}$$

where

$$r_{my} = \pm\left(1 - \left(s_{mx} + \frac{k\lambda_m}{D_x} - \frac{n\Delta z\lambda_m}{D_x D_z}\right)^2 - \left(s_{mz} + \frac{n\lambda_m}{D_z}\right)^2\right)^{1/2} \tag{5}$$

and

$\Delta z$ is the interlace spacing in the z direction, and is defined as the distance between two slots that are adjacent in the x direction (see Figure 2),

$\lambda_m$ is the wavelength in media m.

It can be shown that results obtained interlacing in the x direction are equal to those obtained from the analysis for interlacing in the z direction. Also the solution for geometries interlaced in both directions at once can be evaluated by redefining $D_x$ and $D_z$ to new values.

Now $r_{my}$ may either be real or imaginary. When it is real, $r_{my}$ represents a wave propagating away from the array, hence the plus sign must be used. When it is imaginary, $r_{my}$ represents a wave which attenuates as it moves away from the array, hence the negative sign must be used. For k=n=0, the equation for $\hat{r}_m$ reduces to $\hat{s}_m$ (and the specular direction).

The self admittance is closely approximated by the mutual coupling between the single test element located w/4 (w is the width of the slot) away from the reference element of the array[14]. Assuming that the x components and the z components of $\bar{R}^{(i')}$ and $\bar{R}^{(i)}$ are equal.

$$(\bar{R}^{(i')} - \bar{R}^{(i)}) \cdot \hat{r}_m = \frac{w}{4} r_{my} \tag{6}$$

For mutual admittances, the single test element is assumed to be an element of the other array. Using the given structure with the same assumptions as before, results in

$$(\bar{R}^{(i')} - \bar{R}^{(i)}) \cdot \hat{r}_m = d_3 r_{3y} \quad . \quad \text{(Note: } R_{x,z}^{(i)} = R_{x,z}^{(i')}) \tag{7}$$

Using Equations (6) and (7) will assist in determination of the self and mutual admittances. Appendix A contains a complete list of all the admittances for the structure in Figure 1.

B2. The Pattern Factors

The transmitting and non-transmitting pattern factor for each leg is found through the application of duality to Equations (D14) and (40) in [15] to give

$$p^{vit}(g) = \frac{1}{V^{vit}(0)} \int_0^{\ell^{(g)}} V^{vit}(\ell)\, e^{-j\beta\ell(g)i\hat{p}^{g,i}\cdot\hat{r}}\, d\ell \tag{8}$$

and $g = 1,2,3$

$$p^{vi}(g) = \frac{1}{V^{vi}(0)} \int_0^{\ell^{(g)}} V^{vi}(\ell)\, e^{j\beta\ell(g)i\hat{p}^{g,i}\cdot\hat{r}}\, d\ell \tag{9}$$

respectively, where g is the leg number and i again refers to the array index.

There is a symmetric pattern and an asymmetric pattern corresponding to the symmetric and asymmetric voltage modes respectively. Hence the dummy superscript 'v' for variable becomes an 's' for the symmetric voltage mode and becomes an '$a^T$' for the asymmetric voltage mode.

Note that it is not necessary to specify the media for $\beta$ and $\hat{r}$ since it was assumed that the arrays are planar (i.e., $\hat{p}^{(g)}$ contains no y component). Using Equations (B1) and (B2) in [16] it can be shown that

$$\beta_m\, \hat{p}^{(g)i}\cdot\hat{r}_m = \beta_q\, \hat{p}^{(g)i}\cdot\hat{r}_q \quad \text{(for planar elements only)} \tag{10}$$

where m and q refer to the dielectric media. Hence the media subscripts, m and q, can be eliminated.

The form of $V^{vit}(\ell)$ and $V^{vi}(\ell)$ is usually assumed to be[17]

$$V^{vit}(\ell) = V^{vit}(0)\, \sin\beta_d(\ell_{ef}^{(g)i} - \ell^{(g)i}) \tag{11}$$

and

$$V^{vi}(\ell) = V^{vi}(0)\ \sin\beta_d(\ell_{ef}^{g,i} - \ell^{g,i})^* \tag{12}$$

where

$\beta_d$ is the effective dielectric propagation constant (Equation (C-2) in [18]),

$\ell_{ef}$ is the effective length of the leg due to the inductance at the ends of each leg.

This inductance effectively increases the length of the legs. $V^{vit}(0)$ and $V^{vi}(0)$ are the magnitudes of the voltages for each mode at the terminals (i.e., point where legs join). It must be noted that only the form of the voltages $V^{vit}(\ell)$ and $V^{vi}(\ell)$ is used to calculate the patterns since the magnitude at the terminals divides out. The magnitude of each voltage for the second array will be determined later. It is needed to calculate the transmitted H-field. (Part C).

There is a generalized composite pattern factor for the transmitting and non-transmitting (scattering) case for each voltage mode. By inspection of Figure 7b and the use of Equation (42) in [19] the generalized composite pattern factors for the generalized three-legged elements are

$$\underset{\{\perp\parallel\}}{P_m^{sit}} = (2\hat{p}(1)i_p{}^{s1t} - \hat{p}(2)_p{}^{s2t} - \hat{p}(3)i_p{}^{s3t}) \cdot \underset{\{\perp\parallel\}}{\hat{n}_m} \tag{13}$$

$$\underset{\{\perp\parallel\}}{P_m^{ait}} = (\hat{p}(2)i_p{}^{a2t} - \hat{p}(3)i_p{}^{a3t}) \cdot \underset{\{\perp\parallel\}}{\hat{n}_m} \tag{14}$$

$$\underset{\{\perp\parallel\}}{P_m^{si}} = (2\hat{p}(1)ipsl - \hat{p}(2)ips2 - \hat{p}(3)ps3) \cdot \underset{\{\perp\parallel\}}{\hat{n}_m} \tag{15}$$

$$\underset{\{\perp\parallel\}}{P_m^{ai}} = (\hat{p}(2)_p{}^{a2} - \hat{p}(3)_p{}^{a3}) \cdot \underset{\{\perp\parallel\}}{\hat{n}_m} \tag{16}$$

*An alternate form for $V^{vi}(\ell)$ will be presented in section III, Development of Data and Results. The reasons for this change are discussed in that section.

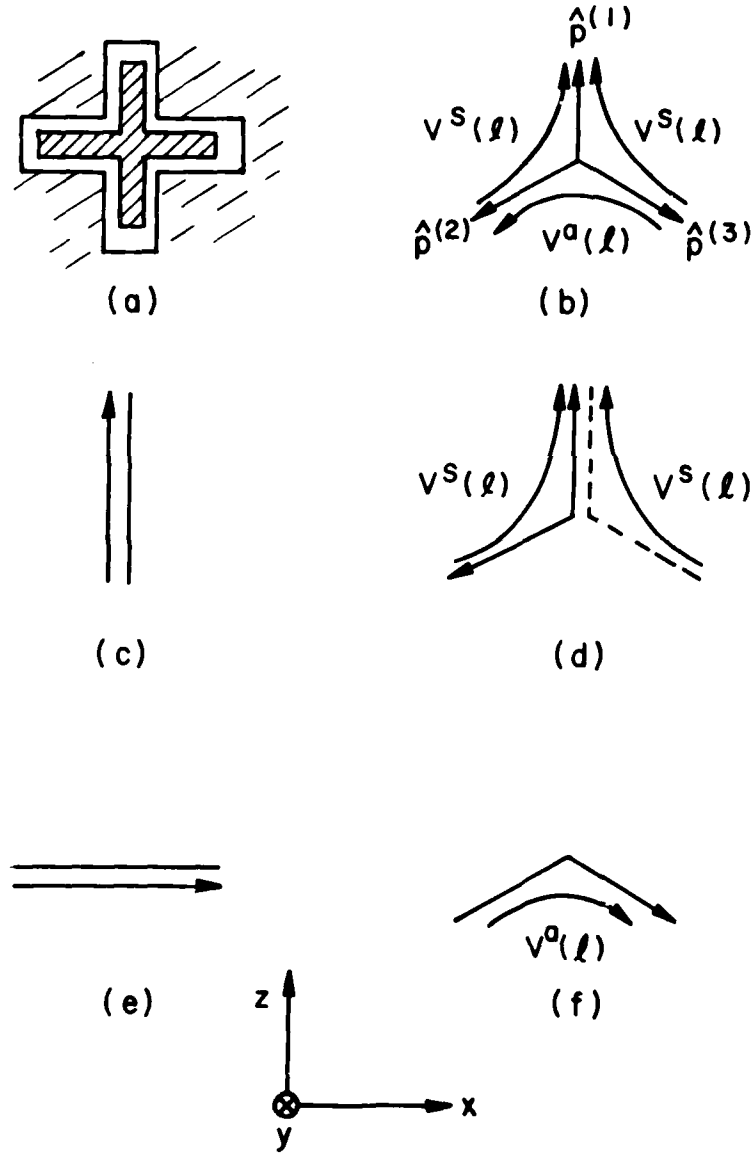


Figure 7. Showing excited modes in YZ SCAN PLANE
(a) Loaded straight slot (L.S.S.)
(b) Three legged direction vectors and voltages defined
(c) L.S.S. for parallel incident polarization
(d) Three legged parallel incident polarization
(e) L.S.S. for orthogonal incident polarization
(f) Three legged orthogonal incident polarization.

The factor of 2 comes from the fact that $V^s(\ell)$ is being counted twice on leg $\ell^{(1)}$. The negative signs appear because the vector 'magnetic current' is going in the opposite direction of the unit vectors of leg directions as shown in Figure 7b. All patterns have now been specified.

## B3. The Transformation Functions

The transformation functions (T factor) needed in admittance calculations are found from Equation (29) in [20] by changing from reflection coefficients for the electric field to reflection coefficients for the magnetic field and generalizing the results to layer m

$$
{}_{\{\frac{\perp}{\parallel}\}}T_m(u^{(i)}, d_m - u^{(i')}) = \left[\left(1 + {}_{\{\frac{\perp}{\parallel}\}}\Gamma_{m,m-1}\, e^{-j2\beta_m u^{(i)} r_{my}}\right)\right.
$$

$$
\left.\times \left(1 + {}_{\{\frac{\perp}{\parallel}\}}\Gamma_{m,m+1}\, e^{-j2\beta_m (d_m - u^{(i')}) r_{my}}\right)\right] \Bigg/
$$

$$
\left(1 - {}_{\{\frac{\perp}{\parallel}\}}\Gamma_{m,m-1}\, {}_{\{\frac{\perp}{\parallel}\}}\Gamma_{m,m+1}\, e^{-j\beta_m d_m r_{my}}\right) \qquad (17)
$$

This is the generalized non-normalized T-factor for slot arrays such that the array and the single test element are separated by at most only one dielectric layer for $u^{(i')} > u^{(i)}$. For $u^{(i)} > u^{(i')}$ see remarks at the end of this section For the given structure, ${}_{\{\frac{\perp}{\parallel}\}}\Gamma_{m,m-1}$ and ${}_{\{\frac{\perp}{\parallel}\}}\Gamma_{m,m+1}$ are the reflection coefficients between two dielectric media whose equations are listed in Appendix D. The T-factors used in admittance calculations can now be computed. See Appendix B.

It was found that expressing the induced currents and the transmitted H-field in a normalized form results in conceptually simpler equations. The T-factors used in these equations are hence normalized. Modification of Equation (33) in [21] in the same manner Equation (29) was modified in [22] gives

$$ {}_{\{\frac{1}{\mu}\}}T_{m/q}(u^{(i)}, d_m - u^{(i')}) = \left(\frac{1 - {}_{\{\frac{1}{\mu}\}}\Gamma_{m,q}}{1 + {}_{\{\frac{1}{\mu}\}}\Gamma_{m,q}}\right) $$

$$ \frac{\left(1 + {}_{\{\frac{1}{\mu}\}}\Gamma_{m,m-1}\, e^{-j2\beta_m u^{(i)} r_{my}}\right)\left(1 + {}_{\{\frac{1}{\mu}\}}\Gamma_{m,m+1}\, e^{-j2\beta_m (d_m - u^{(i')}) r_{my}}\right)}{1 - {}_{\{\frac{1}{\mu}\}}\Gamma_{m,m-1}\, {}_{\{\frac{1}{\mu}\}}\Gamma_{m,m+1}\, e^{-j2\beta_m d_m r_{my}}} \qquad (18) $$

This is the generalized normalized T-factor with $u^{(i')} > u^{(i)}$ and where $q = m \pm 1$ depending on whether calculation of induced currents or transmitted field is involved. For $u^{(i)} > u^{(i')}$ again see the remarks at the end of this section.

The following sign changes must be made for the case $u^{(i)} > u^{(i')}$ as is shown in Appendix D in [23]

| change from | to |
|---|---|
| subscript + | subscript - |
| subscript - | subscript + |

Determination of $V^{s,i}$ and $V^{a,i}$ $i=1,2$

The form of $V^{s,i}(\ell)$ and $V^{a,i}(\ell)$ has been assumed previously (see Equation (12)) in order to calculate the patterns. The magnitude of $V^{s,i}(0)$ and $V^{a,i}(0)$ is now calculated. Denote the load admittances for the symmetric and asymmetric mode by $Y_L^{si}$ and $Y_L^{ai}$, respectively. Hence, from Kirchoff's current law (i.e., the sum of all currents entering a node must equal 0), the load admittance multiplied by the unknown voltage will equal the sum of induced currents.

$$ Y_L^{s1} V^{s,1}(0) = I^{s,in} + I^{s1s1} + I^{s1a1} + I^{s1s2} + I^{s1a2} \qquad (19) $$

$$ Y_L^{a1} V^{a,1}(0) = I^{a,in} + I^{a1s1} + I^{a1a1} + I^{a1s2} + I^{a1a2} \qquad (20) $$

$$ Y_L^{s2} V^{s,2}(0) = 0 + I^{s2a2} + I^{s2a2} + I^{s2s1} + I^{s2a1} \qquad (21) $$

$$Y_L^{a2} V^{a,2}(0) = 0 + I^{a2s2} + I^{a2a2} + I^{a2s1} + I^{a2a1} \tag{22}$$

Using the equations for admittances developed in the preceding section results in:

$$\begin{bmatrix} I^{s,in} \\ I^{a,in} \\ 0 \\ 0 \end{bmatrix} = [Y] \begin{bmatrix} V^{s,1} \\ V^{a,1} \\ V^{s,2} \\ V^{a,2} \end{bmatrix} \tag{23}$$

where [Y] is defined as the admittance matrix

$$[Y] \equiv \begin{bmatrix} Y^{s1s1}+Y_L^{s1} & Y^{s1a1} & Y^{s1s2} & Y^{s1a2} \\ Y^{a1s1} & Y^{a1a1}+Y_L^{a1} & Y^{a1s2} & Y^{a1a2} \\ Y^{s2s1} & Y^{s2a1} & Y^{s2s2}+Y_L^{s2} & Y^{s2a2} \\ Y^{a2s1} & Y^{a2a1} & Y^{a2s2} & Y^{a2a2}+Y_L^{a2} \end{bmatrix} \tag{24}$$

All symmetric and asymmetric voltages for each array can now be found. Since the transmitted H-field into the semi-infinite space, $y>d_4$, is desired, only the node voltages from the second array, $V^{s,2}(0)$ and $V^{a,2}(0)$, need be found. Using Cramer's rule with the determinant of the admittance matrix,

$$D \equiv |Y| \quad , \tag{25}$$

gives

$$V^{s,2}(0) = \frac{1}{D} \begin{vmatrix} Y^{s1s1}+Y_L^{s1} & Y^{s1a1} & I^{s,in} & Y^{s1a2} \\ Y^{a1s1} & Y^{a1a1}+Y_L^{a1} & I^{a,in} & Y^{a1a2} \\ Y^{s2s1} & Y^{s2a1} & 0 & Y^{s2a2} \\ Y^{a2s1} & Y^{a2a1} & 0 & Y^{a2a2}+Y_L^{a2} \end{vmatrix} \tag{26}$$

and

$$V^{a,2}(0) = \frac{1}{D}\begin{vmatrix} Y^{s1s1}+Y_L^{s1} & Y^{s1a1} & Y^{s1s2} & I^{s,in} \\ Y^{a1s1} & Y^{a1a1}+Y_L^{a1} & Y^{a1s2} & I^{a,in} \\ Y^{s2s1} & Y^{s2a1} & Y^{a2s2}+Y_L^{s2} & 0 \\ Y^{a2a1} & Y^{a2a1} & Y^{a2s2} & 0 \end{vmatrix} \qquad (27)$$

This completely determines the magnitudes $V^{s,2}(0)$ and $V^{a,2}(0)$ since all the quantities on the right side of Equations (26) and (27) have been previously determined.

Note that the physical implementation of the load impedance is not important and in fact are assumed to be zero in the computer program. They were included here in order to keep the theory as general as possible.

## C. The Transmitted Field

After having determined the two voltages $V^{s,2}(0)$ and $V^{a,2}(0)$ of the second array, the transmitted field into the semi-infinite space, $y>d_4$, can now be found. No radiation takes place from the first array because of the shielding effect of the second array so by a slight change in notation of Equation (43) in [24], the total transmitted H-field reradiated by $V^{s,2}(0)$ and $V^{a,2}(0)$ is

$$\bar{H}_5^{tot} = \frac{Y_5}{2D_x D_z} \sum_{k=-\infty}^{\infty} \sum_{n=-\infty}^{\infty} \frac{e^{-j\beta_5(\bar{R}-\hat{y}b_4)\cdot\hat{r}_5}\; e^{-j\beta_4(\hat{y}b_4-\bar{R}^{(2)})\cdot\hat{r}_4}}{r_{5y}}$$

$$\left[{}_{\perp}\hat{n}_5\left({}_{\perp}P_5^s V^{s,2}(0)+{}_{\perp}P_5^a V^{a,2}(0)\right){}_{\perp}T_{4/5}(0,0)\right.$$

$$\left. + {}_{\parallel}\hat{n}_5\left({}_{\parallel}P_5^s V^{s,2}(0)+{}_{\parallel}P_5^a V^{a,2}(0)\right){}_{\parallel}T_{4/5}(0,0)\right] \qquad (28)$$

where $Y_5$ is the characteristic admittance in the semi-space $y > b_5$ of Figure 1 and where all other quantities have been previously defined.

Since the total transmitted H-field is desired in the far-field, all evanescent modes have disappeared. So only the k=n=0 term is of importance provided no grating lobes exist. For most practical applications grating lobes are avoided as is the case for this report. They are avoided since a null usually occurs near the frequency at which the grating lobe appears.

From [25] or simply from conservation of energy, it is known that the cross polarized component of the transmitted field should be as small as possible in order to have unit transmission coefficient.

## SECTION III
## DEVELOPMENT OF DATA AND RESULTS

The introduction explained qualtatively the analysis of the structure of Figures 1 and 2. Quantitative values are to be obtained in order to calculate the transmitted field through the structure and hence the bandwidth. To do so, the following observations are useful. Refer to Figure 7 for additional insight.

Assume the incident field is in the YZ-plane ($\alpha$=90°). For an incident field orthogonal to the plane of incidence only the asymmetric mode will be excited ($I^{s,in}$=0). The analysis is reduced to that of an array of bent 'straight' slots shown in Figure 7f. For an incident field parallel to the plane of incidence only the symmetric mode will be excited ($I^{a,in}$=0). This results again in an array of bent 'straight' slots as shown in Figure 7d. Hence for at least the YZ scan plane the structure of Figure 1 is similar to that of the structure in [26]. It is therefore reasonable to use one of the data sets provided in [27] as a basis for the starting data in order to calculate transmission curves. As the leg angle L.A. is decreased from 180° to 120° the above starting data are not necessarily optimum.

From [28] it was demonstrated that a symmetric configuration for a monoplanar structure led to the largest bandwidth of transmission curves for orthogonal and parallel polarizations. Using this for the biplanar structure requires that:

$$d_2 = d_4$$

$$\varepsilon_2 = \varepsilon_4$$

$$\varepsilon_1 = \varepsilon_5$$

Data set P27 given in [29] is then used as the initial data for the structure of Figure 1. For development of the data to this point refer to that reference. Kornbau found that for an equilateral triangular grid ($\Delta z = D_z/2$) a leg angle L.A. of 120° yielded the best performance with respect to low cross polarization. Hence this case is assumed in the data. All initial parameters are now known and computer calculations of the transmission curves can now be produced. It should be noted that although the theory and computer program have been developed to allow for any interlace spacing, leg angle L.A., and dielectric constants, they remain fixed throughout. See Data (TS9) for values, Table 1.

Since a direct synthesis is not feasible at this time, a systematic computer solution approach to increase the bandwidth of the transmission curves was used. This approach is to change one variable and recalculate the curves and keep repeating the process. This is possible because the effect of each variable of the data set is qualitatively known. This allows for prudent choices concerning changes to be made to improve bandwidth.

The important variables that were changed as part of the iterative procedure to improve bandwidth were the slot dimensions, the interelement spacing, the interlace spacing and the width of the middle dielectric layer. The nature of the changes follows.

The length of each leg of the slot was increased in order to lower the resonance frequency. This increased the bandwidth by moving the lower frequency end down in frequency while the change in the upper end was slight. The interelement spacing and interlace spacing were reduced in order to move the upper frequency end up in frequency. The width of the middle dielectric layer determines the mutual coupling between the arrays. Since it was found by inspection of Reference [3] that an increase in the coupling was needed, the width was decreased. Note that these changes were repeated several times.

Each variable is not completely independent of all the other variables so practical limits do exist. As an example, suppose the interelement spacing is reduced while holding the leg length constant. Eventually, the individual slots in each array would overlap. Hence, the results would no longer be correct.

Figures 8 to 11 are the resulting transmission curves for data set TS9 using the voltage distribution given by Equations (11) and (12). Notice that the bandwidth is approaching an octave for both orthogonal and parallel polarizations* in each principle plane ($\alpha$=0 ,90°) for angles of incidence up to 75° from normal. The transmission curves are in fact very similar which is the desired result. The cross polarizations, transmitted polarizations orthogonal to polarizations of the incident field, have been calculated and are found to be -20 dB or less. The cross polarizations are indeed small as desired to provide for unity transmission.

After completion of the above transmission curves some developments occurred concerning similar slot elements. Measurements on a mono-planar slot array imbedded in an asymmetric dielectric configuration, A-sandwich, showed disagreement with calculated transmission curves for frequencies above the first resonance.** (Figures 12 and 13.)*** It should be noted that below that frequency, the curves agree.

---

* This is in reference to the H-field and plane of incidence.

** Resonance is the frequency at which the transmission curve has no loss, i.e., unity gain.

***Figures 12 and 13 were extracted from [30]. For further study see that reference.

Table 1

```
 1 DECIDE ON V DSTR FOR NT PATTERN =1(SINUSOIDAL),=2(COSINUSOIDAL)
 2 1
 3 IF SYMMETRIC CONFIGURATION SET NEXT LINE TO 1
 4 1
 5 DECIDE ON PRINTED OUTPUT
 6 1
 7 FREQL  =    1.0000       LOWEST FREQ USED IN CALCULATIONS IN GHZ
 8 FREQH  =   18.0000       HIGHEST FREQ USED IN GHZ
 9 FINCRM =    0.5000       FREQ INCREMENT IN GHZ
10 D1     =    0.0          DISTANCE FROM ORIGIN
11 D2     =    1.10         THICKNESS OF DIELECTRIC LAYERS IN CM
12 D3          0.50
13 D4     =    1.10
14 D5     -    0.0          DISTANCE TO OBSERVATION PT FROM MEDIA 4
15 READ NUMBER OF INCIDENT ANGLES DESIRED
16 10
17 ANGLES ALPHA,ETA OF INCIDENT FIELD IN DEGREES
18 0.0,1.0 0.0,30.0 0.0,60.0 0.0,70.0 0.0,75.0
19 90.0,1.0 90.0,30.0 90.0,60.0 90.0,70.0 90.0,75.0
20 ER1    =    1.0          RELATIVE PERMITTIVITY OF DIELECTRIC LAYERS
21 ER2    =    1.30
22 ER3    =    1.9
22 ER4    =    1.30
24 ER5    =    1.0
25 DX     =    0.75         INTERELEMENT SPACING X DIRECTION IN CM
26 DZ     =    0.867        INTERELEMENT SPACING Z DIRECTION IN CM
27 DELTZ  =    0.4335       INTERLACE SPACING Z DIRECTION IN CM
28 RL     =    0.75         LENGTH OF LEG OF SLOT IN CM
29 WIDTH  =    0.120        WIDTH OF SLOT XZ PLANE IN CM
30 THIK   =    0.0071       THICKNESS OF SLOT Y DIRECTION IN CM
31 ANGLE BETWEEN LEG 2 & LEG 3 OF ARRAY 1 IN DEGREES
32 120
33 ANGLE BETWEEN LET 2 & LEG 3 OF ARRAY 2 IN DEGREES
34 120
35 ------ END OF INPUT FILE ------
```

DATA SET: TS9: (change line two to a 2 to get DATA SET TS9A).

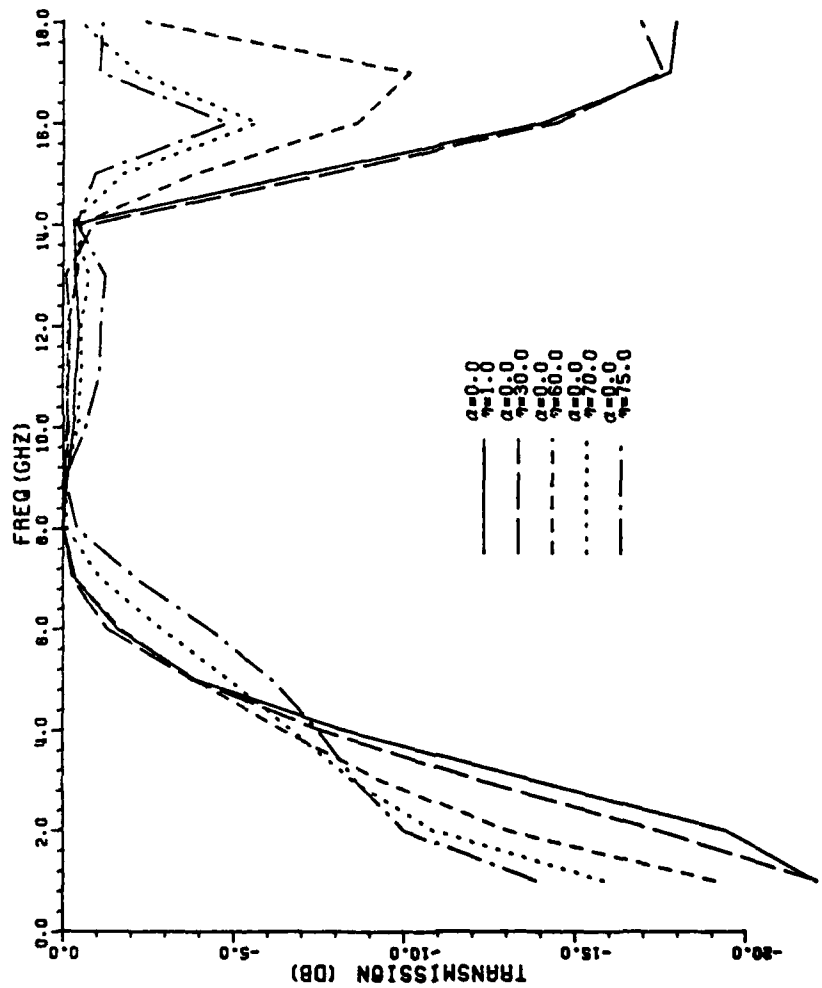


Figure 8. Transmission curves for orthogonal incident and orthogonal transmitted H-field with $\alpha=0°$ using the voltage distributions of Equations (11) and (12). (Data set TS9)

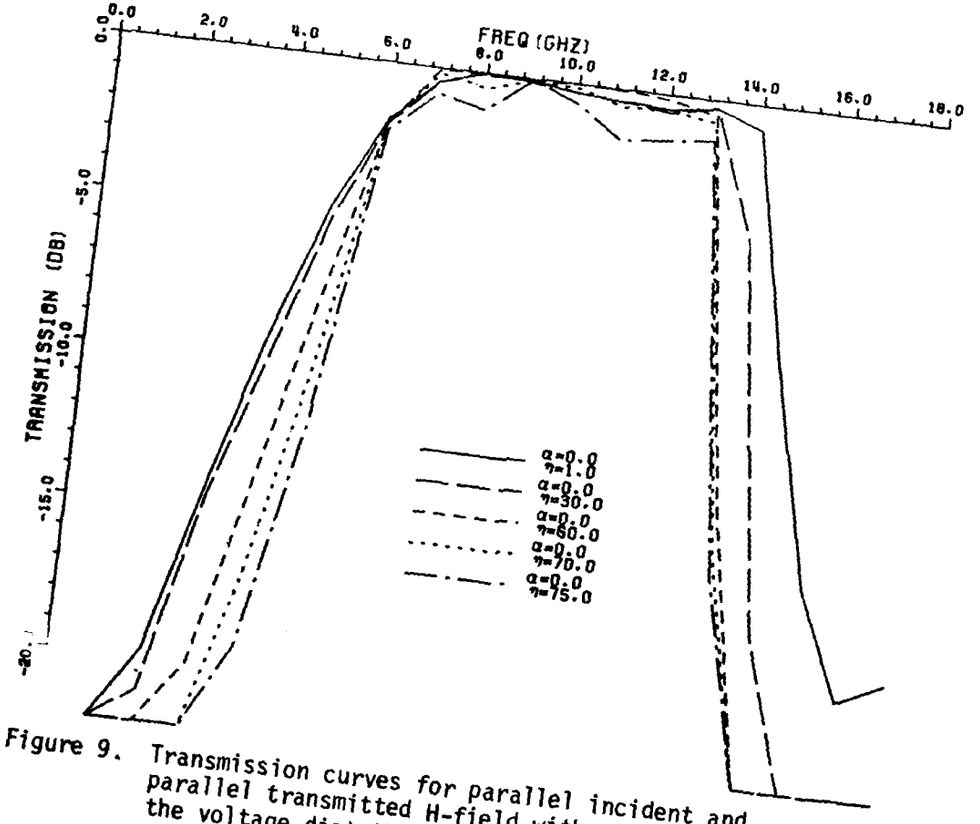


Figure 9. Transmission curves for parallel incident and parallel transmitted H-field with $\alpha=0°$ using the voltage distributions of Equations (11) and (12). (Data set TS9)

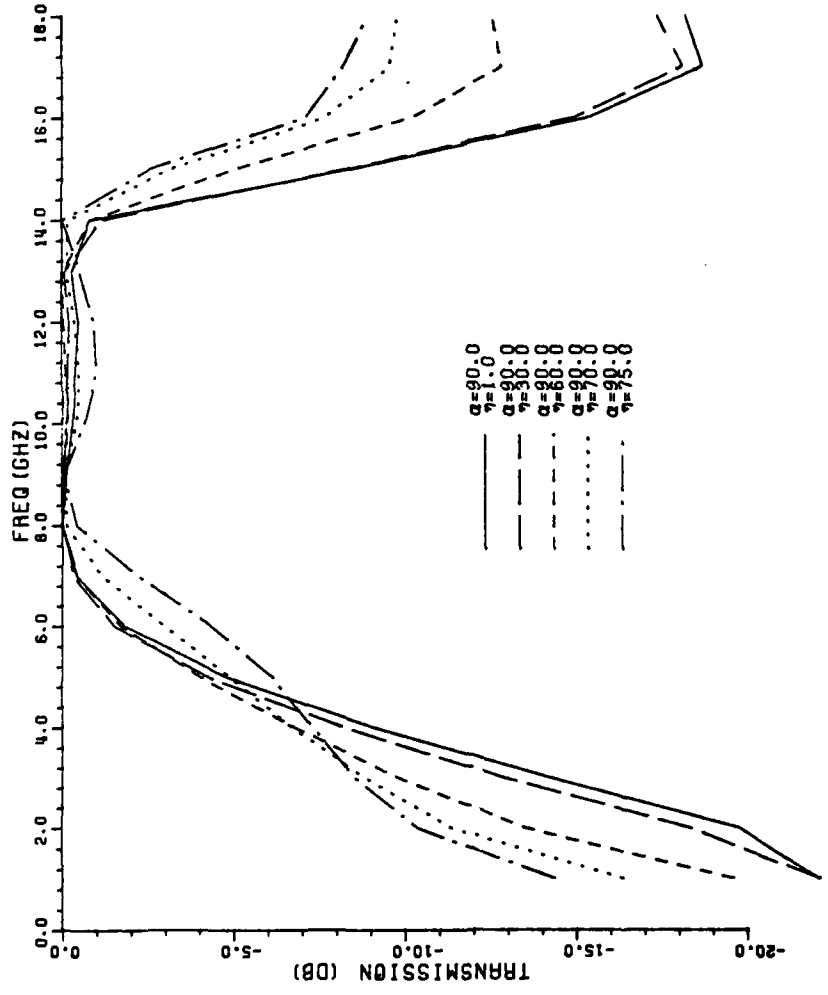


Figure 10. Transmission curves for orthogonal incident and orthogonal transmitted H-field with $\alpha$=90° using the voltage distributions of Equations (11) and (12). (Data set TS9)

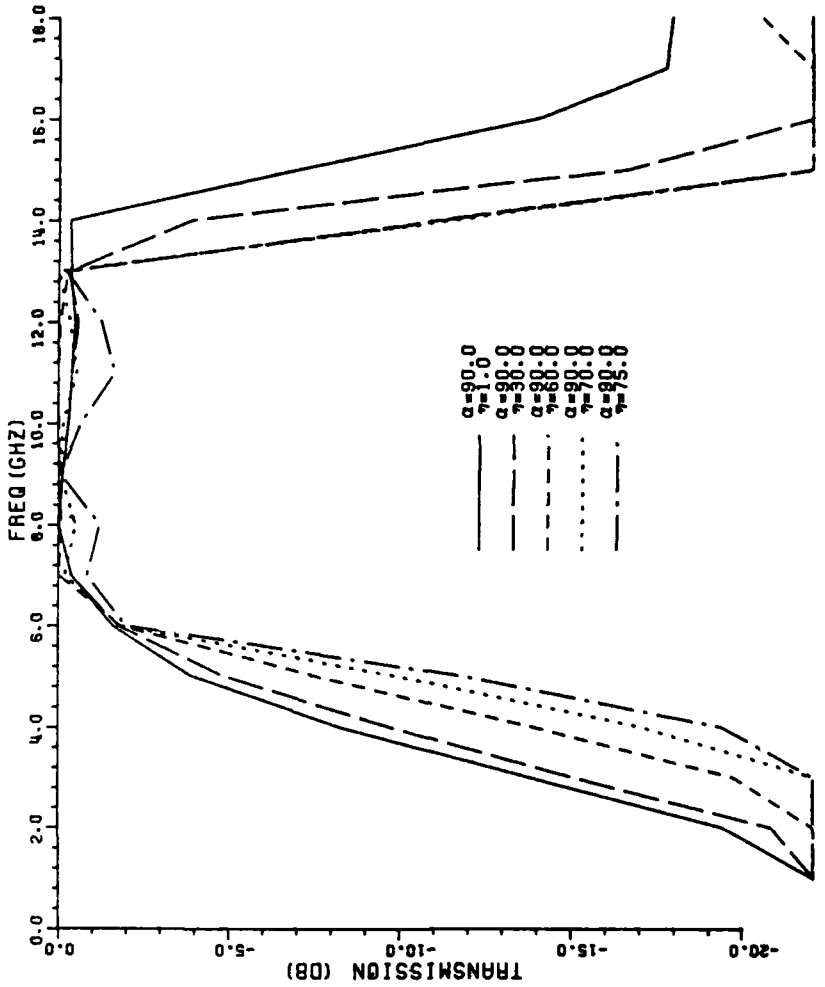


Figure 11. Transmission curves for parallel incident and parallel transmitted H-field with $\alpha$=90° using the voltage distributions of Equations (11) and (12). (Data set TS9)

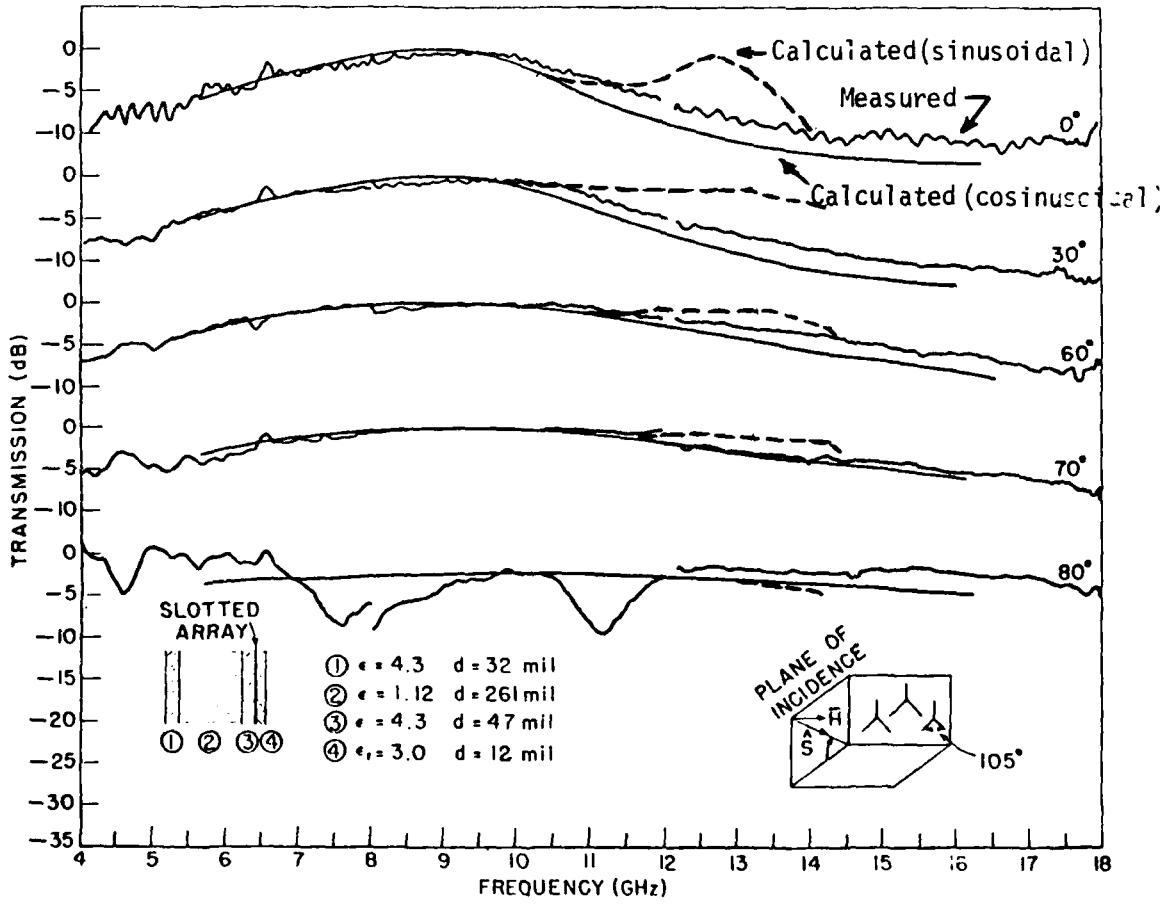


Figure 12. Comparison of calculated and measured transmission curves for orthogonal polarization for a mono-planar slot array using cosinusoidal voltage distribution of Equation (29) or the sinusoidal votage distribution of Equation (12).

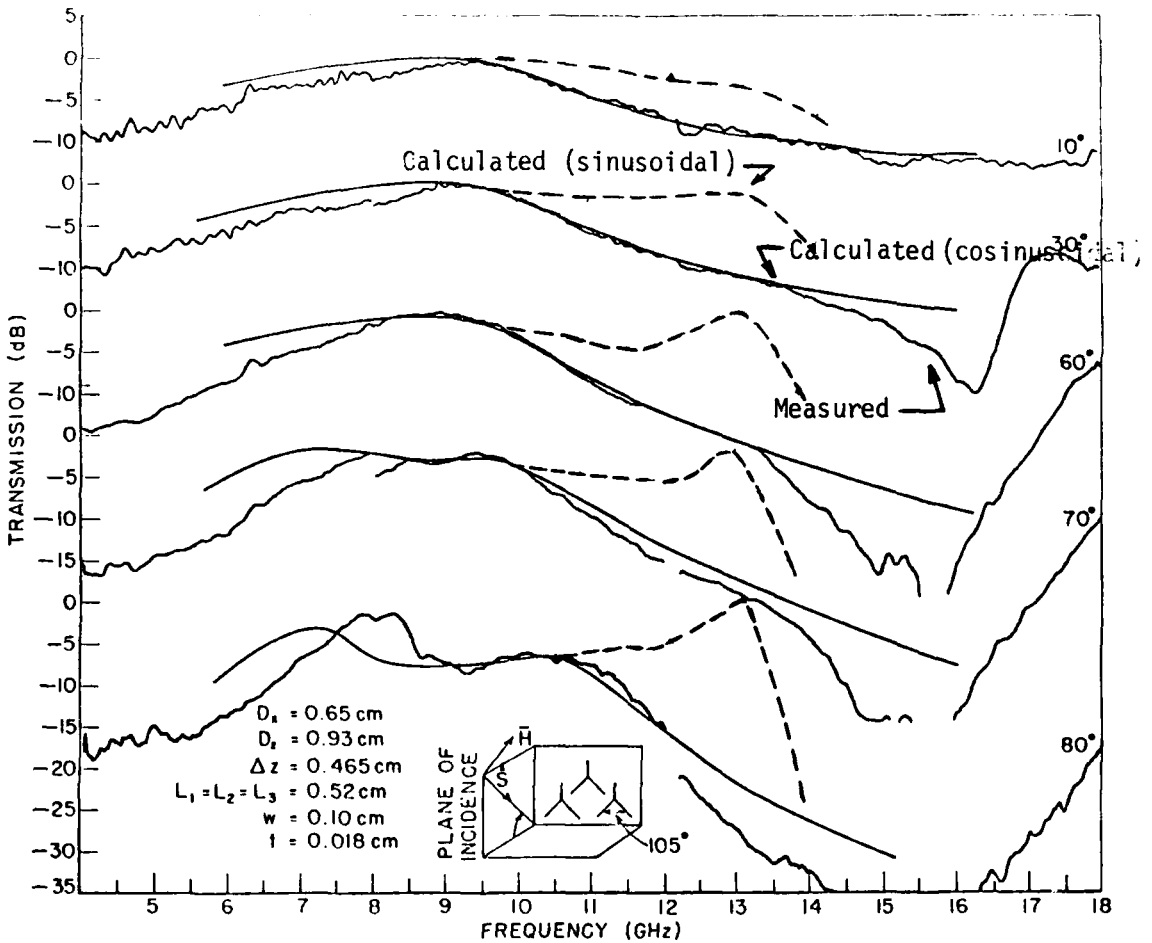


Figure 13. Comparison of calculated and measured transmission curves for parallel polarization for a mono-planar slot array using the voltage distributions of Figure 12.

The measured transmission curves did not contain a second resonance but continued to have greater loss as the frequency increased above resonance. For the structure of Figure 1 no measured results are available. However, the same agreement below resonance and the same general disagreement above resonance would occur.

To achieve closer agreement, a new voltage distribution along the slot elements when in the non-transmitting (scattering) mode is assumed. The new assumed distribution will more closely represent the actual voltage distribution. According to [31] the assumed voltage distribution for an unloaded receiving antenna is of a cosinusoidal form,

$$V^{vi}(\ell) = \frac{\cos\beta_d\ell - \cos\beta_d\ell_{ef}}{1-\cos\beta_d\ell_{ef}} \qquad (29)$$

instead of the assumed form given by Equation (12).

For frequencies below the first resonance the different forms are approximately the same. The transmitted curves below this frequency should be approximately the same. When using Equation (29) in a previously developed program for the mono-planar slot case, the resulting calculated curves agreed with the measured ones for all range of frequencies (Figures 12 and 13). This cosinusoidal equation was then incorporated into the computer program developed for the structure of this report as the voltage distribution for the non-transmitting mode. For the transmitting mode the voltage distribution is the same as before, sinusoidal. At this point, the transmission curves were recalculated. The same iterative procedure used before was not redone. The data previously developed was reused to calculate the new transmission curves. The following Figures 14 to 17 give the new computed transmission curves. It can be seen that the bandwidth is no longer as constant with different incident polarizations. The bandwidth in fact has been reduced. A slight gain also is observed. We have not been able to explain the reason for this gain although the transmission curves are expected to be more accurate than for the sinusoidal case above. It should be possible to slightly improve the bandwidth so that it is nearly constant for the varying angles of incidence and different polarizations. This could possibly be done by decreasing the interelement spacings and the interlace spacing. This would raise the upper frequency end of the transmission curves. Since the interelement spacings and interlace spacing are almost decreased to a point where the slots overlap, not much improvement is expected. However, this has not been attempted at this time.

A slight descrepancy has arisen when using Equation (29) as the voltage distribution of the slot elements in the receiving mode. For this passive structure, a small gain (~ 0.3 dB or less) has occurred for certain incident angles and certain polarizations. See Figure 16. This, of course, is physically impossible.

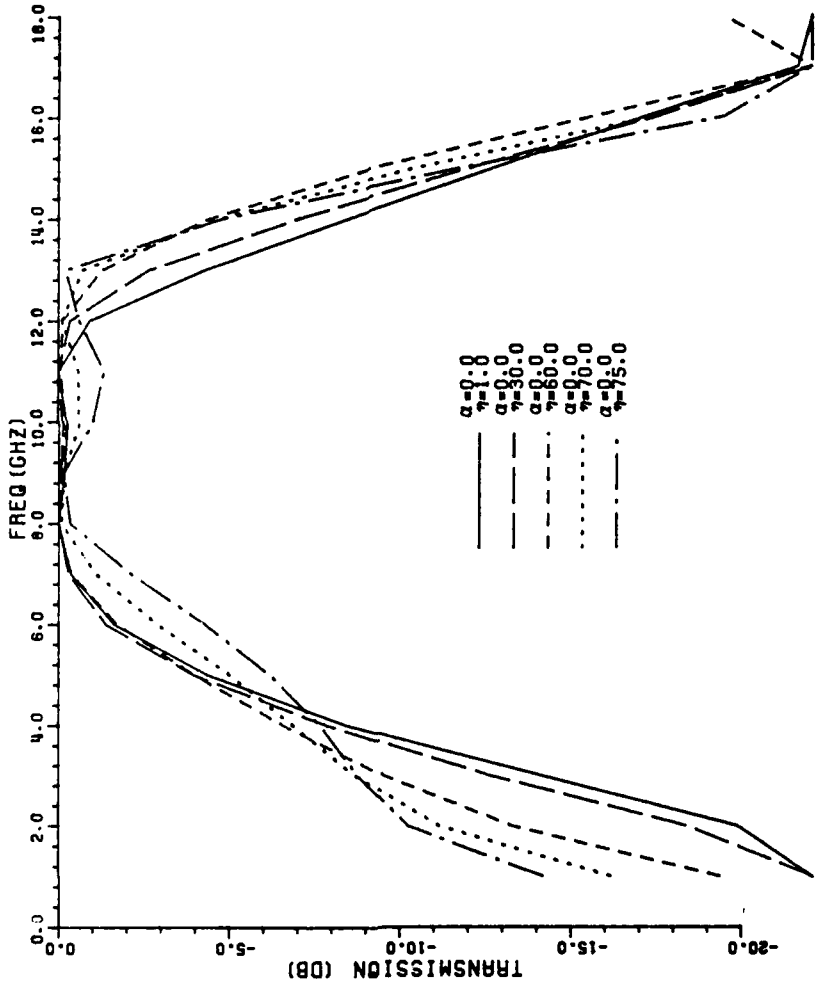


Figure 14. Transmission curves for orthogonal incident and orthogonal transmitted H-field with $\alpha=0°$ using the voltage distributions of Equations (11) and (29). (Data set TS9A)

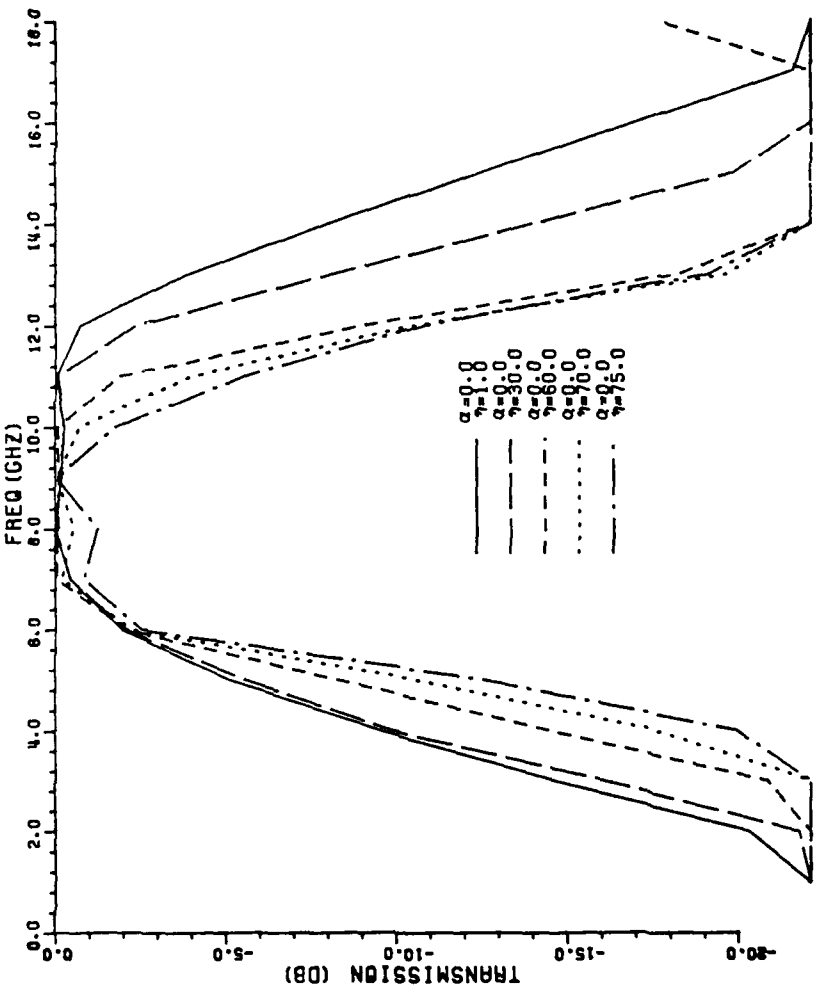


Figure 15. Transmission curves for parallel incident and parallel transmitted H-field with $\alpha=0°$ using the voltage distributions of Equations (11) and (29). (Data set TS9A)

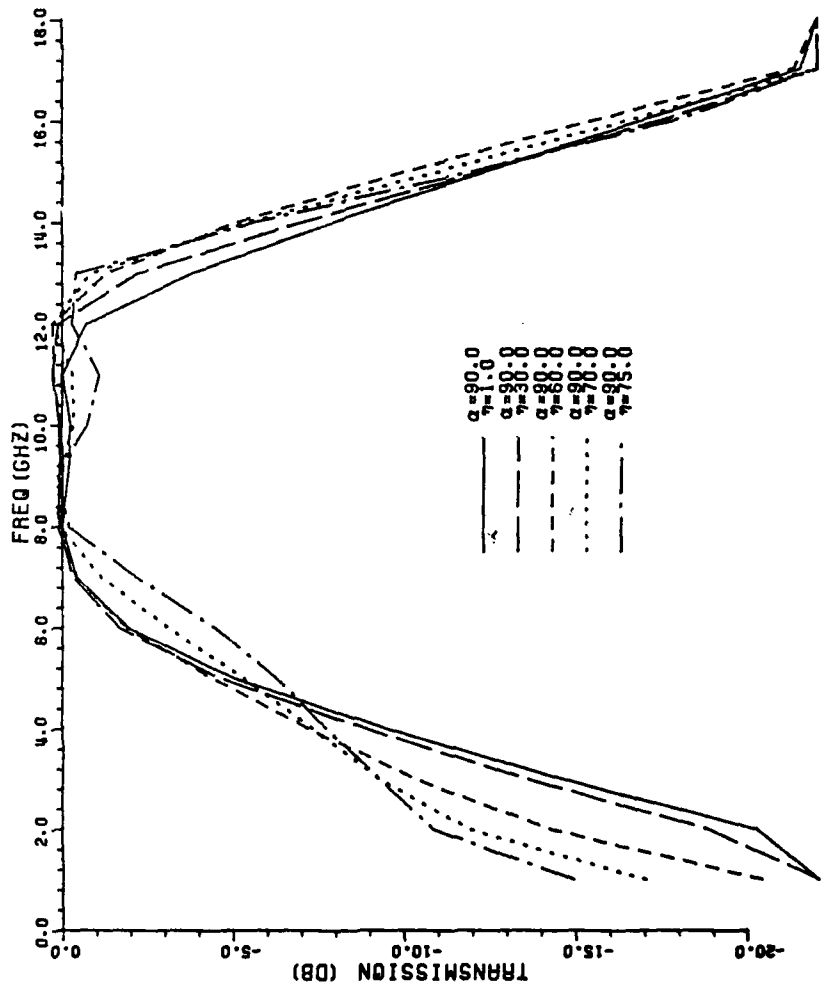


Figure 16. Transmission curves for orthogonal incident and orthogonal transmitted H-field with $\alpha=90°$ using the voltage distributions of Equations (11) and (29). (Data set TS9A)

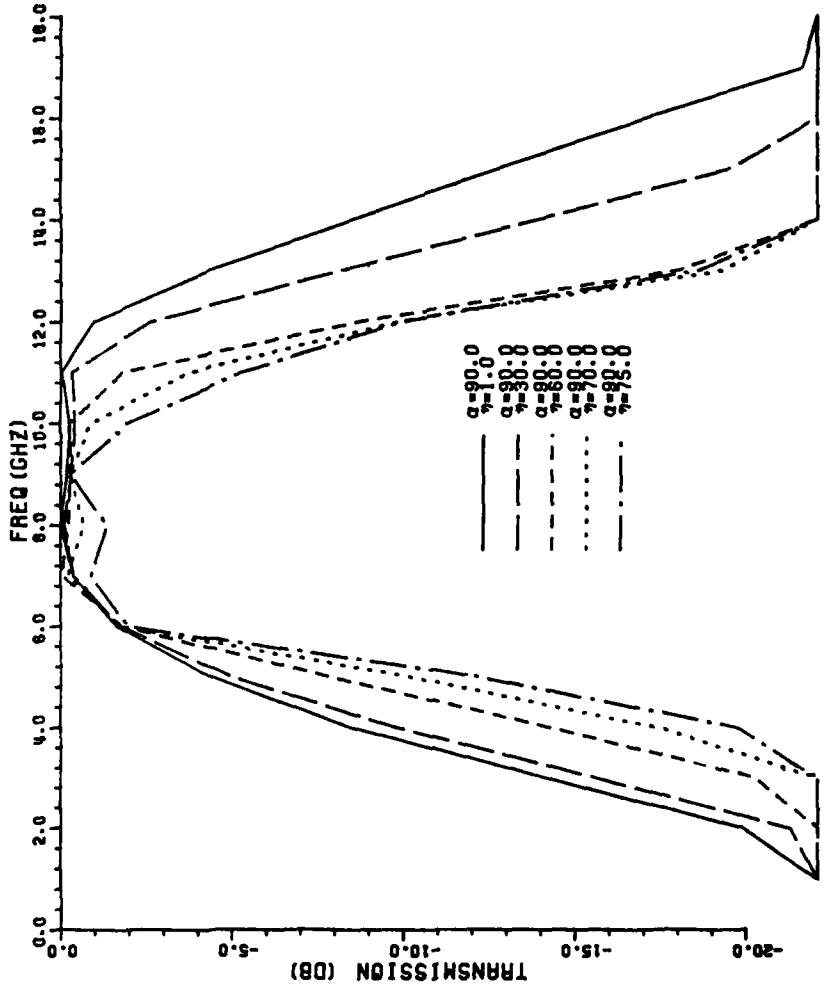


Figure 17. Transmission curves for parallel incident and parallel transmitted H-field with $\alpha$=90° using the voltage distributions of Equations (11) and (29). (Data set TS9A)

The source of this gain has not yet been located although attempts were made to resolve the problem. The computer program was re-examined with no apparent discrepancy between theory and program found. The method of performing the infinite sums through use of the convergence numbers was tested without any changes resulting in the gain.* Certain roundoff errors were considered but to no avail.

Next the slight gain was considered to be caused by the method of handling the end effects of the slots in the manner of an effective length. Ignoring the end effects by setting the effective length equal to the physical length of each leg, reduced the gain slightly (gain $\sim$0.25 dB or less).

Re-examing the voltage distribution being used shows that it was developed for infinitely thin slots. The cause of the gain was then thought to be caused by using slots of finite width. The width of the slots was then reduced by an arbitrarily chosen factor of 4. An effective length was reinstated. The gain was reduced ($\sim$0.15 dB or less). Again neglecting the end effects results in even less gain ($\sim$0.06 dB or less). Figures 18 to 23 show the critical portions of the transmission curves for each of the above cases. Although each step offered improvement through reduced gain, a gain still existed. Lack of time has limited further search for the cause of the gain. However, the effective length does not seem to be the cause since end effects cannot physically be ignored. If the slots were made even thinner the gain would most likely reduce. Since the effective length was small, the final transmission curves were calculated making use of it.

Note that the achieved bandwidth varies from approximately 2 GHz to 6 GHz depending on the angle of incidence and polarization. This is still the largest and most constant bandwidth to date. For angles of incidence from normal (1°) to 60° the bandwidth has a range of 6.5 GHz to 10 GHz.

Interlace Anomaly

Examining the transmission curves given in [32] for the biplanar straight slot case imbedded in three dielectrics results in the following observations. When the plane of incidence is the $\alpha$=0 plane ($\phi$-plane), with polarization orthogonal to the plane, zero transmission occurs at several frequencies. The 'zero' of interest is that one which limits the highest frequency that passes through the filter with little (-1 dB) attenuation. This 'zero' will limit the bandwidth in that plane.

The cause for this is that the structure anticipates the onset of a trapped grating lobe in the middle dielectric.** When this occurs the

---

*The convergence number was decreased from $10^{-3}$ to $10^{-5}$ to allow more terms in the summation to be used.

**Since the middle dielectric has a higher permittivity, the grating lobe will occur there at a lower frequency than in the other dielectric layers.

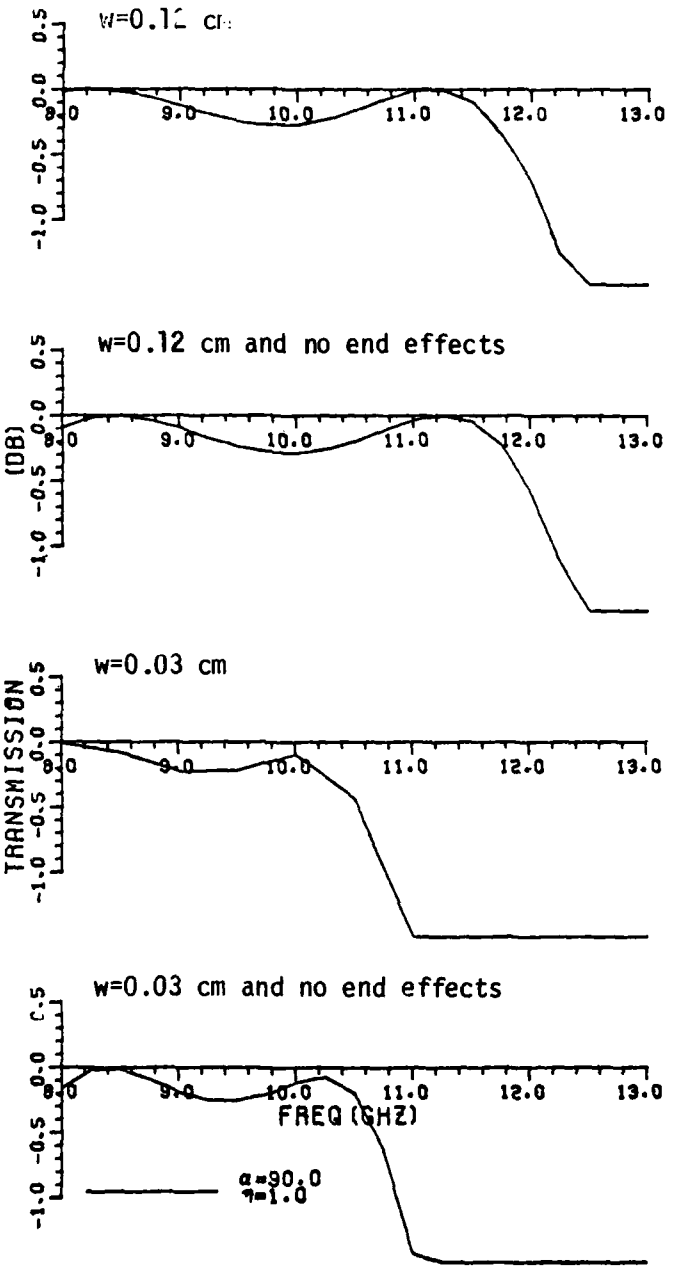


Figure 18. Transmission curves for orthogonal incident and orthogonal transmitted H-field for the various cases used in discussing the slight gain that occurs when using the voltage distributions of Equations (11) and (29). (Data set TS9A except where noted.)

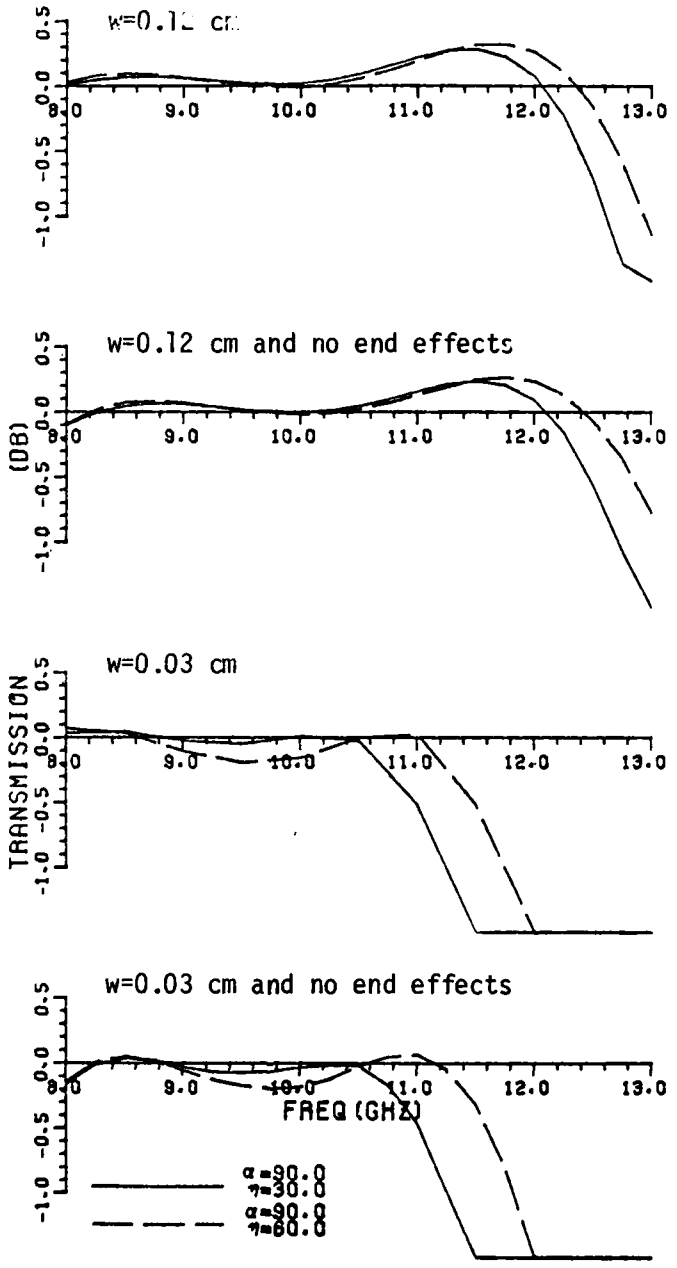


Figure 19. Transmission curves for orthogonal incident and orthogonal transmitted H-field for the various cases used in discussing the slight gain that occurs when using the voltage distributions of Equations (11) and (29). (Data set TS9A except where noted.)

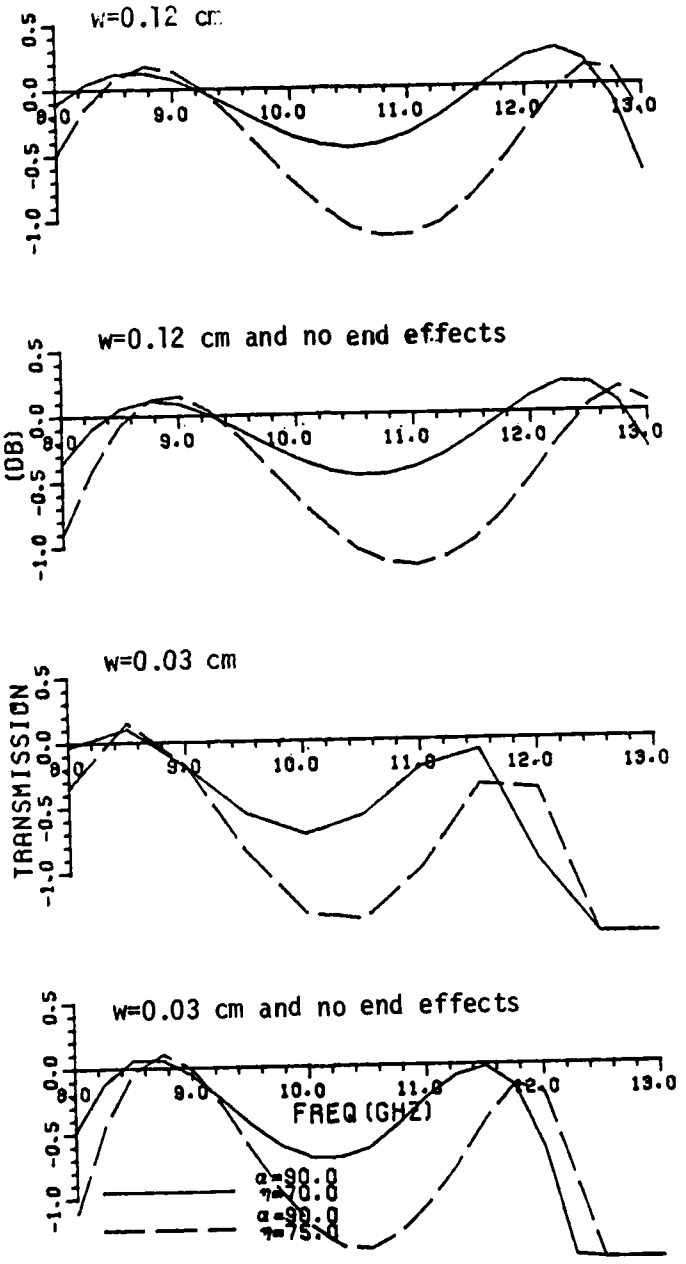


Figure 20. Transmission curves for orthogonal incident and orthogonal transmitted H-field for the various cases used in discussing the slight gain that occurs when using the voltage distributions of Equations (11) and (29). (Data set TS9A except where noted.)

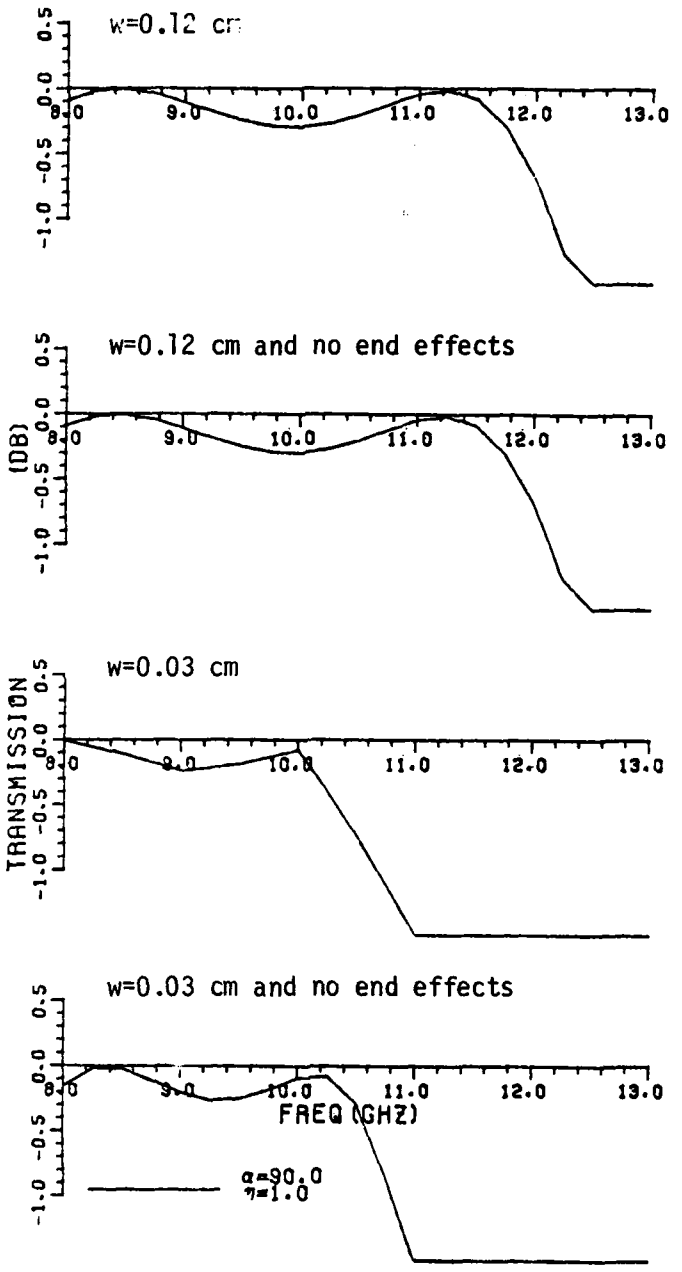


Figure 21. Transmission curves for parallel incident and parallel transmitted H-field for the various cases used in discussing the slight gain that occurs when using the voltage distributions of Equations (11) and (29). (Data set TS9A except where noted.)

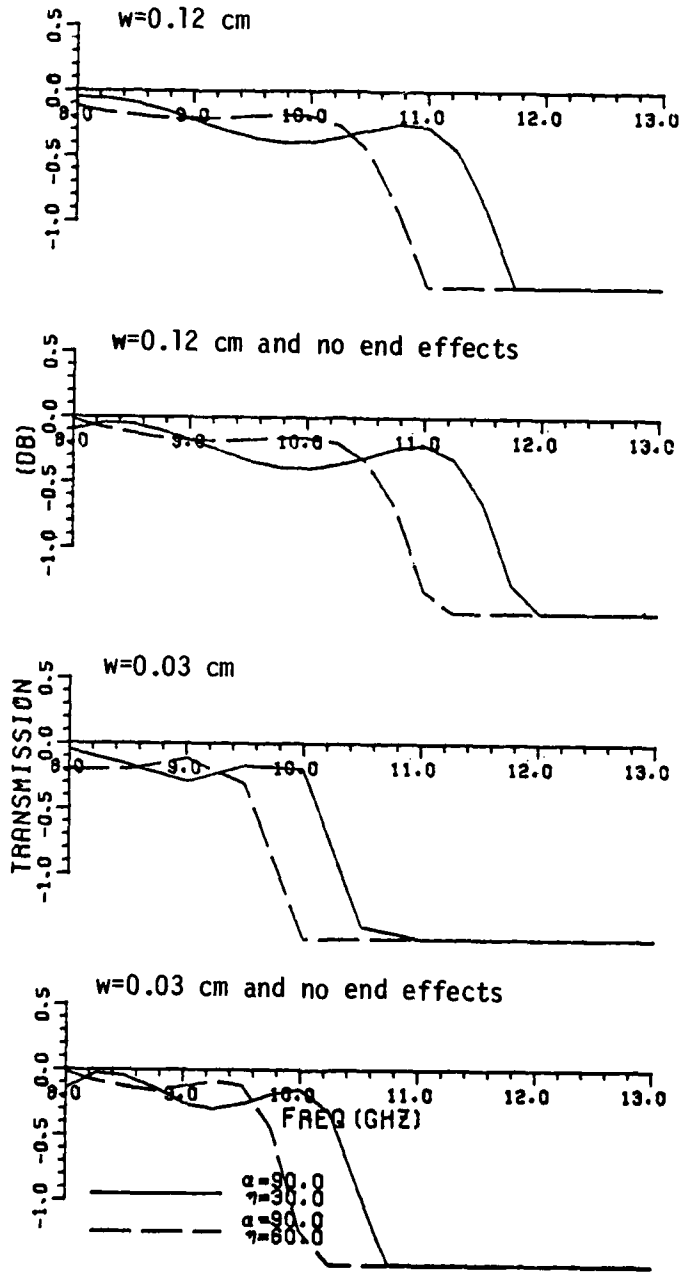


Figure 22. Transmission curves for parallel incident and parallel transmitted H-field for the various cases used in discussing the slight gain that occurs when using the voltage distributions of Equations (11) and (29). (Data set TS9A except where noted.)

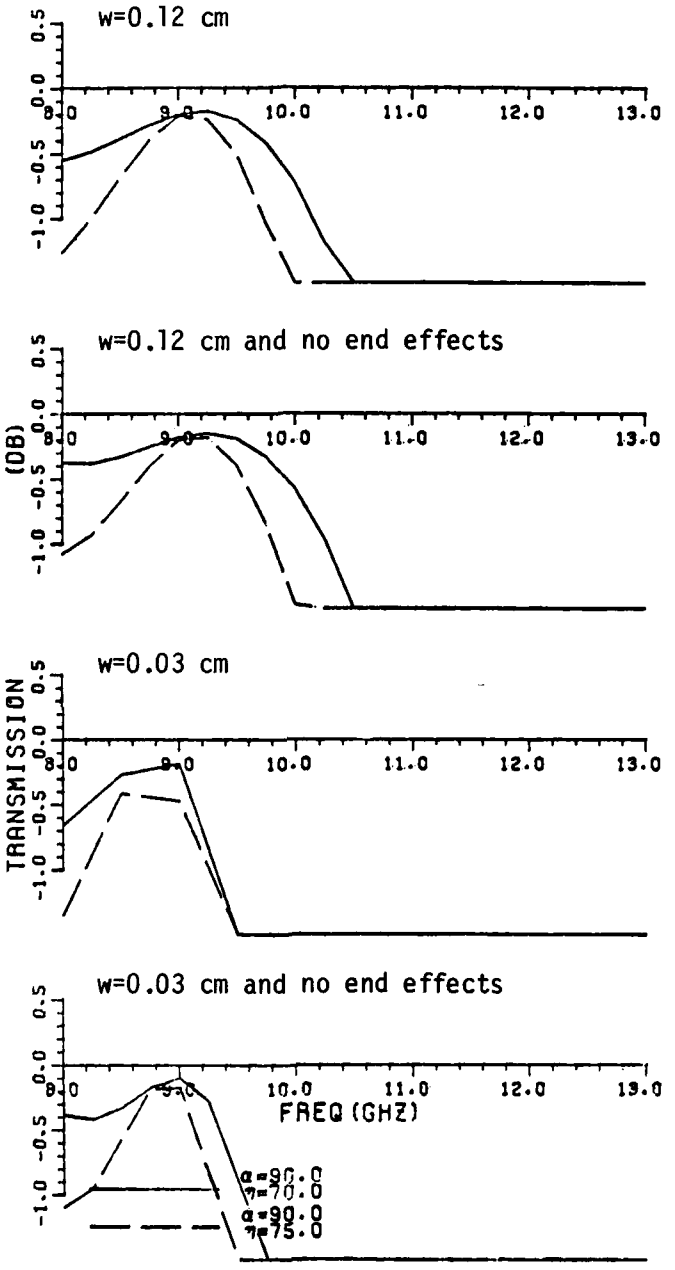


Figure 23. Transmission curves for parallel incident and parallel transmitted H-field for the various cases used in discussing the slight gain that occurs when using the voltage distributions of Equations (11) and (29). (Data set TS9A except where noted.)

evanescent waves begin to increase in strength and will destructively interfere with the principle wave at some frequency. This causes the mutual coupling between the straight slots to go to zero, hence zero transmission occurs. This is referred to as Luebbers anomaly [33].

In the $\alpha=90^{\circ}$ plane ($\theta$-plane), the pattern factor limits the interference between the evanescent waves and the principle wave, consequently a null in the transmission curve corresponding to Luebbers anomaly is not observed for orthogonal polarization. Luebbers anomaly does exist in this plane for parallel polarization.

Since the starting data for the structure of this report came out of the above straight slot case, Luebbers anomaly was expected, but not observed for the computed transmission curves. However, an anomaly (i.e., a null in the transmission curves) does exist for parallel polarization in both the $\alpha=0^{\circ}$ and $\alpha=90^{\circ}$ planes. Investigation of this anomaly is done as before in the $\alpha=90^{\circ}$ plane (see p. 19). It will be recalled that for parallel polarization only the symmetric mode is excited. (Figure 7d). For a null in the transmission curve (Figures 15 and 17) the symmetric mutual coupling, $Y^{s1s2}$ or $Y^{s2s1}$ must go to zero for that point to be an anomaly. Examining results of the computer program shows this to be the case. In the $\alpha=0^{\circ}$ plane both the symmetric and asymmetric modes are excited but none of the modal admittances $Y^{s1s2}$, $Y^{s2s1}$, $Y^{a1a2}$ or $Y^{a2a1}$ goes to zero. However, the anomaly still exists. Hence the "effective mutual" coupling between the arrays must go to zero.

Luebbers anomaly and the newly attained anomaly are of different polarizations. Luebbers exists in the $\alpha=0^{\circ}$ plane for orthogonal polarization and in the $\alpha=90^{\circ}$ plane for parallel polarization, while the new anomaly exists in both the $\alpha=0^{\circ}$ and $\alpha=90^{\circ}$ planes for parallel polarizations.

Through the computer results, it was found that as a direct result of interlacing the slots, Luebbers anomaly changed to the new anomaly. The type of element did not affect the anomalies. Hence the new anomaly is referred to as the interlace anomaly.

This interlace anomaly limits the bandwidth at the upper frequency ends. As was previously stated, the interlace spacing and interelement spacings were reduced to raise the upper frequency end. This moved the anomaly up in frequency.

# CHAPTER IV
# CONCLUSIONS

The transmission properties of a metallic radome configuration of two slot arrays consisting of three-legged elements imbedded in three dielectric layers has been investigated in order to design a bandpass filter with a large bandwidth. Only the symmetrical case consisting of two identical slot arrays with outer dielectric layers of the same material was considered.

A mathematical analysis was not attempted due to the complexity involved. A computer assisted design approach was used. The initial analysis used a sinusoidal voltage distribution. This was used in an iterative process to obtain as large a bandwidth as possible. Unfortunately, this was found, for a mono-planar configuration, to produce erroneous results at the upper portion of the frequency band. Thus, it became necessary to introduce a new cosinusoidal voltage distribution for unloaded three-legged slots in the non-transmitting (scattering) mode. This should improve the accuracy of the transmission curves above resonance. The transmission curves for the design were calculated. The bandwidth was then found to be somewhat smaller than the bandwidth calculated when using the sinusoidal voltage distribution. The bandwidth was also found to vary some with different angles of incidence and different polarization. For angles of incidence from normal ($1^{\circ}$) to $60^{\circ}$ the bandwidth has a range of 6.5 GHz to 10 GHz. Note that the iterations were not repeated when the cosinusoidal voltage mode was introduced. The data developed to that point was reused. It is, therefore, possible that slight improvements could be made to increase and stabilize the bandwidth. The final design still results in the largest and most constant bandwidth to date.

## APPENDIX A
## LIST OF ADMITTANCES FOR GIVEN STRUCTURE

In the main text, the admittances were defined and the general form was given. This appendix lists the admittances explicitly.

$$y^{slsl} \equiv -\frac{I^{slsl}}{V^{sl}(0)} = \frac{Y_2}{2D_xD_z} \sum_{k=-\infty}^{\infty} \sum_{n=-\infty}^{\infty} \frac{e^{-j\beta_2 \frac{w}{4} r_{2y}}}{r_{2y}}$$

$$[{}_{\perp}P_2^{sl\,t}\,{}_{\perp}P_2^{sl}\,{}_{\perp}T_2(0,d_2) + {}_{\parallel}P_2^{sl\,t}\,{}_{\parallel}P_2^{sl}\,{}_{\parallel}T_2(0,d_2)]$$

$$+ \frac{Y_3}{2D_xD_z} \sum_{k=-\infty}^{\infty} \sum_{n=-\infty}^{\infty} \frac{e^{-j\beta_3 \frac{w}{4} r_{3y}}}{r_{3y}}$$

$$[{}_{\perp}P_3^{sl\,t}\,{}_{\perp}P_3^{sl}\,{}_{\perp}T_3(0,d_3) + {}_{\parallel}P_3^{sl\,t}\,{}_{\parallel}P_3^{sl}\,{}_{\parallel}T_3(0,d_3)] \qquad \text{(A1)}$$

$$Y^{slal} \equiv -\frac{I^{slal}}{V^{al}(0)} = \frac{Y_2}{2D_xD_z} \sum_{k=-\infty}^{\infty} \sum_{n=-\infty}^{\infty} \frac{e^{-j\beta_2 \frac{w}{4} r_{2y}}}{r_{2y}}$$

$$[{}_{\perp}P_2^{sl\,t}\,{}_{\perp}P_2^{al}\,{}_{\perp}T_2(0,d_2) + {}_{\parallel}P_2^{sl\,t}\,{}_{\parallel}P_2^{al}\,{}_{\parallel}T_2(0,d_2)]$$

$$+ \frac{Y_3}{2D_xD_z} \sum_{k=-\infty}^{\infty} \sum_{n=-\infty}^{\infty} \frac{e^{-j\beta_3 \frac{w}{4} r_{3y}}}{r_{3y}}$$

$$[{}_{\perp}P_3^{sl\,t}\,{}_{\perp}P_3^{al}\,{}_{\perp}T_3(0,d_3) + {}_{\parallel}P_3^{sl\,t}\,{}_{\parallel}P_3^{al}\,{}_{\parallel}T_3(0,d_3)] \qquad \text{(A2)}$$

$$Y^{s1s2} \equiv -\frac{I^{s1s2}}{V^{s2}(0)} = \frac{Y_3}{2D_xD_z} \sum_{k=-\infty}^{\infty} \sum_{n=-\infty}^{\infty} \frac{e^{-j\beta_3 d_3 r_{3y}}}{r_{3y}}$$

$$[{}_{\perp}P_3^{s1t}\,{}_{\perp}P_3^{s2}\,{}_{\perp}T_3(0,0) + {}_{\parallel}P_3^{s1t}\,{}_{\parallel}P_3^{s2}\,{}_{\parallel}T_3(0,0)] \qquad \text{(A3)}$$

$$Y^{s1a2} \equiv -\frac{I^{s1a2}}{V^{a2}(0)} = \frac{Y_3}{2D_xD_z} \sum_{k=-\infty}^{\infty} \sum_{n=-\infty}^{\infty} \frac{e^{-j\beta_3 d_3 r_{3y}}}{r_{3y}}$$

$$[{}_{\perp}P_3^{s1t}\,{}_{\perp}P_3^{a2}\,{}_{\perp}T_3(0,0) + {}_{\parallel}P_3^{s1t}\,{}_{\parallel}P_3^{a2}\,{}_{\parallel}T_3(0,0)] \qquad \text{(a4)}$$

To define the remaining admittances,

| change from | to |
|---|---|
| superscript s | superscript a |
| superscript a | superscript s |

which results in four more admittances.

Then

| change from | to |
|---|---|
| superscript 1 | superscript 2 |
| superscript 2 | superscript 1 |
| subscript 2 | subscript 4 |
| ${}_{\{\perp}^{\parallel\}}T_3(0,d_3)$ | ${}_{\{\perp}^{\parallel\}}T_3(d_3,0)$ |

which again results in four more admittances.

The last four admittances are found by repeating the first set of changes. All admittances for the structure of Figure 1 are now specified.

## APPENDIX B
## T-FACTOR FOR THE STRUCTURE OF FIGURE 1

Note again that a slot can be considered as a magnetic element in front of an electrically perfectly-conducting ground plane. The reflection coefficient for the H-field from a ground plane is one. When calculating self admittances, the remaining arrays are short circuited causing them to become simply ground planes. Therefore, for either self or mutual admittance calculations the reflection coefficient at each slot array becomes one. For the structure of Figure 1, the reflection coefficients, ${}_{\{\frac{1}{11}\}}\Gamma_{23}$, ${}_{\{\frac{1}{11}\}}\Gamma_{32}$, ${}_{\{\frac{1}{11}\}}\Gamma_{34}$ and ${}_{\{\frac{1}{11}\}}\Gamma_{43}$ are equal to one.

For the self admittance calculations the reference point of the single test element is considered to be one quarter the slot width away from the reference point of the array by definition. However, the T-factor is calculated assuming the reference element and the array coincide. This discrepancy is negligible.

For mutual admittance calculations the reference element coincides with one of the arrays.

Using the above observations in the generalized non-normalized T-factor (Equation (17)) results in the following for the given structure for self admittance calculations;

$$ {}_{\{\frac{1}{11}\}}T_2(0,d_2) = 2.0 \left( \frac{1 + {}_{\{\frac{1}{11}\}}\Gamma_{2,1}\, e^{-j2\beta_2 d_2 r_{2y}}}{1 - {}_{\{\frac{1}{11}\}}\Gamma_{2,1}\, e^{-j2\beta_2 d_2 r_{2y}}} \right) \tag{B1} $$

$$ {}_{\{\frac{1}{11}\}}T_3(0,d_3) = 2.0 \left( \frac{1 + e^{-j2\beta_3 d_3 r_{3y}}}{1 - e^{-j2\beta_3 d_3 r_{3y}}} \right) \tag{B2} $$

$$ {}_{\{\frac{1}{11}\}}T_3(d_3,0) = {}_{\{\frac{1}{11}\}}T_3(0,d_3) \tag{B3} $$

$$ {}_{\{\substack{\perp \\ \parallel}\}}T_4(0,d_4) = 2.0 \times \left( \frac{1 + {}_{\{\substack{\perp \\ \parallel}\}}\Gamma_{4,5}\, e^{-j2\beta_4 d_4 r_{4y}}}{1 - {}_{\{\substack{\perp \\ \parallel}\}}\Gamma_{4,5}\, e^{-j2\beta_4 d_4 r_{4y}}} \right) \tag{B4} $$

and for mutual admittance calculations

$$ {}_{\{\substack{\perp \\ \parallel}\}}T_3(0,0) = 4/\left(1 - e^{-j2\beta_3 d_3 r_{3y}}\right) \tag{B5} $$

This provides all necessary T-factors for admittance calculations.

The normalized T-factors needed for the structure of Figure 1 are:

$$ {}_{\{\substack{\perp \\ \parallel}\}}T(0,0)_{2/1} = 2 \left( \frac{1 - {}_{\{\substack{\perp \\ \parallel}\}}\Gamma_{2,1}}{1 - {}_{\{\substack{\perp \\ \parallel}\}}\Gamma_{2,1}\, e^{-j2\beta_2 d_2 r_{2y}}} \right) \tag{B6} $$

and for transmitted H-field calculations

$$ {}_{\{\substack{\perp \\ \parallel}\}}T(0,0)_{4/5} = 2 \left( \frac{1 - {}_{\{\substack{\perp \\ \parallel}\}}\Gamma_{4,5}}{1 - {}_{\{\substack{\perp \\ \parallel}\}}\Gamma_{4,5}\, e^{-j2\beta_4 d_4 r_{4y}}} \right) \tag{B7} $$

All T-factors have now been determined.

## APPENDIX C
## THE PLANE OF INCIDENCE AND THE PLANES OF SCATTERING

The following formulas were taken from Appendix B in [34] and are generalized and included here for completeness.

The plane of scattering is defined as the plane containing the vector normal to the dielectric interface, $\hat{n}_o$, and the direction of propagation, $\hat{r}_m$, where m refers to the dielectric media.

For unit vectors, ${}_{\perp}\hat{n}_m$, orthogonal to the plane of incidence

$$ {}_{\perp}\hat{n}_m = \frac{\hat{n}_o x \hat{r}_m}{|\hat{n}_o x \hat{r}_m|} = \frac{-\hat{x}r_{mz}+\hat{z}r_{mx}}{(r_{mx}^2+r_{mz}^2)^{1/2}} \qquad (C1) $$

For unit vectors parallel, ${}_{\parallel}\hat{n}_m$, to the plane of scattering and orthogonal to the direction of propagation, $\hat{r}_m$.

$$ {}_{\parallel}\hat{n}_m = {}_{\perp}\hat{n}_m x \hat{r}_m = \frac{1}{(r_{mx}^2+r_{mz}^2)^{1/2}} (-\hat{x}r_{mx}r_{my}+\hat{y}(r_{mx}^2+r_{mz}^2) - \hat{z}r_{my}r_{mz}) \qquad (C2) $$

The plane of incidence is defined as the plane containing the vector $n_o$ normal to the dielectric interface and the direction of propagation $\hat{s}_m$ ($=\hat{r}_m$ for k=n=0), cf. Figure D1.

## APPENDIX D
## REFLECTION COEFFICIENTS FOR THE H-FIELD

The following formulas are found in Appendix C in [35] and are listed here for completeness. The formulas correspond to the following generalized figure.

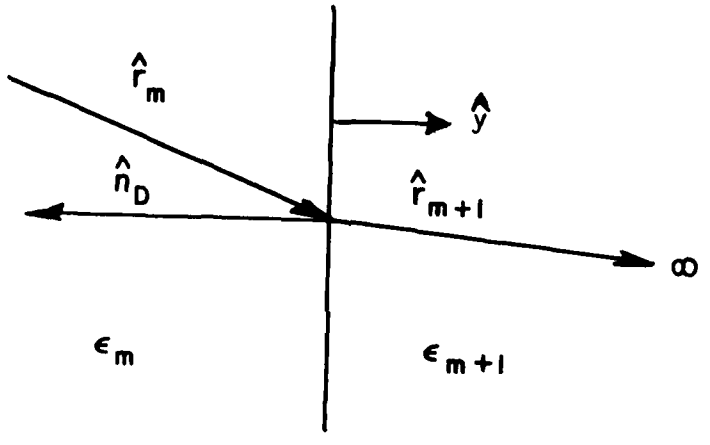


Figure D1. Incident wave on a dielectric boundary.

$$\perp\Gamma_{m,m+1} = \frac{\sqrt{\epsilon_{(m+1)}}r_{my} - \sqrt{\epsilon_m}r_{(m+1)y}}{\sqrt{\epsilon_{(m+1)}}r_{my} + \sqrt{\epsilon_m}r_{(m+1)y}} \tag{D1}$$

$$\parallel\Gamma_{m,m+1} = \frac{\sqrt{\epsilon_{(m+1)}}r_{(m+1)y} - \sqrt{\epsilon_m}r_{my}}{\sqrt{\epsilon_{(m+1)}}r_{(m+1)y} + \sqrt{\epsilon_m}r_{my}} \tag{D2}$$

$$\frac{1+\perp\Gamma_{m,m+1}}{1-\perp\Gamma_{m,m+1}} = \frac{\sqrt{\epsilon_{(m+1)}}r_{my}}{\sqrt{\epsilon_m}r_{(m+1)y}} \tag{D3}$$

$$\frac{1+{}_{\parallel}\Gamma_{m,m+1}}{1-{}_{\parallel}\Gamma_{m,m+1}} = \frac{\sqrt{\epsilon_{(m+1)}}\, r_{(m+1)y}}{\sqrt{\epsilon_m}\, r_{(m+1)y}} \tag{D4}$$

$${}_{\{\frac{1}{\parallel}\}}\Gamma_{m,m+1} = - {}_{\{\frac{1}{\parallel}\}}\Gamma_{m+1,m} \tag{D5}$$

## APPENDIX E
## MUTUAL ADMITTANCE ($Y^{as}$ AND $Y^{sa}$) BETWEEN SYMMETRIC AND ASYMMETRIC MODES

In this appendix we assume that the voltage distribution on the slots is of the same form for both the transmitting and non-transmitting modes, namely sinusoidal. The admittance relationship presented also holds for the cosinusoidal voltage distribution around resonance where the two voltage distributions are approximately equal. Any interlace spacing is allowed, i.e., the relationships hold for straight or interlaced array grids.

The relationships that follow are developed so that easy comparison of computer program results can be made between $Y^{sa}$ and $Y^{as}$. Separating $Y^{sa}$ into real and imaginary parts due to real and imaginary space* yields

$$Y^{sa} = (\mathrm{Re}Y^{sa}+\mathrm{Im}Y^{sa})_{\substack{\text{real}\\\text{space}}} + (\mathrm{Re}Y^{sa}+\mathrm{Im}Y^{sa})_{\substack{\text{imaginary}\\\text{space}}} . \qquad (E1)$$

Similarily

$$Y^{as} = (\mathrm{Re}Y^{as}+\mathrm{Im}Y^{as})_{\substack{\text{real}\\\text{space}}} + (\mathrm{Re}Y^{as}+\mathrm{Im}Y^{as})_{\substack{\text{imaginary}\\\text{space}}} . \qquad (E2)$$

Equating the components to each along with extensive use of Equations (B6), (B7) and (B8) in [36] it was found that

$$\mathrm{Re}Y^{sa}_{\substack{\text{imaginary}\\\text{space}}} = -\,\mathrm{Re}Y^{as}_{\substack{\text{imaginary}\\\text{space}}} \qquad (E3)$$

$$\mathrm{Im}Y^{sa}_{\substack{\text{imaginary}\\\text{space}}} = +\,\mathrm{Im}Y^{sa}_{\substack{\text{imaginary}\\\text{space}}} \qquad (E4)$$

---

*Real space pertains to propagating mode, i.e., k=n=0 for no grating lobes. Imaginary space pertains to evanescent modes, i.e., k and/or n≠0 for no grating lobes.

for a three-legged element, provided that the T-factor is real for imaginary space. This holds if the effective reflection coefficient is real, namely if

1) no grating lobes exist, anywhere, or

2) no dielectric exists (i.e., free space).

An additional case occurs if the reflection coefficient is complex but multiplied by a negligible number, effectively making the T-factor real. This is the case if

1) the electrical thickness $\beta_{m_y} d_{r_{my}}$, of the dielectric slabs is sufficient to insure that the exponentials in the T-factor be negligible.

Equations (E3) and (E4) correspond to Equation (B18) in [37].

For the three-legged elements

$$\hat{p}^{(1)} = \hat{z} \tag{E5}$$

$$\hat{p}^{(2)} = \hat{x}\, p_x^{(2)} + \hat{z}\, p_z^{(2)} \tag{E6}$$

$$\hat{p}^{(3)} = -\hat{x}\, p_x^{(2)} + \hat{z}\, p_z^{(2)} \tag{E7}$$

the relationship between $Y^{sa}$ and $Y^{as}$ in real space is

$$(Y^{sa})_{\substack{\text{real}\\\text{space}}} = -(Y^{as})_{\substack{\text{real}\\\text{space}}} \quad * \tag{E8}$$

or

*Note Equation (E8) and Equation (B16) in [38] have differently defined quantities. Hence they do not contradict.

$$(\mathrm{Re}Y^{sa})_{\substack{\text{real}\\\text{space}}} + (\mathrm{Im}Y^{sa})_{\substack{\text{real}\\\text{space}}} = -(\mathrm{Re}Y^{as})_{\substack{\text{real}\\\text{space}}} - (\mathrm{Im}Y^{as})_{\substack{\text{real}\\\text{space}}} . \quad (E9)$$

For the above relationship to be true it was found that for the symmetric pattern factor, $P^s$, the $\hat{x}$ and $\hat{z}$ components had to be pure imaginary and pure real, respectively, and for the assymmetric pattern factor, $P^a$, the $\hat{x}$ and $\hat{z}$ components had to be pure imaginary and pure real respectively. This must also hold for the transmitting pattern factors. For the given three-legged elements this is indeed true only when the incident field is in the principle planes ($\alpha$=0°,90°).

## APPENDIX F
## PATTERN FACTORS IN THE YZ-PLANE FOR INTERLACE STRUCTURE

This appendix assumes that the voltage distribution on the slots is of the same form for both transmitting and non-transmitting modes. Certain properties of the composite pattern factors, $\{\frac{1}{\|}\}^{pst}$, $\{\frac{1}{\|}\}^{pat}$, $\{\frac{1}{\|}\}^{ps}$ and $\{\frac{1}{\|}\}^{pa}$, will be established for interlacing in the z direction only ($\Delta x=0$). The properties of the composite pattern factors for the non-interlace structure are a special case of those for the interlace structure treated here, (see Appendix D in [39].

When the plane of incidence is the YZ-Plane, $s_{mx}=0$

$$\hat{r}_m = \hat{x}\left(k - \frac{n\Delta z}{D_z}\right)\frac{\lambda_m}{D_x} + \hat{y}\, r_{my} + \hat{z}\left(s_{mz} + \frac{n\lambda_m}{D_z}\right) \tag{F1}$$

where subscript m refers to the media.

Using a three-legged element that is symmetric with respect to the YZ-Plane, results in

$$\hat{p}^{(1)} = \hat{z} \tag{F2}$$

$$\hat{p}^{(2)} = \hat{x}\, p_x^{(2)} + \hat{z}\, p_z^{(2)} \tag{F3}$$

$$\hat{p}^{(3)} = -\hat{x}\, p_x^{(2)} + \hat{z}\, p_z^{(2)} \tag{F4}$$

Since the overall objective is to find certain properties between the composite patterns, certain properties between the patterns of each leg need be found.

To find those properties the following Equation (F5) is assumed since this relates the exponential factor of the patterns of each leg.

$$\hat{p}^{(2)} \cdot \hat{r}_m(k_2,n) = \hat{p}^{(3)} \cdot \hat{r}_m(k_3,n) \tag{F5}$$

where $k_2$ and $k_3$ refer to the summation indice k for leg 2 and 3, respectively.

Substituting Equation (F1) into Equation (F5) gives

$$p_x^{(2)} \left(k_2 - \frac{n\Delta z}{D_z}\right) \frac{\lambda_m}{D_x} + p_z^{(2)} \left(s_{mz} + \frac{n\lambda_m}{D_z}\right)$$

$$= - p_x^{(2)} \left(k_3 - \frac{n\Delta z}{D_z}\right) \frac{\lambda_m}{D_x} + p_z^{(2)} \left(s_{mz} + \frac{n\lambda_m}{D_z}\right) \tag{F6}$$

so

$$k_2 - \frac{n\Delta z}{D_z} = \frac{n\Delta z}{D_z} - k_3 \tag{F7}$$

or

$$\frac{2n\Delta z}{D_z} - k_3 = k_2 \quad . \tag{F8}$$

The relationship between $r_{mx}(k_2,n)$ and $r_{mx}(k_3,n)$, where $r_{mx}$ is the x component of $\hat{r}_m$, can now be found.

$$r_{mx}(k_2,n) = \left(k_2 - \frac{n\Delta z}{D_z}\right) \frac{\lambda_m}{D_x} = \left(\left(\frac{2n\Delta z}{D_z} - k_3\right) - \frac{n\Delta z}{D_z}\right) \frac{\lambda_m}{D_x}$$

$$= \left(\frac{n\Delta z}{D_z} - k_3\right) \frac{\lambda_m}{D_x} \tag{F9}$$

or

$$r_{mx}(k_2,n) = - r_{mx}(k_3,n) \quad . \tag{F10}$$

Also by inspection $r_{mz}(k_2,n) = r_{mz}(k_3,n)$.

Substitution of Equations (F5) and (F8) into the equations for the pattern results in an equation of the form

$$P^{v2}\left(\frac{2n\Delta z}{D_z} - k_3,n\right) = P^{v3}(k_3,n)$$

$$P^{v3}\left(\frac{2n\Delta z}{D_z} - k_3,n\right) = P^{v2}(k_3,n) \qquad \text{(F11)}$$

where $P^v$ is the symmetric, asymmetric, non-transmitting (scattering) and transmitting patterns, $P^s$, $P^a$, $P^{st}$, $P^{at}$ of each leg for scan in the YZ-Plane. v is a dummy variable.

Substituting Equation (F11) into (D10) in [40] with slight notational change yields

$$\perp P_m^s(k_2,n) = \frac{1}{(r_{mx}^2(k_2,n)+r_{mz}^2(k_2,n))^{1/2}}$$

$$[2r_{mx}(k_2,n)P^{s1}(k_2,n)+p_x r_{mz}(k_2,n)(P^{s2}(k_2,n)-P^{s3}(k_2,n)$$

$$-pz\ r_{mx}(k_2,n)(P^{s2}(k_2,n)+P^{s3}(k_2,n)]$$

$$= \frac{1}{(r_{mx}^2(k_3,n)+r_{mz}^2(k_3,n))^{1/2}}$$

$$\left[-2r_{mx}(k_3,n)P^{s1}(k_3,n)+p_x r_{mz}(k_3,n)\left(P^{s2}\left(\frac{2n\Delta z}{D_z} - k_3,n\right) - P^{s3}\left(\frac{2n\Delta z}{D_z} - k_3,n\right)\right)\right.$$

$$\left. + p_z r_{mx}(k_3,n)\left(P^{s2}\left(\frac{2n\Delta z}{D_z} - k_3,n\right) + P^{s3}\left(\frac{2n\Delta z}{D_z} - k_3,n\right)\right)\right] \qquad \text{(F12)}$$

$$= \frac{1}{(r_{mx}(k_3^2,n)+r_{mz}^2(k_3,n))^{1/2}}$$

$$[-2r_{mx}(k_3,n)P^{s1}(k_3,n)+p_x r_{mz}(k_3,n)(P^{s2}(k_3,n)+P^{s3}(k_3,n)$$

$$+p_z r_{mx}(k_3,n)(P^{s2}(k_3,n)+P^{s3}(k_3,n))]$$

$$= -\perp P_m^s(k_3,n)$$

Substituting Equation (F7) into Equation (F12) yields

$$ {}_{\perp}P_m^s\left(\frac{2n\Delta z}{D_z} - k_3, n\right) = {}_{\perp}P_m^s(k_3, n) \tag{F13} $$

Similar derivations using Equations (D11)-(D13) in [41] of non-transmitting modes for parallel and orthogonal components yields

$$ {}_{\parallel}P_m^s\left(\frac{2n\Delta z}{D_z} - k_3, n\right) = {}_{\parallel}P_m^s(k_3, n) \tag{F14} $$

$$ {}_{\perp}P_m^a\left(\frac{2n\Delta z}{D_z} - k_3, n\right) = {}_{\perp}P_m^a(k_3, n) \tag{F15} $$

$$ {}_{\parallel}P_m^a\left(\frac{2n\Delta z}{D_z} - k_3, n\right) = - {}_{\parallel}P_m^a(k_3, n) \tag{F16} $$

The above for equations also hold for the transmitting case.

Note that for k=n=0.

$$ {}_{\perp}P_m^s(0,0) = {}_{\parallel}P^a(0,0) = 0 $$

which is identical to Equation (D18) in [42]. This should be the case since at k=n=0 the principle propagating mode will be the same regardless of grid structure.

If $\Delta z=0$ (non-interlace structure) Equations (F13), (F14), (F15) and (F16) reduce to Equations (D14)-(D17) in [43] given for the non-interlace design.

Equations (D21) and (D22) in [44] only hold for the non-interlace structure.

# APPENDIX G
# COMPUTER LISTING FOR BIPLANAR SLOT ARRAY OF THREE-LEGGED ELEMENTS IN A STRATIFIED DIELECTRIC MEDIUM

| LIST OF IMPORTANT COMPUTER VARIABLES | EXPLANATION AT PROGRAM* LINE NUMBER |
|---|---|
| ABRS | 91 |
| ACPAT | 658 |
| ALPHA | 17 DATA FILE |
| APATX | 641 |
| APATZ | 642 |
| BETA | 85 |
| BETAD | 891 |
| BTD | 586 |
| CA1 | 1202 |
| CS1 | 1201 |
| D | 11 DATA FILE |
| DELTZ | 26 DATA FILE |
| DX | 24 DATA FILE |
| DZ | 25 DATA FILE |
| EFFL | 893 |
| ELEMX | 894 |
| ELEMZ | 894 |
| ER | 19 DATA FILE |
| ETA | 17 DATA FILE |
| EXPT | 1127 |
| EXPYM | 1103 |
| EXPYS | 1077 |
| FINCRM | 9 DATA FILE |
| FREQH | 8 DATA FILE |
| FREQL | 7 DATA FILE |
| IKK | 853 |
| INN | 853 |
| IOC | 52 PRINT |
| IVD | 888 |

* Except when noted otherwise. Explanation then exists at line number given in listed program.

| LIST OF IMPORTANT COMPUTER VARIABLES (cont.) | EXPLANATION AT PROGRAM LINE NUMBER (cont.) |
|---|---|
| NADMT. . . . . | 587 |
| NANGLS . . . . . | 15 DATA FILE |
| OHO. . . . . | 1221 |
| OHP. . . . . | 1222 |
| OPATC. . . . . | 660 |
| PATX . . . . . | 897 |
| PATZ . . . . . | 897 |
| PHO. . . . . | 1223 |
| PHP. . . . . | 1224 |
| PPATC. . . . . | 661 |
| RHO. . . . . | 1042 |
| RL . . . . . | 27 DATA FILE |
| RLA. . . . . | 30 DATA FILE |
| RLAMDA . . . . . | 85 |
| RLF. . . . . | 585 |
| RXKN . . . . . | 859 |
| RYKN . . . . . | 859 |
| RZKN . . . . . | 859 |
| SCPAT. . . . . | 624 |
| SPATX. . . . . | 637 |
| SPATZ. . . . . | 640 |
| SX . . . . . | 105 |
| SZ . . . . . | 105 |
| TFACT. . . . . | 997 |
| THIK . . . . . | 29 DATA FILE |
| VA2. . . . . | 1251 |
| VS2. . . . . | 1250 |
| WIDTH. . . . . | 28 DATA FILE |
| YADMT. . . . . | 590 |
| YADMTL . . . . . | 591 |
| YADMTR . . . . . | 592 |

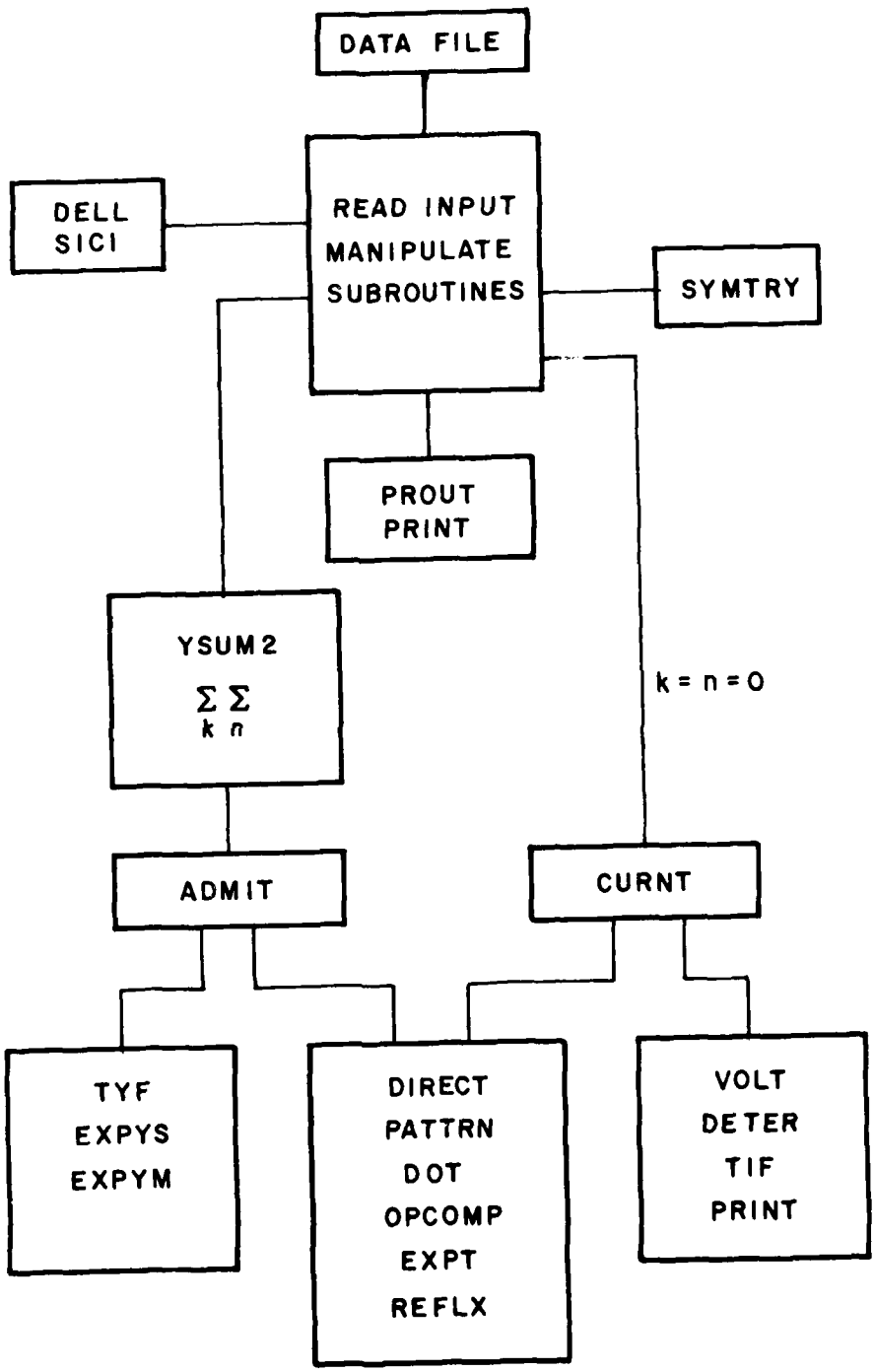


Figure G1. Program structure.

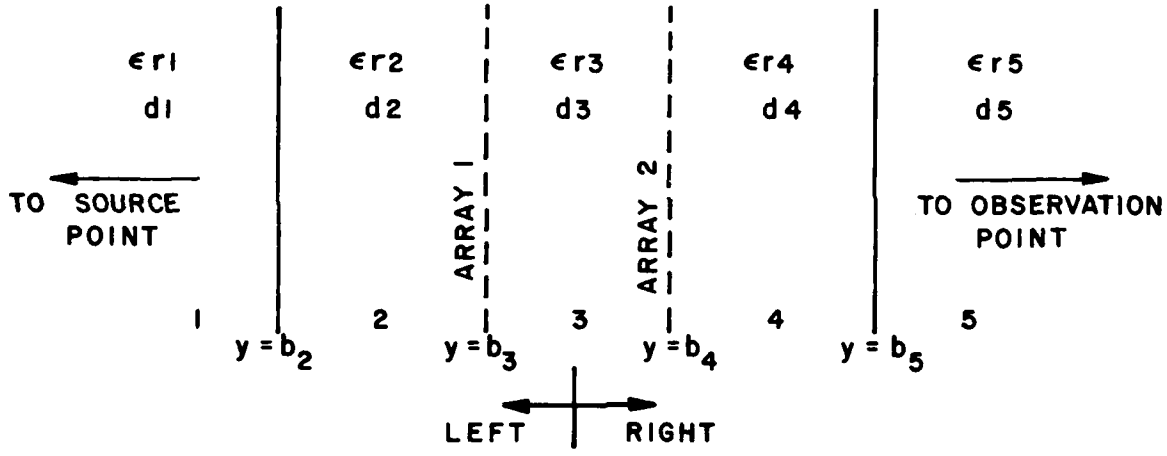


Figure G2. Defining the physical structure.

```
C      WRITTEN BY J.S.ERNST   (UNLESS NOTED OTHERWISE)
C
C      THIS PROGRAM CALCULATES THE TRANSMITTED H FIELD THRU STRUCTURE
C      OF FIGURE 1. THE SELF AND MUTUAL ADMITTANCES ARE ALSO CALCULATED.
C
C      EXPLANATIONS OF VARIABLES ARE EXPLAINED THROUT THE PROGRAM
C
C      INCLUDE SYSTEM SOFTWARE FOR USE IN PRINT ROUTINES
C
       INCLUDE FLSBS,404C:ADLDGB,404C
       INCLUDE PACKB,2969M
       INCLUDE SYSMB,2969M
       INCLUDE STRLGB,2969M
       INCLUDE STRMSB,2969M
       INCLUDE PRINTB,2969M
       LOGICAL LOGIC
       DIMENSION ELEMX(2,5),ELEMZ(2,5),PLF(2),PTD(2),RLAMDA(5)
      1,SX(5),SZ(5),ALPHA(10),ETA(10),ITMA1(3),ITMA2(3),ITMA3(3)
       COMPLEX YADMT(15),YADMTL(16),YADMTR(16)
       COMMON /PRINT/ IOC
       COMMON /ARRAY/ WIDTH
C---COMMON BLOCK
C
       COMMON RXKN,RYKN,RZKN,BETA,D,ER
       COMPLEX RYPN(5),CJ,CZERO
       DIMENSION RXKN(5),RZKN(5),BETA(5),D(5),ER(5)
       DATA CJ,CZERO/(0.0,1.0),(0.0,0.0)/
C-----
       DATA RED,PI/0.0174532925,3.14159265/
C*** COMPUTE TIMING & FILE INITIALIZATION ***
C
C  GETTIM & GETDAT ARE USED TO GET THE TIME OF DAY & THE DATE
C  GETCP IS USED TO GET THE CURRENT CPU CLOCK IN 10'S OF MSEC
       CALL GETTIM(ITMA1)
       CALL GETDAT(ITMA2)
       CALL GETCP(JTM1)
```

```
      ITM4=0
      CALL PRINTL
C      SET UP INITIALIZATIONS--SEE DATA FILE
      READ(5,5007)
      READ(5,-)IVP
      READ(5,5007)
      READ(5,-)ISYMY
      READ(5,5007)
      READ(5,-)IOC
C      READ IN DIELECTRIC PARAMETERS AND ALL NON ANTENNA
C      PARAMETERS--SEE DATA FILE
      READ(5,5006) FRELL
      READ(5,5006) FREHI
      READ(5,5006) FINCR
      DO 10 I=1,5
10    READ(5,5006)EL(I)
      READ(5,5007)
      READ(5,-)NANGLS
      READ(5,5007)
      READ(5,-) (ALPHA(I),ETA(I),I=1,NANGLS)
      DO 15 L=1,5
15    READ(5,5006)ER(L)
      READ(5,5006)DX
      READ(5,5006)DZ
      READ(5,5006)DELTZ
      READ(5,5006)RL
      READ(5,5006)WIDTH
      READ(5,5006)THTK
C      ASSUMPTIONS: LEG1 IS ON +Z AXIS, LEG2 AND LEG3 ARE IN
C      - Z DIRECTION -X,+X DIRECTION RESPECTIVLY
      DO 20 LSLOT=1,2
      READ(5,5007)
      READ(5,-)RLA
      RLAR=RLA*RAD
      ELEMX(LSLOT,1)=0.0
```

```
      ELEMZ(LSLOT,1)=1.0
      ELEMX(LSLOT,2)=-SIN(RLAR/2.0)
      ELEMZ(LSLOT,2)=-COS(RLAR/2.0)
      ELEMX(LSLOT,3)=-ELEMX(LSLOT,2)
20    ELEMZ(LSLOT,3)=ELEMZ(LSLOT,2)
5006  FORMAT(8X,F12.6)
5007  FORMAT(2X)
      CALL GETCP(ITM2)
C      DETERMINE FREQ
      NPOINT=(FREQH-FREQL)/FINCRM+1.2
      DO 50 M=1,NPOINT
      RM=M-1
      FREQ=FREQL+RM*FINCRM
C      CALCULATE THE WAVELENGTH AND PROPAGATION CONSTANT IN
C      EACH DIELECTRIC MEDIA
      DO 25 I=1,5
      RLAMDA(I)=30.0/(FREQ*SQRT(ER(I)))
25    BETA(I)=2.*PI/RLAMDA(I)
C      CALCULATE THE EFFECTIVE LENGTH AND BETAD FOR EACH ARRAY
      ABRS=SQRT((ER(2)+ER(5))/2.0)
      RLAM=RLAMDA(1)
      CALL DELL(RL,WIDTH,THIK,PLAM,ABRS,DL)
      RLF(1)=RL+DL
      BTD(1)=ABRS*BETA(1)/SQRT(ER(1))
      ABRS=SQRT((ER(3)+ER(4))/2.0)
      CALL DELL(RL,WIDTH,THIK,PLAM,ABRS,DL)
      RLF(2)=RL+DL
      BTD(2)=ABRS*BETA(1)/SQRT(ER(1))
C      DETERMINE THE SCAN ANGLE
      DO 45 INDEX=1,NANGLS
      ALPHAR=RPD*ALPHA(INDEX)
      ETAR=RPD*ETA(INDEX)
      DO 30 L=1,5
C      COMPONENTS OF INCIDENT PLANE WAVE SIGNAL
```

```
      SX(L)=SIN(ETAR)*COS(ALPHAR)*SQRT(ER(1))/SQRT(ER(L))
   30 SZ(L)=SIN(ETAR)*SIN(ALPHAR)*SQRT(ER(1))/SQRT(ER(L))
      DUMMY1=ALPHA(INDEX)
      DUMMY2=BETA(INDEX)
      CALL PRINTF(FREQ,DUMMY1,DUMMY2)
C      SYMMETRY CONDITION USED
   35 IXSY=1
      IF(ISYMY.EQ.1) IXSY=4
      DO 40 NADMT=1,IXSY
C      PERFORM THE DOUBLE SUMMATION TO CALCULATE ADMITTANCES
      CALL YADMZ(IVO,ELEMX,ELEMZ,PLF,BTO,PLAMDA,SX,SZ
     1,DX,DZ,DELTZ,RL,NADMT,YADMT,YADMTL,YADMTR)
      YADMT(NADMT)=YADMT(NADMT)/(2.0*DX*DZ*376.82)
      YADMTL(NADMT)=YADMTL(NADMT)/(2.0*DX*DZ*376.82)
      YADMTR(NADMT)=YADMTR(NADMT)/(2.0*DX*DZ*376.82)
      IF(ISYMY.EQ.1) CALL SYMTRY(NADMT,YADMT,YADMTL,YADMTR)
C      PRINT OUT ADMITTANCE RESULTS
      CALL PRTOUT(NADMT,YADMT,YADMTL,YADMTR)
   40 CONTINUE
C      CALCULATE THE TRANSMITTED H FIELD
      CALL CURNT(IVO,ELEMX,ELEMZ,RLF,BTO,RLAMDA
     1,SX,SZ,DX,DZ,DELTZ,RL,YADMT)
      ITM4=ITM4+1
   45 CONTINUE
   50 CONTINUE
C
C*** END OF RUN ***
C
      CALL GETCP(ITM3)
      CALL GETTIM(ITMA3)
      ITM1=(ITM3-ITM1)/100
      ITM4=((ITM3-ITM2)/ITM4)/100
      CALL PRINTE(ITMA1,ITMA2,ITMA3,ITM1,ITM4)
      STOP
      END
```

```
141 C  ***********************************************************************
142 C
143 C***SYMTRY
144 C
145 C      THIS SUBROUTINE USES SYMMETRY OF THE STRUCTURE TO REDUCE CALCULATION
146 C      TIME. WHEN SYMMETRIC ARRAY 1 IS THE SAME AS ARRAY 2 IN THE
147 C      SAME PHYSICAL SURROUNDING THE ADMITTANCES CALCULATED FOR ARRAY 1
148 C      ARE THE SAME AS THOSE OF ARRAY 2
149 C
150        SUBROUTINE SYMTRY(NADMT,YADMT,YADMTL,YADMTR)
151        COMPLEX YADMT(16),YADMTL(16),YADMTR(16)
152        GOTO (1,1,1,1,2,2,2,2),NADMT
153 1      YADMT(NADMT+12)=YADMT(NADMT)
154        YADMTL(NADMT+12)=YADMTL(NADMT)
155        YADMTR(NADMT+12)=YADMTR(NADMT)
156        RETURN
157 2      YADMT(NADMT+4)=YADMT(NADMT)
158        RETURN
159        END
160 C  ***********************************************************************
161 C
162 C***PROUT
163 C
164 C      THIS SUBROUTINE JUSTS SETS UP THE LABELING SYSTEM TO PRINT OUT
165 C      DATA
166 C
167        SUBROUTINE PROUT(NADMT,YADMT,YADMTL,YADMTR)
168        COMPLEX YADMT(16),YADMTL(16),YADMTR(16)
169        DIMENSION LAB(2),LFT(2),IRT(2)
170        DATA LB1,LB2,LB3,LB4/3HY S,3HY A,3H1A1,3H1S1/
171        DATA LB5,LB6,LB7,LB8/3H2A1,3H1A2,3H2S1,3H1S2/
172        DATA LB9,LB10/3H2A2,3H2S2/
173        DATA LB11,LB12,LB13,LB14/3HYLS,3HYRS,3HYLA,3HYRA/
174 C
175        GOTO(1,2,3,4,5,6,7,8,9,10,11,12,13,14,15,16),NADMT
```

```
176 1     LAB(1)=LB1
177       LAB(2)=LB4
178       LFT(1)=LB11
179       IRT(1)=LB12
180       IPRNT=2
181       GOTO 17
182 2     LAB(1)=LB1
183       LAB(2)=LB3
184       LFT(1)=LB11
185       IRT(1)=LB12
186       IPRNT=2
187       GOTO 17
188 3     LAB(1)=LB2
189       LAB(2)=LB4
190       LFT(1)=LB13
191       IRT(1)=LB14
192       IPRNT=2
193       GOTO 17
194 4     LAB(1)=LB2
195       LAB(2)=LB3
196       LFT(1)=LB13
197       IRT(1)=LB14
198       IPRNT=2
199       GOTO 17
200 5     LAB(1)=LB1
201       LAB(2)=LB8
202       IPRNT=4
203       GOTO 18
204 6     LAB(1)=LB1
205       LAB(2)=LB6
206       IPRNT=4
207       GOTO 18
208 7     LAB(1)=LB2
209       LAB(2)=LB8
210       IPRNT=4
```

```
      GOTO 19
8     LAB(1)=LB2
      LAB(2)=LB6
      IPRNT=4
      GOTO 18
9     LAB(1)=LB1
      LAB(2)=LB7
      IPRNT=8
      GOTO 18
10    LAB(1)=LB1
      LAB(2)=LB5
      IPRNT=8
      GOTO 18
11    LAB(1)=LB2
      LAB(2)=LB7
      IPRNT=8
      GOTO 18
12    LAB(1)=LB2
      LAB(2)=LB5
      IPRNT=8
      GOTO 18
13    LAB(1)=LB1
      LAB(2)=LB10
      LFT(1)=LB11
      IRT(1)=LB12
      IPRNT=16
      GOTO 17
14    LAB(1)=LB1
      LAB(2)=LB9
      LFT(1)=LB11
      IRT(1)=LB12
      IPRNT=16
      GOTO 17
15    LAB(1)=LB2
      LAB(2)=LB10
```

```
      LFT(1)=LB13
      IRT(1)=LB14
      IPRNT=15
      GOTO 17
16    LAB(1)=LB2
      LAB(2)=LB9
      LFT(1)=LB13
      IRT(1)=LB14
      IPRNT=16
17    LFT(2)=LAB(2)
      IRT(2)=LAB(2)
      CALL PRINTC(LFT,YADMTL(NADMT),32,0)
      CALL PRINTC(IRT,YADMTR(NADMT),32,0)
18    CALL PRINTC(LAB,YADMT(NADMT),IPRNT,0)
      RETURN
      END
C  ***********************************************************************
C
C***YSUM2
C
C     WRITTEN BY C.J.LARSON--MODIFIED BY J.S.ERNST
C
C     THIS SUBROUTINE MANAGES THE DOUBLE SUMMATION IN THE POISSON
C     SUM FORMULA AND CHECKS FOR CONVERGENCE
C
C     THE VARIABLES ARE READ THRU AND DEFINED IN OTHER PARTS OF THE
C     PROGRAM
C
      SUBROUTINE YSUM2(IVD,ELEMX,ELEMZ,RLF,BTD,RLAMDA,SX,SZ
     1,DX,DZ,DELTZ,RL,NADMT,YADMT,YADMTL,YADMTR)
      DIMENSION ELEMX(2,3),ELEMZ(2,3),RLF(2,5),BTD(2),RLAMDA(5)
     1,SX(5),SZ(5)
      COMPLEX YADMT(16),YADMTL(16),YADMTR(16)
      COMPLEX Y,Y1,Y2,Y3,Y4,Y5,Y6,Y7,Y8,Y9
      COMPLEX YLT,YL1,YL2,YL3,YL4,YL5,YL6,YL7,YL8,YL9
```

```
     1,YRT,YR1,YR2,YR3,YR4,YR5,YR6,YR7,YR8,YR9
      INTEGER TEST1,TEST2,TEST3,TEST4,TEST5,TEST6,TEST7,
     1TEST8,TEST9,TEST10,TEST11,TEST12
C---COMMON BLOCK
C
      COMMON RXKN,RYKN,RZKN,BETA,D,ER
      COMPLEX RYKN(5),CJ,CZERO
      DIMENSION RXKN(5),RZKN(5),BETA(5),D(5),ER(5)
      DATA CJ,CZERO/(0.0,1.0),(0.0,0.0)/
C-----
C
C
C
C     CONVERGENCE NUMBER (COMPA)
C
      COMP=0.
      DO 1 I=1,3
      N=I-2
      DO 1 M=1,3
      K=M-2
      CALL ADMIT(IVD,ELEMX,ELEMZ,RLF,BTD,RLAMDA,SX,SZ
     1,DX,DZ,DELTZ,RL,NADMT,K,N,YADMT,YADMTL,YADMTR)
      A=ABS(AIMAG(YADMT(NADMT)))
1     COMP=COMP+A
      COMPA=COMP/1E+3
C
C     K=N=0, TERM
C
      K=0
      N=0
      CALL ADMIT(IVD,ELEMX,ELEMZ,RLF,BTD,RLAMDA,SX,SZ
     1,DX,DZ,DELTZ,RL,NADMT,K,N,YADMT,YADMTL,YADMTR)
      Y1=YADMT(NADMT)
      YL1=YADMTL(NADMT)
      YR1=YADMTR(NADMT)
```

```
C
C       SUM ALONG +K AXIS
C
        Y2=(0.,0.)
        YL2=(0.,0.)
        YR2=(0.,0.)
        TEST1=1
        DO 2 I=1,200
        K=I
        KCONP=I
        CALL ADMIT(IVD,ELEMX,ELEMZ,RLF,BTD,RLAMDA,SX,SZ
       1,DX,DZ,DELTZ,RL,NADMT,K,N,YADMT,YADMTL,YADMTR)
        Y2=Y2+YADMT(NADMT)
        YL2=YL2+YALMTL(NADMT)
        YR2=YR2+YADMTR(NADMT)
        BBR=ABS(AIMAG(YADMT(NADMT)))
        IF(BBR.LT.COMPA) GO TO 10
        GO TO 11
10      TEST1=TEST1+1
        IF(TEST1.EQ.3)GO TO 12
        GO TO 2
11      TEST1=0
2       CONTINUE
C
C       SUM ALONG -K AXIS
C
12      Y3=(0.,0.)
        YL3=(0.,0.)
        YR3=(0.,0.)
        TEST2=0
        DO 3 I=1,200
        K=-I
        KCONM=I
        CALL ADMIT(IVD,ELEMX,ELEMZ,RLF,BTD,RLAMDA,SX,SZ
       1,DX,DZ,DELTZ,RL,NADMT,K,N,YADMT,YADMTL,YADMTR)
```

```
      Y3=Y3+YADMT(NADMT)
      YL3=YL3+YADMTL(NADMT)
      YR3=YR3+YADMTR(NADMT)
      C=ABS(AIMAG(YADMT(NADMT)))
      IF(C.LT.COMPA)GO TO 20
      GO TO 21
20    TEST2=TEST2+1
      IF (TEST2.EQ.3)GO TO 22
      GO TO 3
21    TEST2=0
3     CONTINUE
C
C     SUM ALONG +N AXIS
C
22    K=0
      YL4=(0.,0.)
      YR4=(0.,0.)
      Y4=(0.,0.)
      TEST3=0
      DO 4 I=1,200
      N=I
      NCONP=I
      CALL ADMIT(IVD,ELEMX,ELEMZ,RLP,BTD,RLAMDA,SX,SZ
     1,DX,DZ,DELTZ,RL,NADMT,K,N,YADMT,YADMTL,YADMTR)
      Y4=Y4+YADMT(NADMT)
      YL4=YL4+YADMTL(NADMT)
      YR4=YR4+YADMTR(NADMT)
      DAB=ABS(AIMAG(YADMT(NADMT)))
      IF(DAB.LT.COMPA)GO TO 30
      GO TO 31
30    TEST3=TEST3+1
      IF(TEST3.EQ.3)GO TO 32
      GO TO 4
31    TEST3=0
4     CONTINUE
```

```
C
C       SUM ALONG -M AXIS
C
32      Y5=(0.,0.)
        YL5=(0.,0.)
        YR5=(0.,0.)
        TEST4=1
        DO 5 I=1,200
        N=-I
        NCONM=I
        CALL ADMIT(IVD,ELEMX,ELEMZ,RLF,BTD,RLAMDA,SX,SZ
     1,DX,DZ,DELTZ,RL,NADMT,M,N,YADMT,YADMTL,YADMTR)
        Y5=Y5+YADMT(NADMT)
        YL5=YL5+YADMTL(NADMT)
        YR5=YR5+YADMTR(NADMT)
        E=ABS(AIMAG(YADMT(NADMT)))
        IF(E.LT.COMPA)GO TO 40
        GO TO 41
40      TEST4=TEST4+1
        IF(TEST4.EQ.3)GO TO 42
        GO TO 5
41      TEST4=0
5       CONTINUE
C
C       SUM IN FIRST QUAD K(+) N(+)
C
42      Y6=(0.,0.)
        YL6=(0.,0.)
        YR6=(0.,0.)
        TEST5=0
        TEST6=0
        DO 6 I=1,200
        K=I
        N=I
        CALL ADMIT(IVD,ELEMX,ELEMZ,RLF,BTD,RLAMDA,SX,SZ
```

```
421         1,DX,DZ,DELTZ,RL,NADMT,K,N,YADMT,YADMTL,YADMTR)
422          Y6=Y6+YADMT(NADMT)
423          YL6=YL6+YADMTL(NADMT)
424          YR6=YR6+YADMTR(NADMT)
425          F=ABS(AIMAG(YADMT(NADMT)))
426          IF(F.LT.COMPA)GO TO 50
427          GO TO 51
428   50     TEST5=TEST5+1
429          IF(TEST5.EQ.3)GO TO 55
430          GO TO 52
431   51     TEST5=0
432   52     TEST6=0
433          DO 7 M=2,200
434          K=M
435          CALL ADMIT(IVD,ELEMX,ELEMZ,RLF,BTD,PLAMDA,SX,SZ
436         1,DX,DZ,DELTZ,RL,NADMT,K,N,YADMT,YADMTL,YADMTR)
437          Y6=Y6+YADMT(NADMT)
438          YL6=YL6+YADMTL(NADMT)
439          YR6=YR6+YADMTR(NADMT)
440          G=ABS(AIMAG(YADMT(NADMT)))
441          IF(G.LT.COMPA)GO TO 53
442          GO TO54
443   53     TEST6=TEST6+1
444          IF(TEST6.EQ.3)GO TO 6
445          GO TO 7
446   54     TEST6=0
447   7      CONTINUE
448   6      CONTINUE
449   C
450   C      SUM IN SECOND QUAD K(-) K(+)
451   C
452   55     Y7=(0.,0.)
453          YL7=(0.,0.)
454          YR7=(0.,0.)
455          TEST7=0
```

```
      TEST8=
      DO 8 I=1,200
      K=-1
      M=I
      CALL ADMIT(IVD,ELEMX,ELEMZ,RLF,BTD,RLAMDA,SX,SZ
     1,DX,DZ,DELTZ,RL,YADMT,K,M,YADMT,YADMTL,YADMTR)
      Y7=Y7+YADMT(NADMT)
      YL7=YL7+YADMTL(NADMT)
      YR7=YR7+YADMTR(NADMT)
      H=ABS(AIMAG(YADMT(NADMT)))
      IF(H.LT.COMPA)GO TO 60
      GOTO61
60    TEST7=TEST7+1
      IF(ITEST7.EQ.3)GO TO 65
      GO TO 62
61    TEST7=0
62    TEST8=0
      DO 9 M=2,200
      K=-M
      CALL ADMIT(IVD,ELEMX,ELEMZ,RLF,BTD,RLAMDA,SX,SZ
     1,DX,DZ,DELTZ,RL,YADMT,K,M,YADMT,YADMTL,YADMTR)
      Y7=Y7+YADMT(NADMT)
      YL7=YL7+YADMTL(NADMT)
      YR7=YR7+YADMTR(NADMT)
      O=ABS(AIMAG(YADMT(NADMT)))
      IF(O.LT.COMPA)GO TO 63
      GO TO 64
63    TESTA=TEST8+1
      IF(TEST8.EQ.3)GO TO 8
      GO TO 9
64    TEST8=0
9     CONTINUE
8     CONTINUE
```

```
C
C     SUM IN THIRD QUAD K(-) N(-)
C
65    Y8=(0.,0.)
      YL8=(0.,0.)
      YR8=(0.,0.)
      TEST9=0
      TEST10=0
      DO 13 I=1,200
      K=-1
      N=-I
      CALL ADMIT(IVD,ELEMX,ELEMZ,RLF,BTD,RLAMDA,SX,SZ
     1,DX,DZ,DELTZ,RL,NADMT,K,N,YADMT,YADMTL,YADMTR)
      Y8=Y8+YADMT(NADMT)
      YL8=YL8+YADMTL(NADMT)
      YR8=YR8+YADMTR(NADMT)
      P=ABS(AIMAG(YADMT(NADMT)))
      IF(P.LT.COMPA)GO TO 70
      GO TO 71
70    TEST9=TEST9+1
      IF(TEST9.EQ.3)GO TO 75
      GO TO 72
71    TEST9=0
72    TEST10=0
      DO 14 M=2,200
      K=-M
      CALL ADMIT(IVD,ELEMX,ELEMZ,RLF,BTD,RLAMDA,SX,SZ
     1,DX,DZ,DELTZ,RL,NADMT,K,N,YADMT,YADMTL,YADMTR)
      Y8=Y8+YADMT(NADMT)
      YL8=YL8+YADMTL(NADMT)
      YR8=YR8+YADMTR(NADMT)
      Q=ABS(AIMAG(YADMT(NADMT)))
      IF(Q.LT.COMPA)GO TO 75
      GO TO 74
73    TEST10=TEST10+1
```

```
      IF(TEST10.EQ.3)GO TO 13
      GO TO 14
74    TEST10=0
14    CONTINUE
15    CONTINUE
C
C     SUM IN FOURTH QUAD K(+) N(-)
C
75    Y9=(0.,0.)
      YL9=(0.,0.)
      YR9=(0.,0.)
      TEST11=0
      TEST12=0
      DO 15 I=1,200
      K=1
      N=-I
      CALL ADMIT(IVD,ELEMX,ELEMZ,RLF,BTD,RLAMDA,SX,SZ
     1,DX,DZ,DELTZ,RL,NADMT,K,N,YADMT,YADMTL,YADMTR)
      Y9=Y9+YADMT(NADMT)
      YL9=YL9+YADMTL(NADMT)
      YR9=YR9+YADMTR(NADMT)
      R=ABS(AIMAG(YADMT(NADMT)))
      IF(R.LT.COMPA)GO TO 80
      GO TO 81
80    TEST11=TEST11+1
      IF(TEST11.EQ.3)GO TO 85
      GO TO 82
81    TEST11=0
82    TEST12=0
      DO 16 M=2,200
      K=M
      CALL ADMIT(IVD,ELEMX,ELEMZ,RLF,BTD,RLAMDA,SX,SZ
     1,DX,DZ,DELTZ,RL,NADMT,K,N,YADMT,YADMTL,YADMTR)
      Y9=Y9+YADMT(NADMT)
      YL9=YL9+YADMTL(NADMT)
```

```
      YR9=YR9+YALPTR(NADMT)
      S=ABS(AIMAG(YADMT(NADMT)))
      IF(S.LT.COMPA)GO TO 83
      GO TO 84
83    TEST12=TEST12+1
      IF(TEST12.LT.0.3)GO TO 15
      GO TO 16
84    TEST12=0
16    CONTINUE
15    CONTINUE
C
85    Y=Y1+Y2+Y3+Y4+Y5+Y6+Y7+Y8+Y9
      YLT=YL1+YL2+YL3+YL4+YL5+YL6+YL7+YL8+YL9
      YRT=YR1+YR2+YR3+YR4+YR5+YR6+YR7+YR8+YR9
      YADMTL(NADMT)=YLT
      YADMTR(NADMT)=YRT
      YADMT(NADMT)=Y
      RETURN
      END
C  ***************************************************************
C
C***ADMIT
C
C     THIS SUBROUTINE CALCULATES THE SELF AND MUTUAL ADMITTANCES
C
C     INPUT VARIABLES
C      RLE(A)=EFFECTIVE LENGTH OF EACH ARRAY A
C      BTO(A)=EFFECTIVE PROPAGATION CONSTANT OF EACH ARRAY A
C      NADMT=DECIDES WHICH ADMITTANCE IS BEING CALCULATED ,THE NUMBER
C       FOLLOWING THE COMMENTS ON THE ADMITTANCES BELOW IS NADMT
C     OUTPUT VARIABLES
C      YADMT=TOTAL ADMITTANCE FOR EACH IKK,IM
C      YADMTL=ADMITTANCE LOOKING LEFT
C      YADMTR=ADMITTANCE LOOKING RIGHT
C
```

```
C      THE REMAINING VARIABLES ARE EXPLAINED IN THE INDIVIDUAL SUBROUTINES
C
       SUBROUTINE ADMITT(IKD,ELEMX,ELEMZ,RLF,BTU,RLAMDA
      1,SX,SZ,DX,DZ,DELTZ,RL,NADMT,IKA,INN,YADMT
      2,YADMTL,YADMTR)
       COMPLEX PATX(3),PATZ(3),SPATX(2,2),SPATZ(2,2)
      1,APATX(2,2),APATZ(2,2),XPAT,ZPAT,SCPAT(2,5,2)
      2,ACPAT(2,5,2),TPACT(2,5),YADMT(16),DPATC,PPATC,EXPYS,EXPYN
       COMPLEX YADMTL(16),YADMTR(16)
       DIMENSION ELEMX(2,3),ELEMZ(2,3),RLAMDA(5),SX(5),SZ(5)
      1,BTU(2),RLF(2)
C---COMMON BLOCK
C
       COMMON RXKN,RYKN,RZKN,BETA,D,ER
       COMPLEX RYKN(5),CU,CZERO
       DIMENSION RXKN(5),RZKN(5),BETA(5),D(5),ER(5)
       DATA CU,CZERO/(0.0,1.0),(0.0,0.0)/
C-----
       CALL DIRECT(IKK,INN,RLAMDA,SY,SZ,DX,DZ,DELTZ)
C      SET UP MEDIA NUMBERS AND SLOT NUMBERS ACCORDING TO NADMT
       GOTO (20,20,20,20,25,25,25,25,25,25,25,25,30,30,30,30),NADMT
20     MEDL=2
       MEDR=3
       LS1=1
       LS2=1
       GOTO 35
25     MEDL=3
       MEDR=3
       LS1=1
       LS2=2
       GOTO 35
30     MEDL=3
       MEDR=4
       LS1=2
       LS2=2
```

```
      GOTO 35
35    DO 40 LSLOT=LS1,LS2
      DO 40 NTRNS=1,2
      BETAD=BTU(LSLOT)
      EFFL=RLF(LSLOT)
      CALL PATTRN(IVD,NTRNS,BETAL,PL,EFF,ELEMX,ELEMZ,LSLOT
     1,PATX,PATZ)
C
C       SPATX(A,B)=X COMPONENT OF SYMMETRIC PATTERN
C             WHERE A=ARRAY NUMBER
C                   B=1(TRANSMITTING),2(NON-TRANSMITTING)
C       SPATZ(A,B)=Z COMPONENT
C       APATX(A,B)=X COMPONENT OF ASYMMETRIC PATTERN
C       APATZ(A,B)=Z COMPONENT
C
      SPATX(LSLOT,NTRNS)=2.0*PATX(1)-PATX(2)
     1-PATX(3)
      SPATZ(LSLOT,NTRNS)=2.0*PATZ(1)-PATZ(2)
     1-PATZ(3)
      APATX(LSLOT,NTRNS)=PATX(2)-PATX(3)
      APATZ(LSLOT,NTRNS)=PATZ(2)-PATZ(3)
40    CONTINUE
C
C       DEFINING VARIABLES FOR THE REST OF THE SUBROUTINE
C
C       SCPAT(A,B,C)=SYMMETRIC COMPOSITE PATTERN FACTOR
C             WHERE A=1(ORTHOGONAL),2(PARALLEL)
C                   B=MEDIA NUMBER
C                   C=1(TRANSMITTING),2(NON-TRANSMITTING)
C       ACPAT(A,B,C)=ASYMMETRIC COMPOSITE PATTERN FACTOR
C             WHERE A,B,C ARE DEFINED ABOVE
C       OPATC=ORTHOGONAL PATTERN COMPONENT
C       PPATC=PARALLEL PATTERN COMPONENT
C
      GOTO (1,2,3,4,5,6,7,8,9,10,11,12,1,2,3,4),NADMT
```

```
C
C    Y(S1,S1) #1 OF  Y(S2,S2) #13
C
1      DO 16  EDIA=MEDL,MEDR
       DO 16 NTRNS=1,2
       XPAT=SPATX(LS1,NTRNS)
       ZPAT=SPATZ(LS1,NTRNS)
       CALL OPCOMP(MEDIA,XPAT,ZPAT,OPATC,PPATC)
       SCPAT(1,MEDIA,NTRNS)=OPATC
16     SCPAT(2,MEDIA,NTRNS)=PPATC
       CALL TYP(NADMT,TFACT)
C
       YADMTL(NADMT)=EXPYS(MEDL)*(SCPAT(1,MEDL,1)*SCPAT(1,MEDL,2)
     1*TFACT(1,MEDL)+SCPAT(2,MEDL,1)*SCPAT(2,MEDL,2)*TFACT(2,MEDL))
       YADMTR(NADMT)=
     2 EXPYS(MEDR)*(SCPAT(1,MEDR,1)*SCPAT(1,MEDR,2)*TFACT(1,MEDR)
     3+SCPAT(2,MEDR,1)*SCPAT(2,MEDR,2)*TFACT(2,MEDR))
       YADMT(NADMT)=YADMTL(NADMT)+YADMTR(NADMT)
       RETURN
C
C    Y(S1,A1) #2 OF Y(S2,A2) #14
C
2      DO 22 MEDIA=MEDL,MEDR
       XPAT=SPATX(LS1,1)
       ZPAT=SPATZ(LS1,1)
       CALL OPCOMP(MEDIA,XPAT,ZPAT,OPATC,PPATC)
       SCPAT(1,MEDIA,1)=OPATC
       SCPAT(2,MEDIA,1)=PPATC
       XPAT=APATX(LS1,2)
       ZPAT=APATZ(LS1,2)
       CALL OPCOMP(MEDIA,XPAT,ZPAT,OPATC,PPATC)
       ACPAT(1,MEDIA,2)=OPATC
22     ACPAT(2,MEDIA,2)=PPATC
       CALL TYP(NADMT,TFACT)
       YADMTL(NADMT)=EXPYS(MEDL)*(SCPAT(1,MEDL,1)*ACPAT(1,MEDL,2)
```

```
699          1*TFACT(1,MEDL)+SCPAT(2,MEDL,1)*ACPAT(2,MEDL,2)*TFACT(2,MEDL))
700           YADMTR(NADMT)=
701          2 EXPYS(MEDR)*(SCPAT(1,MEDR,1)*ACPAT(1,MEDR,2)*TFACT(1,MEDR)
702          3+SCPAT(2,MEDR,1)*ACPAT(2,MEDR,2)*TFACT(2,MEDR))
703           YADMT(NADMT)=YADMTL(NADMT)+YADMTR(NADMT)
704           RETURN
705  C
706  C     Y(A1,S1) #3 OR Y(A2,S2) #15
707  C
708  3        DO 32 MEDIA=MEDL,MEDR
709           XPAT=APATX(LS1,1)
710           ZPAT=APATZ(LS1,1)
711           CALL OPCOMP(MEDIA,XPAT,ZPAT,OPATC,PPATC)
712           ACPAT(1,MEDIA,1)=OPATC
713           ACPAT(2,MEDIA,1)=PPATC
714           XPAT=SPATX(LS1,2)
715           ZPAT=SPATZ(LS1,2)
716           CALL OPCOMP(MEDIA,XPAT,ZPAT,OPATC,PPATC)
717           SCPAT(1,MEDIA,2)=OPATC
718  32       SCPAT(2,MEDIA,2)=PPATC
719           CALL TYP(NADMT,ITACT)
720           YADMTL(NADMT)=EXPYS(MEDL)*(ACPAT(1,MEDL,1)*SCPAT(1,MEDL,2)
721          1*TFACT(1,MEDL)+ACPAT(2,MEDL,1)*SCPAT(2,MEDL,2)*TFACT(2,MELL))
722           YADMTR(NADMT)=
723          2 EXPYS(MEDR)*(ACPAT(1,MEDR,1)*SCPAT(1,MEDR,2)*TFACT(1,MEDR)
724          3+ACPAT(2,MEDR,1)*SCPAT(2,MEDR,2)*TFACT(2,MELR))
725           YADMT(NADMT)=YADMTL(NADMT)+YADMTR(NADMT)
726           RETURN
727  C
728  C     Y(A1,A1) #4 OR Y(A2,A2) #16
729  C
730  4        DO 42 MEDIA=MEDL,MEDR
731           DO 42 NTRNS=1,2
732           XPAT=APATX(LS1,NTRNS)
733           ZPAT=APATZ(LS1,NTRNS)
```

```
      CALL OPCOMP(MEDIA,XPAT,ZPAT,OPATC,PPATC)
      ACPAT(1,MEDIA,MTERMS)=OPATC
     &ACPAT(2,MEDIA,MTERMS)=PPATC
      CALL TYP(NADMT,IFACT)
      YADMTL(NADMT)=EXPYS(MEDL)*(ACPAT(1,MEDL,1)*ACPAT(1,MEDL,2)
     1*IFACT(1,MEDL)+ACPAT(2,MEDL,1)*ACPAT(2,MEDL,2)*IFACT(2,MEDL))
      YADMTR(NADMT)=
     < EXPYS(MEDR)*(ACPAT(1,MEDR,1)*ACPAT(1,MEDR,2)*IFACT(1,MEDR)
     3+ACPAT(2,MEDR,1)*ACPAT(2,MEDR,2)*IFACT(2,MEDR))
      YADMT(NADMT)=YADMTL(NADMT)+YADMTR(NADMT)
      RETURN
C
C   Y(S1,S2) #5 OR Y(S2,S1) #9
C
      XPAT=SPATX(LS1,1)
      ZPAT=SPATZ(LS1,1)
      CALL OPCOMP(3,XPAT,ZPAT,OPATC,PPATC)
      SCPAT(1,3,1)=OPATC
      SCPAT(2,3,1)=PPATC
      XPAT=SPATX(LS2,2)
      ZPAT=SPATZ(LS2,2)
      CALL OPCOMP(3,XPAT,ZPAT,OPATC,PPATC)
      SCPAT(1,3,2)=OPATC
      SCPAT(2,3,2)=PPATC
      CALL TYP(NADMT,IFACT)
      YADMT(NADMT)=EXPYM(3)*(SCPAT(1,3,1)*SCPAT(1,3,2)
     1*IFACT(1,3)+SCPAT(2,3,1)*SCPAT(2,3,2)*IFACT(2,3))
      YADMTL(NADMT)=(0.0,0.0)
      YADMTR(NADMT)=(0.0,0.0)
      RETURN
C
C   Y(S1,A2) #6 OR Y(S2,A1) #10
C
     &XPAT=SPATX(LS1,1)
      ZPAT=SPATZ(LS1,1)
```

```
      CALL OPCOMP(3,XPAT,ZPAT,OPATC,PPATC)
      SCPAT(1,3,1)=OPATC
      SCPAT(2,3,1)=PPATC
      XPAT=APATX(LS2,2)
      ZPAT=APATZ(LS2,2)
      CALL OPCOMP(3,XPAT,ZPAT,OPATC,PPATC)
      ACPAT(1,3,2)=OPATC
      ACPAT(2,3,2)=PPATC
      CALL TYP(NADMT,IFACT)
      YADMT(NADMT)=FXPYM(3)*(SCPAT(1,3,1)*ACPAT(1,3,2)
     1*IFACT(1,3)+SCPAT(2,3,1)*ACPAT(2,3,2)*IFACT(2,3))
      YADMTL(NADMT)=(0.0,0.0)
      YADMTR(NADMT)=(0.0,0.0)
      RETURN
C
C   Y(A1,S2) #7 OR Y(A2,S1) #11
C
7     XPAT=APATX(LS1,1)
      ZPAT=APATZ(LS1,1)
      CALL OPCOMP(3,XPAT,ZPAT,OPATC,PPATC)
      ACPAT(1,3,1)=OPATC
      ACPAT(2,3,1)=PPATC
      XPAT=SPATX(LS2,2)
      ZPAT=SPATZ(LS2,2)
      CALL OPCOMP(3,XPAT,ZPAT,OPATC,PPATC)
      SCPAT(1,3,2)=OPATC
      SCPAT(2,3,2)=PPATC
      CALL TYP(NADMT,IFACT)
      YADMT(NADMT)=FXPYM(3)*(ACPAT(1,3,1)*SCPAT(1,3,2)
     1*IFACT(1,3)+ACPAT(2,3,1)*SCPAT(2,3,2)*IFACT(2,3))
      YADMTL(NADMT)=(0.0,0.0)
      YADMTR(NADMT)=(0.0,0.0)
      RETURN
C
C   Y(A1,A2) #8 OR Y(A2,A1) #12
```

```
C
8  XPAT=APATX(LS1,1)
   ZPAT=APATZ(LS1,1)
   CALL OPCOMP(5,XPAT,ZPAT,OPATC,PPATC)
   ACPAT(1,5,1)=OPATC
   ACPAT(2,5,1)=PPATC
   XPAT=APATX(LS2,2)
   ZPAT=APATZ(LS2,2)
   CALL OPCOMP(3,XPAT,ZPAT,OPATC,PPATC)
   ACPAT(1,3,2)=OPATC
   ACPAT(2,3,2)=PPATC
   CALL TYP(NADMT,IFACT)
   YADMT(NADMT)=EXPYM(5)*(ACPAT(1,3,1)*ACPAT(1,3,2)
  1*IFACT(1,3)+ACPAT(2,3,1)*ACPAT(2,3,2)*IFACT(2,3))
   YADMTL(NADMT)=(0.0,0.0)
   YADMTR(NADMT)=(0.0,0.0)
   RETURN
C
C  Y(S2,S1) #9
C
9  LS1=2
   LS2=1
   GOTO 5
C
C  Y(S2,A1) #10
C
10 LS1=2
   LS2=1
   GOTO 6
C
C  Y(A2,S1) #11
C
11 LS1=2
   LS2=1
   GOTO 7
```

```
C
C    Y(A2,A1) =12
C
12      LS1=2
        LS2=1
        GOTO 8
        END
C  ***********************************************************************
C
C***DIRECT
C
C       THIS SUBROUTINE DECIDES THE DIRECTIONS THE WAVE IS PROPAGATING
C
C       INPUT VARIABLES
C        IKK,INN=SUMMATION INDICES
C        RLAMDA=WAVELENGTH IN EACH DIELECTRIC
C        SX,SZ=X,Z COMPONENTS OF INCIDENT WAVE VECTOR
C        DX,DZ=X,Z INTERELEMENT SPACING
C        DELTZ=INTERLACE SPACING IN Z DIRECTION
C       OUTPUT VARIABLES
C        RXKN,RYKN,RZKN=X,Y,Z COMPONENTS OF PROPAGATING WAVE
C
      SUBROUTINE DIRECT(IKK,INN,RLAMDA,SX,SZ,DX,DZ,DELTZ)
      DIMENSION RLAMDA(5),SX(5),SZ(5)
C---COMMON BLOCK
C
      COMMON RXKN,RYKN,RZKN,BETA,D,ER
      COMPLEX RYKN(5),CO,CZERO
      DIMENSION RXKN(5),RZKN(5),BETA(5),D(5),ER(5)
      DATA CO,CZERO/(0.0,1.0),(0.0,0.0)/
C-----
      DO 1 L=1,5
      RXKN(L)=SX(L)+IKK*RLAMDA(L)/DX-INN*RLAMDA(L)*DELTZ/(DX*DZ)
      RZKN(L)=SZ(L)+INN*RLAMDA(L)/DZ
      YR=1.0-RXKN(L)*RXKN(L)-RZKN(L)*RZKN(L)
```

```
874         IF(YR .LT. 0.0)RYKN(L)=CMPLX(0.0,-SQRT(-YR))
875         IF(YR .GT. 0.0)RYKN(L)=CMPLX(SQRT(YR),0.0)
876 1       CONTINUE
877         RETURN
878         END
879 C  ***************************************************************
880 C
881 C***PATRN
882 C
883 C       THIS SUBROUTINE CALCULATES THE PATTERN FUNCTION ASSUMING
884 C       EITHER A SINUSOIDAL OR COSINUSOIDAL VOLTAGE DISTRIBUTION
885 C       FOR TRANSMITTING AND NON-TRANSMITTING MODES (SEE IVD)
886 C
887 C       INPUT VARIABLES
888 C        IVD=1(SINUSOIDAL V DSTR IS USED FOR T AND NT MODES)
889 C           =2(SINUSOIDAL V DSTR IS USED FOR T MODE AND COSINUSOIDAL
890 C              IS USED FOR NT MODE)
891 C        BETAD=RELATIVE PROPAGATION CONSTANT
892 C        RL=LENGTH OF EACH LEG
893 C        EFFL=EFFECTIVE LENGTH OF EACH LEG
894 C        ELEMX,ELEMZ=X,Z COMPONENTS OF LEG DIRECTIONS
895 C        LSLOT=1(ONE ARRAY),=2(THE OTHER ARRAY)
896 C       OUTPUT VARIABLES
897 C        PATX,PATZ=X,Z COMPONENTS OF THE TOTAL PATTERN OF EACH LEG
898 C
899         SUBROUTINE PATTRN(IVD,NTRNS,BETAL,RL,EFFL,ELEMX
900        1,ELEMZ,LSLOT,PATX,PATZ)
901         COMPLEX PATX(3),PATZ(3),PAT,CELEMX,CELEMZ,DF
902        1,CRXKN,CRZKN,DOT
903        2,CXP1,CXP2,CXP3,CXP4
904         DIMENSION ELEMX(2,3),ELEMZ(2,3)
905 C---COMMON BLOCK
906 C
907         COMMON RXKN,RYKN,RZKN,BETA,D,ER
908         COMPLEX RYKN(5),CJ,CZERO
```

```
      DIMENSION RXKN(5),RZKN(5),BETA(5),U(5),PR(5)
      DATA CJ,CZERO/(0.0,1.0),(0.0,0.0)/
C-----
      CRXKN=CMPLX(RXKN(1),0.0)
      CRZKN=CMPLX(RZKN(1),0.0)
      IF(IVO.EQ.1) GOTO 1
      GOTO (1,3),NTRNS
C      ASSUMES SINUSOIDAL VOLTAGE DISTRIBUTION
1     BELE=BETAD*EFFL
      DENOM=2.0*SIN(BELE)
      BTME=-BETA(1)
      IF(NTRNS.EQ.2)BTME=-BTME
      DO 2 LEG=1,3
      CELEMX=CMPLX(ELEMX(LSLOT,LEG),0.0)
      CELEMZ=CMPLX(ELEMZ(LSLOT,LEG),0.0)
      DP=DOT(CELEMX,CZERO,CELEMZ,CRXKN,RYKN(1),CRZKN)
      PAT=(CEXP(CJ*(BELE-BETAD*RL+BTME*DP*PL))
     1-CEXP(CJ*BELE))/(BETAD-BTME*DP)
     2+(CEXP(-CJ*(BELE-BETAD*RL-BTME*DP*RL))
     3-CEXP(-CJ*BELE))/(BETAD+BTME*DP)
      PATX(LEG)=ELEMX(LSLOT,LEG)*PAT/DENOM
2     PATZ(LEG)=ELEMZ(LSLOT,LEG)*PAT/DENOM
      RETURN
C      ASSUMES COSINUSOIDAL VOLTAGE DISTRIBUTION
3     CXP2=CEXP(CJ*BETAD*RL)
      CXP3=CEXP(-CJ*BETAD*RL)
      BELEC=COS(BETAD*EFFL)
      DENOM=2.0*(1.0-BELEC)
      DO 4 LEG=1,3
      CELEMX=CMPLX(ELEMX(LSLOT,LEG),0.0)
      CELEMZ=CMPLX(ELEMZ(LSLOT,LEG),0.0)
      DP=DOT(CELEMX,CZERO,CELEMZ,CRXKN,RYKN(1),CRZKN)
      CXP1=CEXP(CJ*BETA(1)*RL*DP)
      CXP4=RL/CJ
      IF(CABS(DP).NE.0.0) CXP4=(1.0-CXP1)/(BETA(1)*DP)
```

AD-A084 663 OHIO STATE UNIV COLUMBUS ELECTROSCIENCE LAB F/G 9/5
BROADBAND METALLIC RADOME.(U)
SEP 79 J S ERNST F33615-76-C-1024
UNCLASSIFIED ESL-784346-11 AFAL-TR-79-1142 NL

2 OF 2
AD
A084963

END
DATE FILMED
6-80
DTIC

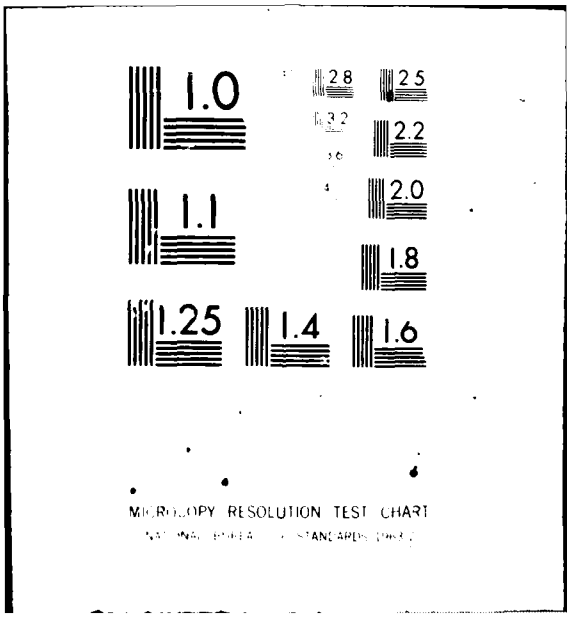
1.0
2.8
2.5
3.2
2.2
2.0
1.1
1.8
1.25
1.4
1.6
MICROCOPY RESOLUTION TEST CHART

```
      PAT=(1.0-CXP2*CXP1)/(BETAD+BETA(1)*DP)
     1+(CXP3*CXP1-1.0)/(BETAD-BETA(1)*DP)
     2-2.0*BELEC*CXP4
C       COMPONENTS OF THE PATTERN DUE TO EACH LEG
      PATX(LEG)=ELEMX(LSLOT,LEG)*PAT*CJ/DENOM
     4  PATZ(LEG)=ELEMZ(LSLOT,LEG)*PAT*CJ/DENOM
      RETURN
      END
C
C***OPCOMP
C
C     THIS SUBROUTINE CALCULATES THE ORTHOGONAL AND PARALLEL
C     COMPONENTS OF THE COMPOSITE PATTERN FACTORS
C
C     INPUT VARIABLES
C      MEDIA=MEDIA IN WHICH PROPAGATION VECTOR IS CALCULATED
C      CXCOMP,CYCOMP,CZCOMP=VECTOR COMPONENTS OF WHICH ORTHOGONAL
C       OR PARALLEL COMPONENTS TO PLANE OF INCIDENCE IS DESIRED
C     OUTPUT VARIABLES
C      OTOT=ORTHOGONAL RESULT
C      PTOT=PARALLEL RESULT
C
      SUBROUTINE OPCOMP(MEDIA,CXCOMP,CZCOMP,OTOT,PTOT)
      COMPLEX CXCOMP,CZCOMP,OTOT,PTOT,CRXKN,CRZKN,DOT
C---COMMON BLOCK
C
      COMMON RXKN,RYKN,RZKN,BETA,D,ER
      COMPLEX RYKN(5),CJ,CZERO
      DIMENSION RXKN(5),RZKN(5),BETA(5),D(5),ER(5)
      DATA CJ,CZERO/(0.0,1.0),(0.0,0.0)/
C-------
      CRXKN=CMPLX(RXKN(MEDIA),0.0)
      CRZKN=CMPLX(RZKN(MEDIA),0.0)
      RXZ=SQRT(RXKN(MEDIA)*RXKN(MEDIA)+RZKN(MEDIA)*RZKN(MEDIA))
C        CALCULATE THE ORTHOGONAL PATTERN FACTOR
```

```
      OTOT=DOT(CXCOMP,CZERO,CZCOMP,-CRZKN/RXZ
     1,CZERO,CRXKN/RXZ)
C         CALCULATE THE PARALLEL PATTERN FACTOR
      PTOT=DOT(CXCOMP,CZERO,CZCOMP,-CRXKN
     2*RYKN(MEDIA)/RYZ,CZERO,-CRZKN*RYKN(MEDIA)/RXZ)
      RETURN
      END
C  ***********************************************************
C
C***TYF
C
C     THIS SUBROUTINE CALCULATES THE NON-NORMALIZED TRANSFORMATION
C     FUNCTION USED IN ADMITTANCE CALCULATIONS
C
C     INPUT VARIABLES
C      NADMT=NUMBER OF ADMITTANCE BEING CALCULATED--SEE
C           SUBROUTINE ADMIT
C     OUTPUT VARIABLES
C      TFACT(A,B)=NON-NORMALIZED TRANSFORMATION FUNCTION
C        WHERE A=1(ORTHOGONAL),2(PARALLEL)
C              B=DIELECTRIC MEDIA NUMBER
C
      SUBROUTINE TYF(NADMT,TFACT)
      COMPLEX RHO(5,5),TFACT(2,5),FXPT,EXP2,EXP3,EXP4
C---COMMON BLOCK
C
      COMMON RAKN,RYKN,RZKN,BETA,D,ER
      COMPLEX RYKN(5),CJ,CZERO
      DIMENSION RXKN(5),RZKN(5),BETA(5),D(5),ER(5)
      DATA CJ,CZERO/(0.0,1.0),(0.0,0.0)/
C-----
      GOTO (1,1,1,1,2,2,2,2,2,2,2,3,3,3,3),NADMT
1     EXP2=EXPT(2,2.0)
      EXP3=EXPT(3,2.0)
      DO 4 LORTHO=1,2
```

```
      CALL REFLX(LORTHO,2,RHO)
      TFACT(LORTHO,2)=2.0*(1.0+RHO(2,1)
     1*EXP2)/(1.0-RHO(2,1)*EXP2)
      TFACT(LORTHO,3)=2.0*(1.0+EXP3)/(1.0-EXP3)
      RETURN
    2 EXP3=EXPT(3,2.0)
      DO 5 LORTHO=1,2
    5 TFACT(LORTHO,3)=4.0/(1.0-EXP3)
      RETURN
    3 EXP4=EXPT(4,2.0)
      EXP5=EXPT(5,2.0)
      DO 6 LORTHO=1,2
      CALL REFLX(LORTHO,5,RHO)
      TFACT(LORTHO,4)=2.0*(1.0+RHO(4,5)
     1*EXP4)/(1.0-RHO(4,5)*EXP4)
    6 TFACT(LORTHO,3)=2.0*(1.0+EXP3)/(1.0-EXP3)
      RETURN
      END
C
C***REFLX
C
C     THIS SUBROUTINE CALCULATES THE REFLECTION COEFFICIENTS FOR
C     H-FIELD AT DIELECTRIC INTERFACES
C
C     INPUT VARIABLES
C      LORTHO=1(ORHTOGONAL),2(PARALLEL)  RHO IS CALCULATED
C      L=MEDIA NUMBER OF ONE OF THE DIELECTRICS RHO IS NEEDED
C     OUTPUT VARIABLES
C      RHO=REFLECTION COEFFICIENT
C
      SUBROUTINE REFLX(LORTHO,L,RHO)
      COMPLEX RHO(5,3)
C---COMMON BLOCK
C
      COMMON RXKN,RYKN,RZKN,RETA,D,ER
      COMPLEX RYKN(5),CJ,CZERO
```

```
      DIMENSION RXKN(5),RZKN(5),BETA(5),U(5),ER(5)
      DATA CJ,CZERO/(0.0,1.0),(0.0,0.0)/
C-----
      SQ1=SQRT(ER(L-1))
      SQ2=SQRT(ER(L))
      GOTO (1,2),LORTHO
C    ORTHOGONAL H
 1    RHO(L-1,L)=(SQ2*RYKN(L-1)-SQ1
     1*RYKN(L))/(SQ2*RYKN(L-1)+SQ1*RYKN(L))
      RHO(L,L-1)=-RHO(L-1,L)
      RETURN
C    PARALLEL H
 2    RHO(L-1,L)=(SQ2*RYKN(L)-SQ1
     1*RYKN(L-1))/(SQ2*RYKN(L)+SQ1*RYKN(L-1))
      RHO(L,L-1)=-RHO(L-1,L)
      RETURN
      END
C  ***********************************************************************
C
C***EXPYS
C
C     THIS FUNCTION SUBROUTINE CALCULATES THE NEEDED EXPONENTIAL
C     FOR SELF ADMITTANCE CALCULATIONS
C
C     INPUT VARIABLES
C      MEDIA=DETERMINES IN WHICH DIELECTRIC CALCULATIONS ARE MADE
C     OUTPUT VARIABLES
C      EXPYS=COMPLEX EXPONENTIAL ADMITTANCE SELF
C
      COMPLEX FUNCTION EXPYS(MEDIA)
      COMPLEX ARGUM,PHASE
      COMMON/EXPNY/WIDTH
C
C---COMMON BLOCK
C
```

```
      COMMON RXKN,RYKN,RZKN,BETA,D,ER
      COMPLEX RYKN(5),CJ,CZERO
      DIMENSION RXKN(5),RZKN(5),BETA(5),D(5),ER(5)
      DATA CJ,CZERO/(0.0,1.0),(0.0,0.0)/
C-----
      ARGUM=BETA(MEDIA)*WIDTH/2.0*RYKN(MEDIA)
C      THE FOLLOWING TWO STATEMENTS ELIMINATES ANY ERROR MESSAGES
C      WHEN EXPONENTIALS EXCEED CERTAIN LIMITS--NO ACTUAL ERROR
      IF(AIMAG(ARGUM).LE.-50.0)PHASE=CMPLX(0.0,0.0)
      IF(AIMAG(ARGUM).GT.-50.0)PHASE=CEXP(-CJ*ARGUM)
      IF(REAL(RYKN(MEDIA)).NE.0.0)PHASE=CMPLX(1.0,0.0)
      EXPYS=SQRT(ER(MEDIA))*PHASE/RYKN(MEDIA)
      RETURN
      END
C  ***************************************************************
C
C***EXPYM
C
C      THIS FUNCTION SUBROUTINE CALCULATES THE NEEDED EXPONENTIAL
C      FOR MUTUAL ADMITTANCE CALCULATIONS
C
C      INPUT VARIABLES
C       MEDIA=DETERMINES IN WHICH DIELECTRIC CALCULATIONS ARE MADE
C      OUTPUT VARIABLES
C       EXPYM=COMPLEX EXPONENTIAL ADMITTANCE MUTUALS
C
      COMPLEX FUNCTION EXPYM(MEDIA)
      COMPLEX EXPT
C---COMMON BLOCK
C
      COMMON RXKN,RYKN,RZKN,BETA,D,ER
      COMPLEX RYKN(5),CJ,CZERO
      DIMENSION RXKN(5),RZKN(5),BETA(5),D(5),ER(5)
      DATA CJ,CZERO/(0.0,1.0),(0.0,0.0)/
C-----
```

```
      EXPYM=SQRT(ER(MEDIA))*EXPT(MEDIA,1.0)/RYKN(MEDIA)
      RETURN
      END
C  ***************************************************************
C
C***EXPT
C
C     THIS FUNCTION SUBROUTINE CALCULATES A FREQUENTLY USED
C     COMPLEX EXPONENTIAL
C
C     INPUT VARIABLES
C      RMULT=REAL MULTIPLIER,VALUE DEPENDS ON PHYSICAL SITUATION
C      MEDIA=DETERMINES IN WHICH DIELECTRIC CALCULATIONS ARE MADE
C     OUTPUT VARIABLES
C      EXPT=COMPLEX EXPONENTIAL
C
      COMPLEX FUNCTION EXPT(MEDIA,RMULT)
      COMPLEX ARGUM
C
C---COMMON BLOCK
C
      COMMON RXKN,RYKN,RZKN,BETA,D,ER
      COMPLEX RYKN(5),CJ,CZERO
      DIMENSION RXKN(5),RZKN(5),BETA(5),D(5),ER(5)
      DATA CJ,CZERO/(0.0,1.0),(0.0,0.0)/
C-----
      ARGUM=RMULT*BETA(MEDIA)*D(MEDIA)*RYKN(MEDIA)
C      SEE COMMENT IN PREVIOUS SUBROUTINE EXPYS
      IF(AIMAG(ARGUM).GT.-50.0)EXPT=CEXP(-CJ*ARGUM)
      IF(AIMAG(ARGUM).LE.-50.0)EXPT=CMPLX(0.0,0.0)
      RETURN
      END
C  ***************************************************************
C
C***CURNT
C
```

```
C      THIS SUBROUTINE CALCULATES THE INCIDENT AND TRANSMITTED H FIELD
C
C      SEE SUBROUTINE ADMIT FOR VARIABLE LISTING
C
       SUBROUTINE CURNT(IVD,ELEMX,ELEMZ,RLF,BTD,RLAMDA
      1,SX,SZ,DX,DZ,DELTZ,RL,YADMT)
       COMPLEX PATX(3),PATZ(3),SPATX(2,2),SPATZ(2,2)
      1,APATX(2,2),APATZ(2,2),XPAT,ZPAT,SCPAT(2,5,2)
      2,ACPAT(2,5,2),TFACT(2,5),YADMT(16),CPATC,PPATC,EXPT
      3,FACTOR,CS1(2),CA1(2),VS2(2),VA2(2),CHO,CHP,PHO,PHP
       DIMENSION ELEMX(2,3),ELEMZ(2,3),PLAMDA(5),SX(5),SZ(5)
      1,BTD(2),RLF(2)
C---COMMON BLOCK
C
       COMMON RXKN,RYKN,RZKN,BETA,D,ER
       COMPLEX RYKN(5),CJ,CZERO
       DIMENSION RXKN(5),RZKN(5),BETA(5),D(5),ER(5)
       DATA CJ,CZERO/(0.0,1.0),(0.0,0.0)/
C-----
       CALL DIRECT(0.0,0.0,PLAMDA,SX,SZ,DX,DZ,DELTZ)
       DO 1 LSLOT=1,2
C   THE FOLLOWING STATEMENT JUST WORKS,NO PHYSICAL MEANING
       NTRNS=LSLOT
       BETAD=BTD(LSLOT)
       EFFL=RLF(LSLOT)
       CALL PATTRN(IVD,NTRNS,BETAD,RL,EFFL,ELEMX,ELEMZ,LSLOT
      1,PATX,PATZ)
       SPATX(LSLOT,NTRNS)=2.0*PATX(1)-PATX(2)
      1-PATX(3)
       SPATZ(LSLOT,NTRNS)=2.0*PATZ(1)-PATZ(2)
      1-PATZ(3)
       APATX(LSLOT,NTRNS)=PATX(2)-PATX(3)
1      APATZ(LSLOT,NTRNS)=PATZ(2)-PATZ(3)
       XPAT=SPATX(1,1)
       ZPAT=SPATZ(1,1)
```

```
      CALL OPCOMP(1,XPAT,ZPAT,OPATC,PPATC)
      SCPAT(1,1,1)=OPATC
      SCPAT(2,1,1)=PPATC
      XPAT=APATX(1,1)
      ZPAT=APATZ(1,1)
      CALL OPCOMP(1,XPAT,ZPAT,OPATC,PPATC)
      ACPAT(1,1,1)=OPATC
      ACPAT(2,1,1)=PPATC
      DO 2 LORTHO=1,2
      CALL TIF(LORTHO,IFACT)
C      CS1(A)=SYMMETRIC CURRENT OF ARRAY 1
C      CA1(A)=ASYMMETRIC CURRENT OF ARRAY 2
C        WHERE A=1(ORTHOGONAL),2(PARALLEL)
      CS1(LORTHO)=SCPAT(LORTHO,1,1)*IFACT(LORTHO,2)*EXPT(2,1,0)
     1*EXPT(1,1,0)
2     CA1(LORTHO)=ACPAT(LORTHO,1,1)*IFACT(LORTHO,2)*EXPT(2,1,0)
     1*EXPT(1,1,0)
      CALL VOLT(YADMT,CS1,CA1,VS2,VA2)
      XPAT=SPATX(2,2)
      ZPAT=SPATZ(2,2)
      CALL OPCOMP(5,XPAT,ZPAT,OPATC,PPATC)
      SCPAT(1,5,2)=OPATC
      SCPAT(2,5,2)=PPATC
      XPAT=APATX(2,2)
      ZPAT=APATZ(2,2)
      CALL OPCOMP(5,XPAT,ZPAT,OPATC,PPATC)
      ACPAT(1,5,2)=OPATC
      ACPAT(2,5,2)=PPATC
      FACTOR=EXPT(4,1.0)*EXPT(5,1.0)*SQRT(ER(5))/
     1(RYKN(5)*2.0*DX*DZ*376.82)
C      OHO=ORTHOGONAL INCIDENT H FIELD ORTHOGONAL TRANSMITTED
C      OHP=     "          "    "    "    PARALLEL       "
C      PHO= PARALLEL       "    "    "   ORTHOGONAL      "
C      PHP=     "          "    "    "    PARALLEL       "
      OHO=(VS2(1)*SCPAT(1,5,2)+VA2(1)*ACPAT(1,5,2))
     1*IFACT(1,4)*FACTOR
```

```
      OHP=(VS2(1)*SCPAT(2,5,2)+VA2(1)*ACPAT(2,5,2))
     1*TFACT(2,4)*FACTOR
      PHO=(VS2(2)*SCPAT(1,5,2)+VA2(2)*ACPAT(1,5,2))
     1*TFACT(1,4)*FACTOR
      PHP=(VS2(2)*SCPAT(2,5,2)+VA2(2)*ACPAT(2,5,2))
     1*TFACT(2,4)*FACTOR
      CALL PRINTC(6HOHO...,OHO,1,1)
      CALL PRINTC(6HOHP...,OHP,1,1)
      CALL PRINTC(6HPHO...,PHO,1,1)
      CALL PRINTC(6HPHP...,PHP,1,1)
      RETURN
      END
C  ***************************************************************
C
C***VOLT
C
C     THIS SUBROUTINE SETS UP THE MATRICES FOR CALCULATING THE
C     VOLTAGES ON SLOT ARRAY NUMBER 2
C
C     INPUT VARIABLES
C      YADMT=THE ADMITTANCES
C      CS1,CA1=SEE SUBROUTINE CURNT
C     OUTPUT VARIABLES
C      VS2(A)=SYMMETRIC VOLTAGE OF ARRAY 2
C      VA2(A)=ASYMMETRIC VOLTAGE OF ARRAY 2
C        WHERE A=1(ORTHOGONAL),2(PARALLEL)
C
      SUPROUTINE VOLT(YADMT,CS1,CA1,VS2,VA2)
      COMPLEX YADMT(16),CS1(2),CA1(2),VS2(2),VA2(2),Z(4,4)
     1,DET,DETD
      DO 1 I=1,5
      Z(1,1)=YADMT(1)
      Z(1,2)=YADMT(2)
      Z(2,1)=YADMT(3)
      Z(2,2)=YADMT(4)
```

```
1262          Z(3,1)=YADMT(9)
1263          Z(3,2)=YADMT(10)
1264          Z(4,1)=YADMT(11)
1265          Z(4,2)=YADMT(12)
1266          GOTO (2,3,3,4,4),I
1267  2       Z(1,3)=YADMT(5)
1268          Z(1,4)=YADMT(6)
1269          Z(2,3)=YADMT(7)
1270          Z(2,4)=YADMT(8)
1271          Z(3,3)=YADMT(13)
1272          Z(3,4)=YADMT(14)
1273          Z(4,3)=YADMT(15)
1274          Z(4,4)=YADMT(16)
1275          CALL DETER(Z,DET)
1276          DETD=DET
1277          GOTO 1
1278  3       LORTHO=I-1
1279          Z(1,3)=CS1(LORTHO)
1280          Z(1,4)=YADMT(6)
1281          Z(2,3)=CA1(LORTHO)
1282          Z(2,4)=YADMT(8)
1283          Z(3,3)=CMPLX(0.0,0.0)
1284          Z(3,4)=YADMT(14)
1285          Z(4,3)=CMPLX(0.0,0.0)
1286          Z(4,4)=YADMT(16)
1287          CALL DETER(Z,DET)
1288          VS2(LORTHO)=DET/DETD
1289          GOTO 1
1290  4       LORTHO=I-3
1291          Z(1,3)=YADMT(5)
1292          Z(1,4)=CS1(LORTHO)
1293          Z(2,3)=YADMT(7)
1294          Z(2,4)=CA1(LORTHO)
1295          Z(3,3)=YADMT(13)
1296          Z(3,4)=CMPLX(0.0,0.0)
1297          Z(4,3)=YADMT(15)
```

```
1298          Z(4,4)=CMPLX(0.0,0.0)
1299          CALL DETER(Z,DET)
1300          VAR(LORTHO)=DET/DETO
1301    1     CONTINUE
1302          RETURN
1303          END
1304    C     ***************************************************************
1305    C
1306    C***TIF
1307    C
1308    C     THIS SUBROUTINE CALCULATES THE NORMALIZED TRANSFORMATION FUNCTION
1309    C     NEEDED IN CALCULATING THE INCIDENT FIELD AND TRANSMITTED FIELD
1310    C
1311    C     SEE SUBROUTINE TYF FOR VARIABLE LISTING
1312    C
1313          SUBROUTINE TIF(LORTHO,TFACT)
1314          COMPLEX TFACT(2,5),RHO(5,5),EXPT
1315    C---COMMON BLOCK
1316    C
1317          COMMON RXKN,RYKN,RZKN,BETA,D,ER
1318          COMPLEX RYKN(5),CJ,CZERO
1319          DIMENSION RXKN(5),RZKN(5),BETA(5),D(5),ER(5)
1320          DATA CJ,CZERO/(0.0,1.0),(0.0,0.0)/
1321    C-----
1322          CALL REFLX(LORTHO,2,RHO)
1323          TFACT(LORTHO,2)=2.0*(1.0-RHO(2,1))
1324         1/(1.0-RHO(2,1)*EXPT(2,2.0))
1325          CALL REFLX(LORTHO,5,RHO)
1326          TFACT(LORTHO,4)=2.0*(1.0-RHO(4,5))
1327         1/(1.0-RHO(4,5)*EXPT(4,2.0))
1328          RETURN
1329          END
1330    C     ***************************************************************
1331    C
1332    C***DETER
1333    C
```

```
1334 C      WRITTEN JACK RICHMOND--MODIFIED BY J.S.ERNST
1335 C
1336 C      THIS SUBROUTINE CALCULATES THE DETERMINATE OF THE ADMITTANCE
1337 C      MATRIX
1338 C
1339 C      INPUT VARIABLE
1340 C       Z=YAUNT=SELF AND MUTUAL ADMITTANCES
1341 C      OUTPUT VARIABLE
1342 C       DET=DETERMINATE
1343 C
1344        SUBROUTINE DETER(Z,DET)
1345        COMPLEX Z(4,4),BIGZ,HOLD,DET
1346        DIMENSION L(4),M(4)
1347        N=4
1348        DET=(1.,0.)
1349        DO 80 K=1,N
1350        L(K)=K
1351        M(K)=K
1352        BIGZ=Z(K,K)
1353        DO 20 J=K,N
1354        DO 20 I=K,N
1355   10   IF(CABS(BIGZ)-CABS(Z(I,J)))15,19,19
1356   15   BIGZ=Z(I,J)
1357        L(K)=I
1358        M(K)=J
1359 19     CONTINUE
1360 20     CONTINUE
1361        J=L(K)
1362        IF(J-K)35,35,25
1363 25     CONTINUE
1364        DO 30 I=1,N
1365        HOLD=-Z(K,I)
1366        Z(K,I)=Z(J,I)
1367   30   Z(J,I)=HOLD
1368 35     I=M(K)
```

```
      IF(I-K) 45,45,38
38    CONTINUE
      DO 40 J=1,N
      HOLD=-Z(J,K)
      Z(J,K)=Z(J,I)
40    Z(J,I)=HOLD
45    CONTINUE
      DO 55 I=1,N
      IF(I-K)50,55,50
50    Z(I,K)=Z(I,K)/(-BIGZ)
55    CONTINUE
      DO 65 I=1,N
      DO 65 J=1,N
      IF(I-K)60,64,60
60    IF(J-K)62,64,62
62    Z(I,J)=Z(I,K)*Z(K,J)+Z(I,J)
64    CONTINUE
65    CONTINUE
      DO 75 J=1,N
      IF(J-K)70,75,70
70    Z(K,J)=Z(K,J)/BIGZ
75    CONTINUE
      DET=DET*BIGZ
      Z(K,K)=1./BIGZ
80    CONTINUE
      RETURN
      END
C     ***************************************************************
```

```
C PRINT SUBROUTINES FOR 2989M V:04
C
C J.F.STOSIC  NOV.6,78
C
C$$$$$$
C
      SUBROUTINE PRINTK(LAB,X,IVAR,IDB)
C
C PRINT REAL X: VALUE,(OPTION,DB)
C
C.IN  LAB   :A 6 CHARACTER HOLLERITH IDENTIFIER
C.IN  X     :THE VARIABLE TO BE PRINTED
C.IN  IVAR  :THE BINVARY CODE OF THIS VARIABLE
C.          :IF IVAR < 0, A BLANK LINE IS PRINTED FIRST
C.          :IF IVAR > 0, NO BLANK LINE IS PRINTED
C.IN  IDB   :IF IDB=1, MAGNITUDE IS ALSO PRINTED IN DB
C.COM IOC   :IS THE I/O CODE, BINARY SUM OF DESIRED OUTPUTS
C
      DIMENSION LAB(2)
      COMMON /PRINT/ IOC
C
      IF((IABS(IVAR).AND.IOC).EQ.0) RETURN
      IF(IVAR.LT.0) WRITE(6,10)
10    FORMAT('*')
      IF(IDB.NE.1) GOTO 120
      B=-100.00
      IF(X.GT.0.0) B=20.0*ALOG10(X)
      WRITE(6,20) LAB,X,B
20    FORMAT(2A3,'=',(1X,1PG13.4),2X,0PF8.4)
      RETURN
120   WRITE(6,20) LAB,X
      RETURN
      END
C
C$$$$$$
```

```
C
      SUBROUTINE PRINTC(LAB,X,IVAR,IOB)
C
C PRINT COMPLEX X; REAL,IMAGINARY,MAGNITUDE,PHASE(DEG).;MAG,DB
C
C
      COMPLEX X
      DIMENSION LAB(2)
      COMMON /PRINT/ IOC
C
C.IN  LAB    :A 6 CHARACTER HOLLERITH IDENTIFIER
C.IN  X      :THE VARIABLE TO BE PRINTED
C.IN  IVAR   :THE BINARY CODE OF THIS VARIABLE
C.           :IF IVAR < 0, A BLANK LINE IS PRINTED FIRST
C.           :IF IVAR > 0, NO BLANK LINE IS PRINTED
C.IN  IOB    :IF IOB=1. MAGNITUDE IS ALSO PRINTED IN DB
C.COM IOC    :IS THE I/O CODE. BINARY SUM OF DESIRED OUTPUTS
C
      IF((IABS(IVAR).AND.IOC).EQ.0) RETURN
      IF(IVAR.LT.0) WRITE(6,10)
10    FORMAT('*')
      A=CABS(X)
      P=57.295779*ATAN2(AIMAG(X),REAL(X))
      IF(IOB.NE.1) GOTO 120
      B=-100.00
      IF(A.GT.0.0) B=20.0*ALOG10(A)
      WRITE(6,30) LAB,X,A,P,B
30    FORMAT(2A3,'=',3(1X,1PG13.4),1X,0PF7.2,1X,0PF8.4)
      RETURN
120   WRITE(6,30) LAB,X,A,P
      RETURN
      END
C
C$$$$$$
C
```

```
      SUBROUTINE PRINTI(LAB,I1,X,IVAR,IDB)
C
C PRINT COMPLEX 'X' WITH SINGLE INDEX (SEE 'PRINTC')
C
C.IN  LAB    :A 6 CHARACTER HOLLERITH IDENTIFIER
C.           :THE LAST TWO CHARACTERS ARE REPLACED
C.IN  I1     :INDEX OF VARIABLE NAME
C
      COMPLEX X
      DIMENSION LAB(2)
C
      LAB(2)=LAB(2).AND.'77600000
      LAB(2)=LAB(2)+('54)*256+('60+I1)
      CALL PRINTC(LAB,X,IVAR,IDB)
      RETURN
      END
C
C$$$$$$
C
      SUBROUTINE PRINTD(LAB3,I1,I2,X,IVAR,IDB)
C
C PRINT COMPLEX 'X' WITH DOUBLE INDICIES (SEE 'PRINTC')
C
C.IN  LAB3  :A 3 CHARACTER HOLLERITH IDENTIFIER
C.IN  I1,I2 :ARE THE INDICIES OF THE VARIABLE
C
      COMPLEX X
      DIMENSION LAB(2)
C
      LAB(1)=LAB3
      LAB(2)=('60+I1)*65536+('54)*256+('60+I2)
      CALL PRINTC(LAB,X,IVAR,IDB)
      RETURN
      END
```

```
105 C
106 C$$$$$$
107 C
108       SUBROUTINE PRINTL
109 C
110 C INITIALIZATION
111 C
112       DIMENSION IBUF(24),IFILE(2),IUSER(2)
113       LOGICAL LOGIC
114       DATA IEND/3H EN/
115 C
116 C*** ASSIGN NAMES TO INPUT(5) & OUTPUT(6) FILES ***
117 C
118 100   WRITE(8,10)
119 10    FORMAT('INPUT')
120       CALL RDFLNM(IFILE,IUSER)
121       CALL ASSIGN(IFILE,IUSER,5,$100)
122 110   WRITE(8,11)
123 11    FORMAT('OUTPUT')
124       CALL RDFLNM(IFILE,IUSER)
125       CALL ADNWOL(IFILE,IUSER,6,$110)
126 C
127 C*** DECISION ON BACKGROUND PROCESSING, PROGRESS(4) FILE ***
128 C
129       WRITE(8,12)
130 12    FORMAT('BACKGROUND (T OR F)?')
131       READ(8,=) LOGIC
132       IF(.NOT.LOGIC) GOTO 140
133 190   WRITE(8,13)
134 13    FORMAT('PROGRESS')
135       CALL RDFLNM(IFILE,IUSER)
136       CALL ASSIGN(IFILE,IUSER,4,$130)
137       CLOSE 4
138       CALL DEASSN
139 140   CONTINUE
```

```
140 C
141 C*** DELETE THE TEMPORARY FILE CREATED BY THE COMPILER ***
142 C
143       CALL LUDEL(3)
144 C
145 C*** TRANSFER THE INPUT FILE TO THE OUTPUT FILE ***
146 C
147 150   READ(5,30) (IBUF(I),I=1,24)
148 30    FORMAT(24A3)
149       WRITE(6,40) (IBUF(I),I=1,24)
150 40    FORMAT(1H ,24A3)
151       IF(IBUF(3).NE.IEND) GOTO 150
152 C
153 C*** PRINT THE OUTPUT HEADER ***
154 C
155       CALL PRINTH
156 C
157       CLOSE 5
158       RETURN
159       END
160 C
161 C$$$$$
162 C
163       SUBROUTINE PRINTH
164 C
165 C PRINT AN OUTPUT HEADER
166 C
167       WRITE(6,90)
168 90    FORMAT('COMPLEX VALUES: REAL,IMAGINARY,MAGNITUDE,'
169      # 'PHASE(DEG),[MAG.(DB)]'
170      # /'FREQ(GHZ), ALPHA-ETA(DEG), ADMITTANCES(MHOS)')
171       RETURN
172       END
173 C
174 C$$$$$
175 C
```

```
      SUBROUTINE PRINTF(FREQ,ALPHA,ETA)
C
C PRINT FREQUENCY AND ANGLES
C
      WRITE(6,50) FREQ,ALPHA,ETA
50    FORMAT(66('*')/'*'/'FREQ='F8.5'  ALPHA='
     # F6.2'    ETA='F6.2)
C
C*** UPDATE THE PROGRESS FILE ***
C
      WRITE(4,60) FREQ,ALPHA,ETA
60    FORMAT('FREQ,ALPHA,ETA: ',3(1X,F6.2))
      CLOSE 4
      RETURN
      END
C
C$$$$$$
C
      SUBROUTINE PRINTE(ITA1,ITA3,ITA2,IT1,IT4)
C
C TIME AND DATE, END OF FILE
C
      DIMENSION ITA1(3),ITA2(3),ITA3(3)
      WRITE(6,90) ITA1,ITA3,ITA2,IT1,IT4
90    FORMAT(66('*')/'*'/'START TIME   = '3A3' DATE= '3A3
     # /'STOP TIME    = '3A3/'CPU TIME(SEC)= 'I8
     # /'  CPU AVGERAGE CASE TIME(SEC)= 'I4)
C
      CALL LODEL(4)
      RETURN
      END
C
```

```
C WRITTEN BY C.J.LARSON--MODIFIED BY J.F.STOSIC
C GENERAL SUBROUTINES NEEDED FOR PROGRAM
C
C$$$$$$
C
      FUNCTION DOT(AX,AY,AZ,BX,BY,BZ)
C
C COMPUTE THE DOT PRODUCT OF TWO COMPLEX VECTORS
C.IN  AX,AY,AZ  :X,Y,Z COMPONENTS OF THE A VECTOR
C.IN  BX,BY,BZ  :X,Y,Z COMPONENTS OF THE B VECTOR
C
      COMPLEX AX,AY,AZ,BX,BY,BZ,DOT
      DOT=AX*BX+AY*BY+AZ*BZ
      RETURN
      END
C
C$$$$$$
C
      SUBROUTINE DELL(HL,W,T,RLAMDA,SRER,DL)
C
C CALCULATION OF AN INCREMENTAL LENGTH TO BE ADDED TO
C A SLOT OR FLAT WIRE DIPOLE DUE TO END EFFECTS.
C SEE DISSERTATION BY B. MUNK, APPENDIX A
C XHAT: EQ(A-19), XHAT: EQ(A-33), DL: EQ(A-23) & EQ(A-30)
C
C ALL OF THE DIMENSIONS HAVE THE SAME UNITS, EG. CM
C.IN  HL      :HALF-LENGTH
C.IN  W,T     :WIDTH & THICKNESS OF SLOT OR DIPOLE
C.IN  RLAMDA  :FREE SPACE WAVELENGTH
C.IN  SRER    :SQUARE ROOT OF EFFECTIVE DIELECTRIC CONSTANT
C.OUT DL      :'DELTA L', TO BE ADDED TO HALF-LENGTH
C
      DATA PI,P12 /3.14159265, 1.57079633/
      B=2.0*PI/RLAMDA
C
```

```
C*** CALCULATE ELECTRICAL LENGTHS ***
C
      EL=ABS(HL)*SRER
      E*=W*SRER
      ET=T*SRER
      BL=B*EL
      BL2=2.0*BL
      BL4=4.0*BL
C
      CALL SICI(SIBL,CIBL,BL)
      SIPL=SIBL+PI2
      CALL SICI(SI2BL,CI2BL,BL2)
      SI2BL=SI2BL+PI2
      CALL SICI(SI4BL,CI4BL,BL4)
      SI4BL=SI4BL+PI2
C
      KHAT=120.0*(ALOG(RLAMDA/(PI*FW))+CIBL+0.769357926)
      IF(2.0*EL/EW.LT.15.0)KHAT=KHAT-41.58886085
C
      XHAT=60.0*SI2BL+30.0*(2.0*SI2BL-SI4BL)*COS(BL2)+30.0*(CI4BL
     # +2.0*CIBL-2.0*CI2BL-ALOG(BL4)+2.19537305)*SIN(BL2)
C
      EDL=XHAT/(B*KHAT)+1.8E-3*EW*KHAT/ALOG(1.5*EW/ET)
C
      DL=EDL/SRER
C
      RETURN
      END
C
C$$$$$
C
      SUBROUTINE SICI(SI,CI,X)
C
C COMPUTATION OF SINE & COSINE INTEGRALS
C
```

```
C.IN  X      :ARGUMENT
C.OUT SI     :VALUE OF SINE INTEGRAL
C.OUT CI     :VALUE OF COSINE INTEGRAL
C
      Z=ABS(X)
      IF(Z-4.0) 100,100,400
100   Y=(4.0-Z)*(4.0+Z)
      SI=-1.570797E0
      IF(Z) 300,200,300
200   CI=-1.0E68
      RETURN
300   SI=X*(((((1.753141E-5*Y+1.568968E-7)*Y+1.374168E-5)*Y
     #+6.939089E-4)*Y+1.564682E-2)*Y+4.395509E-1+SI/X)
      CI=((5.772156E-1+ALOG(Z))/Z-Z*(((((1.066985E-10*Y
     #+1.584796E-8)*Y+1.725752E-6)*Y+1.165995E-4)*Y+4.990920E-3)*Y
     #+1.315306E-1))*Z
      RETURN
400   SI=SIN(Z)
      Y=COS(Z)
      Z=4.0/Z
      U=(((((((((4.048069E-3*Z-2.279143E-2)*Z+5.515070E-2)*Z
     #-7.261642E-2)*Z+4.987716E-2)*Z-3.332519E-3)*Z-2.314617E-2)*Z
     #-1.134958E-5)*Z+6.250011E-2)*Z+2.583969E-10
      V=((((((((((-5.108699E-3*Z+2.813179E-2)*Z-6.537283E-2)*Z
     #+7.902634E-2)*Z-4.400416E-2)*Z-7.945556E-3)*Z+2.601293E-2)*Z
     #-5.764000E-4)*Z-3.122418E-2)*Z-6.646441E-7)*Z+2.500000E-1
      CI=Z*(SI*V-Y*U)
      SI=-Z*(SI*U+Y*V)
      IF(X) 500,600,600
500   SI=-3.141593E0-SI
600   RETURN
      END
C
C$$$$$
C
```

## REFERENCES


[1] B.A. Munk and T.W. Kornbau, "Mono-Planar Arrays of Generalized Three-Legged Elements in a Stratified Dielectric Medium," Report 4346-6, May 1978, The Ohio State University ElectroScience Laboratory, Department of Electrical Engineering; prepared under Contract F33615-76-C-0124 for Air Force Avionics Laboratory, Wright-Patterson Air Force Base, Ohio. (AFAL-TR-78-43) (AD/B030 753L)

[2] T.W. Kornbau, "Application of the Plane Wave Expansion Method to Periodic Arrays Having a Skewed Grid Geometry," Report 4346-3, June 1977, The Ohio State University ElectroScience Laboratory, Department of Electrical Engineering; prepared under Contract F33615-76-C-0124 for Air Force Avionics Laboratory, Wright-Patterson Air Force Base, Ohio. (AFAL-TR-77-112) (AD/A047 311)

[3] B.A. Munk and R.D. Fulton, "Transmission Through a Bi-planar Slot Array Sandwiched Between Dielectric Layers," Report 3622-7, February 1976, The Ohio State University ElectroScience Laboratory, Department of Electrical Engineering; prepared under Contract F33615-73-C-1173 for Air Force Avionics Laboratory, Wright-Patterson Air Force Base, Ohio. (AFAL-TR-76-18) (AD/A032 160)

[4] B.A. Munk, G.A. Burrell and T.W. Kornbau, "A General Theory of Periodic Surfaces in Stratified Dielectric Media," Report 4346-1, November 1977, The Ohio State University ElectroScience Laboratory, Department of Electrical Engineering; prepared under Contract F33615-76-C-0124 for Air Force Avionics Laboratory (AFAL/WRP), Air Force Wright Aeronautical Laboratories, Wright-Patterson Air Force Base, Ohio. (AFAL-TR-77-219) (AD/B030 544L)

[5] B.A. Munk and R.D. Fulton, op. cit., pp. 15-17.

[6] E.L. Pelton, "Scattering Properties of Periodic Arrays Consisting of Resonant Multi-mode Elements," Ph.D. Dissertation, The Ohio State University, 1975. Also published as Report 3622-3, June 1975, The Ohio State University ElectroScience Laboratory, Department of Electrical Engineering; prepared under Contract F33615-73-C-1173 for Air Force Avionics Laboratory, Wright-Patterson Air Force Base, Ohio. (AFAL-TR-75-98) (AD/A 016 950)

[7] B.A. Munk and T.W. Kornbau, op. cit., p. 3.

[8] E.C. Jordan and K.G. Balmain, Electromagnetic Waves and Radiating Systems, Prentice-Hall, Inc., 1968, pp. 517-519.

[9] B.A. Munk and T.W. Kornbau, op. cit., p. 10.

[10] B.A. Munk, G.A. Burrell and T.W. Kornbau, op. cit., p. 17.

[11] Ibid., p. 36.

[12] Ibid., p. 61.

[13] T.W. Kornbau, op.cit., p. 11.

[14] S.A. Schelkunoff and H.T. Friis, Antennas, Theory and Practice, John Wiley and Sons, 1952, pp. 407-420.

[15] B.A. Munk, G.A. Burrell and T.W. Kornbau, op.cit., pp. 68,34.

[16] Ibid., p. 54.

[17] S.A. Schelkunoff and H.T. Früs, op.cit., pp. 241-243.

[18] B.A. Munk, R.J. Luebbers and T.L. Oliver, "Reflection Properties of a Periodic Array of Dipoles in a Dielectric Slab," Report 2989-6, December 1972, The Ohio State University ElectroScience Laboratory, Department of Electrical Engineering; prepared under Contract F33615-67-C-1439 for Air Force Avionics Laboratory, Wright-Patterson Air Force Base, Ohio. (AFAL-TR-72-381) (AD 906 372L)

[19] B.A. Munk, G.A. Burrell and T.W. Kornbau, op.cit., p. 35.

[20] Ibid., p. 25.

[21] Ibid., p. 27.

[22] Ibid., p. 25.

[23] Ibid., pp. 61-80.

[24] B.A. Munk and T.W. Kornbau, op.cit., p. 20.

[25] Ibid., p. 21.

[26] B.A. Munk and R.D. Fulton, op.cit.

[27] Ibid., p. 44.

[28] B.A. Munk and T.W. Kornbau, op. cit., pp. 34-37.

[29] B.A. Munk and R.D. Fulton, op.cit., p. 44.

[30] T.W. Kornbau, B.A. Munk, and C.J. Larson, "Design of a Metallized Radome for the C-140 Aircraft," Report 4346-4, May 1979, The Ohio State University ElectroScience Laboratory, Department of Electrical Engineering; prepared under Contract F33615-76-C-1024 for Air Force Avionics Laboratory, Wright-Patterson Air Force Base, Ohio. (AFAL-TR-79-1103)

[31] S.A. Schelkunoff and H.T. Friis, op. cit., p. 242.

[32] B.A. Munk and R.D. Fulton, op.cit., pp. 11-13.

[33] Ibid., pp. 12.

[34] B.A. Munk, G.A. Burrell and T.W. Kornbau, op.cit., p. 55.

[35] Ibid., pp. 58-60.

[36] B.A. Munk and T.W. Kornbau, op.cit., p. 55.

[37] Ibid., p. 59.

[38] Ibid., p. 59.

[39] Ibid., pp. 65-68.

[40] Ibid., p. 66.

[41] Ibid., p. 66.

[42] Ibid., p. 67

[43] Ibid., p. 70.

[44] Ibid., p. 68.



*U.S.Government Printing Office: 1980 — 657-084/600

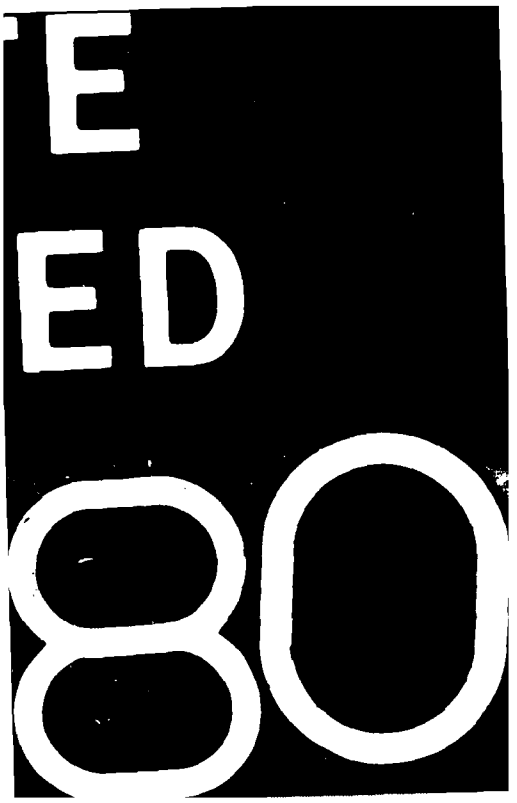
E
ED
80